NORADRENERGIC ACTIVATION OF GLYCOGENOLYSIS IN THE RAT NEOCORTEX AND HIPPOCAMPUS

MARIA FARA-ON

NORADRENERGIC ACTIVATION OF GLYCOGENOLYSIS IN THE RAT NEOCORTEX AND HIPPOCAMPUS

BY

MARIA FARA-ON

A THESIS SUBMITTED TO THE SCHOOL OF GRADUATE STUDIES
IN PARTIAL FULFILLMENT OF THE REQUIREMENTS FOR THE DEGREE
OF MASTER OF SCIENCE

DEPARTMENT OF PSYCHOLOGY
MEMORIAL UNIVERSITY OF NEWFOUNDLAND

2001

ST. JOHN'S NEWFOUNDLAND

ABSTRACT

In the central nervous system (CNS) glycogen and its catabolic enzyme glycogen phosphorylase (GP) are localized primarily in glial cells. Little is known about the distribution and localization of this energy source throughout the brain. Neuronally-secreted noradrenaline (NA) is known to activate glycogenolysis by stimulating adrenergic receptors (AR) found on glial cells, however, many aspects of this metabolic interaction have yet to be elucidated. Using *in vivo* and *in situ* techniques, this study aims to map the discrete areas of the brain where high levels of both active (aGP) and available (tGP) glycogen phosphorylase exist, where NA exerts significant glycogenolytic effects and to identify which AR subtypes may be involved in mediating these effects.

We investigated the effects of noradrenergic agents on glycogenolysis through IP administration of the α2 adrenergic autoreceptor antagonist, idazoxan (5 mg/kg), the α1-AR agonist, phenylephrine (3 mg/kg), or both á1- and β1/ β2-AR antagonists, prazosin (3 mg/kg) and propranolol (5 mg/kg). Drug effects on glycogenolysis were assayed by histochemical assessment of aGP and tGP no longer than 45 minutes following injection of drug or vehicle. Relative optical density (ROD) measures of regions of the neocortex, hippocampus, selected thalamic, diencephalic and striatal sites were taken using computer-assisted densitometric software (MCID). AGP and tGP were found to be distributed differentially throughout the sites investigated. Layer 4 of the neocortex, stratum lacunosum moleculare, medial habenula, reticular nucleus of the thalamus and the globus pallidus all demonstrated particularly high levels of both aGP and tGP under normal conditions. Idazoxan administration was found to induce significant increases in aGP levels in all layers of the upper limb of the primary somatosensory cortex, all layers of CA1, and some layers in CA3 and dentate gyrus, all thalamic nuclei examined and the caudate putamen. Results from our receptor study using specific AR subtype agonists and antagonists were inconclusive, but idazoxan was a much more effective activator than phenylephrine supporting the hypothesis that â, rather than á-ARs, play the primary role in mediating glycogenolysis induced by NA release. In addition the use of an á- and â-AR antagonist cocktail suggested noradrenergic modulation contributes only weakly to

basal enzymic activation. The range of glycogenolytic activation/inhibition induced by adrenergic agents appears to be 0-12% of total available GP.

The distribution of aGP and tGP we have found is consistent with the aGP distribution previously described by Harley and Bielajew (1992). Levels of aGP in the absence of drug manipulation appear to be less than 80% of tGP. Our neocortical results are also consistent with previous data showing significant increases in aGP in the somatosensory cortex following medial forebrain bundle (MFB) stimulation, suggesting an important interaction between sensory processing and noradrenergic modulation of glycogenolysis. The novel finding that NA induces significant activation of glycogenolysis in the hippocampus suggests activation of glycogenolysis may phy a part in NA's learning and mnemonic effects in this region.

ACKNOWLEDGMENTS

This thesis was made possible only through the contribution of many people from the Psychology Department of Memorial University of Newfoundland. In particular, I would like to express my gratitude to my supervisors, Dr. Carolyn W. Harley and Dr. John H. Evans for their invaluable guidance, assistance and support throughout. I am very grateful for the fellowship support I received from the School of Graduate Studies. Special thanks to Steve Milway, B.Sc., for laboratory support and assistance, Doris Babstock, M.Sc., for helping me with densitometry procedures and computer-generated images and Christian Lupien for technical help. I would also like to thank Dr. Michael Nolan and Tyson Garbe, M.A., for their unflagging encouragement and editorial assistance. Finally, I would like to thank Emmanuel Fara-On without whose assistance (too numerous to list) I might never have finished.

TABLE OF CONTENTS

LIST OF TABLES

LIST OF FIGURES

LIST OF GRAPHS

LIST OF IMAGES

LIST OF ABBREVIATIONS

Neocortex

BF3	Barrel field layer 3/4
BF4	Barrel field layer 4
BF5a	Barrel field layer 5a
BF5b	Barrel field layer 5b
BF6	Barrel field layer 6
SSPul3	Primary somatosensory cortex, upper limb section, layer 3/4
SSPul4	Primary somatosensory cortex, upper limb section, layer 4
SSPul5a	Primary somatosensory cortex, upper limb section, layer 5a
SSPul5b	Primary somatosensory cortex, upper limb section, layer 5b
SSPul6	Primary somatosensory cortex, upper limb section, layer 6
SSPll3	Primary somatosensory cortex, lower limb section, layer 3/4
SSPll4	Primary somatosensory cortex, lower limb section, layer 4
SSPll5a	Primary somatosensory cortex, lower limb section, layer 5a
SSPll5b	Primary somatosensory cortex, lower limb section, layer 5b
SSPll6	Primary somatosensory cortex, lower limb section, layer 6
SSS3	Secondary somatosensory cortex layer 3/4
SSS4	Secondary somatosensory cortex layer 4
SSS5a	Secondary somatosensory cortex layer 5a
SSS5b	Secondary somatosensory cortex layer 5b
SSS6	Secondary somatosensory cortex layer 6

Hippocampus

CA1so	CA1 stratum oriens
CA1sp	CA1 stratum pyramidale
CA1sr	CA1 stratum radiatum
CA1slm	CA1 stratum lacunosum moleculare
CA3so	CA3 stratum oriens
CA3sp	CA3 stratum pyramidale
CA3sr	CA3 stratum radiatum
CA3slm	CA3 stratum lacunosum moleculare
DGlbmo	Dentate gyrus, lateral blade, molecular layer
DGlbsg	Dentate gyrus, lateral blade, granular layer
DGlbpo	Dentate gyrus, lateral blade, polymorphic layer
DGmbsg	Dentate gyrus, medial blade, granular layer
DGmbmo	Dentate gyrus, medial blade, molecular layer

Thalamic, Diencephalic and Striatal Sites

CP	Caudate putamen
FF	Fornia fimbrix
GP	Globus pallidus
LD	Laterodorsal nucleus of the thalamus
PVT	Paraventricular nucleus of the thalamus
IC	Internal capsule
RT	Reticular nucleus of the thalamus
MH	Medial habenula

Please note that abbreviations listed above were taken from Swanson, (1992).

Glial function in the CNS

Of the two major cell types in the brain, neurons and glia, neurons have received greater empirical attention. In recent years, however, this imbalance is beginning to be redressed. Several lines of investigation have demonstrated the inadequacy of perceiving glia primarily as passive supporting cells. The critical importance of glia for maintenance of optimal central nervous system (CNS) functioning and for safeguarding healthy CNS dynamics from early development until death, is now well documented in the literature (Butterworth, 1993; Yamamoto *et al.*, 1989; and for reviews see Federoff *et al.*, 1993). Glia ensure proper CNS formation by guiding neuronal migration and growth (Bunge *et al.*, 1962 and Rakic, 1972), both ontogenetically (Hansson *et al.*, 1990; Pfeiffer *et al.*, 1992; and Rakic, 1971) and during regeneration (Hodges-Savola, 1996). They act as phagocytes by destroying dead and unhealthy tissue in response to brain trauma (Bunge, 1962; and Kimelberg, 1988). Moreover, glia are also known to secrete trophic and nutrient factors as well as second messengers to ensure neuronal survival (Lindsay, 1979) and facilitate CNS communication (Federoff *et al.*, 1993; Heal and Marsden, 1990; and Yudkoff *et al.*, 1993).

These important glial functions, related to safeguarding the integrity of the extracellular environment and to recycling and replenishing neuronal substrates (Butterworth, 1993; and Yamamoto *et al.*, 1989), strongly imply that glia are able to sense neuronal activity in the extracellular milieu. In order for such tightly coordinated interactions to be possible, there must exist an effective mode of communication between glial and neuronal elements in the CNS. Glial metabolism in particular appears to be especially sensitive to neuronal activity. Sensory stimulation-induced excitation of neurons has been reported to activate glycogenolysis (Swanson *et al.*, 1992; and

Tsacopoulos and Magistretti, 1996), whereas decreased neuronal activity during such conditions as hibernation or under anaesthesia results in an accumulation of glycogen (Swanson. 1991). Brazitikos and Tsacopoulos (1991) reported that photo-stimulation of honeybee drone retina activates glial metabolism. Photo-stimulation was found to be accompanied by increases in the conversion of labelled 2-deoxyglugcose (2DG) to labelled 2 deoxyglucose-6-phosphate (2DG-6-P) (this conversion is the first step toward glycogen synthesis). Since photo-stimulation is detected by photoreceptors and not glial cells, this finding suggests a metabolic interaction between the two cell types.

Glial cells express functional receptors for a plethora of neuronally-secreted substances, including those neurochemicals which have been reported to activate glycogenolysis and other glial functions (Deecher *et al.*, 1993; Hirata *et al.*, 1983; Hosli *et al.*, 1982; Salm and McCarthy, 1992; Stone and Ariano, 1989; Stone and John, 1991; and Stone *et al.*, 1991). These functional receptors, which can be activated by various neurochemicals, suggest a potential mechanism through which rapid and continuous communication between neurons and glia might occur. Signaling between astrocytes and neurons is complex, mediated by a range of neurotransmitters (Cambray-Deakin *et al.*, 1988; Deecher *et al.*, 1993; and Harik *et al.*, 1982), including neuropeptides (Sorg and Magistretti, 1992) and other neuromodulators (Cambray-Deakin *et al.*, 1988; Sorg *et al.*, 1995; and Woolf, 1987). The effects of these neurochemicals depend on the action of intracellular messengers (McCarthy and Vellis, 1979; Subbarao *et al.*, 1995; Takarama and Graves, 1991; and Ververken *et al.*, 1982).

Neuronal activation likely increases the metabolic demands on astrocytes, which are responsible for, among other functions, maintaining the sensitivity and integrity of neurons and the synaptic milieu in order to facilitate further stimulation. These added

energetic demands may be met by the non-oxidative metabolic processes such as breakdown of glycogen via glycogenolysis. For instance, astrocytes assist in the maintenance of the proper ionic environment for neuronal communication through removal of excess potassium ions (K^+) from the synapse (Woodward *et al.*, 1979). Astroglia have also been found to possess uptake carriers for amino acids and neurotransmitters, in addition to enzyme systems responsible for inactivating neurotransmitters (Hansson and Ronnback, 1992). They actively participate in synthesis, uptake, metabolism and release of GABA and glutamate (Hansson and Ronnback, 1981; and Hansson and Ronnback, 1991) to terminate rapidly and efficiently the effects of these substances in the synaptic cleft, and to resupply substrates to the active terminal (Woodward *et al.*, 1979).

Glutamate is the major excitatory transmitter in the mammalian CNS (Fonnum, 1984) and the most extensively distributed excitatory amino acid transmitter in the cerebral cortex (Hansson and Ronnback, 1991). Astrocytic processing of glutamate is crucial to maintaining effective glutamatergic transmission. In order for this transmission to be effective, the concentration of glutamate in the extracellular fluid must be kept low to reduce noise, and the supply of glutamate must be continuously replenished and transported to neurons without inducing depolarization (Fahrig, 1993). Glutamate removal from the synaptic cleft is primarily the responsibility of astrocytes. Neuronal capacity for glutamatergic re-uptake is considerably less than that of astrocytes (Schousboe and Westergaard, 1993). Following reuptake, astrocytes convert glutamate to glutamine via catalysis by glutamine synthetase, an enzyme which is localized primarily at astrocytic loci (Norenberg and Martinez-Hernandez, 1979). Glutamine is then safely transported to neurons in a manner that does not activate glutamate receptors. Neurons

contain the mitochondrial enzyme, glutaminase, which converts glutamine back into glutamate (Hertz, 1979). Interruption of astrocytic processing of glutamate would result in dangerously high synaptic glutamatergic concentrations, which would be harmful or even lethal to neuronal tissue (Yamamoto *et al.*, 1989; and Yudkoff *et al.*, 1993), and might lead to neuronal loss through excitotoxicity (Butterworth, 1993; and Schousboe and Westergaard, 1993).

In addition, evidence suggests that glial cells provide neurons with substrates, which can be used to replenish anaplerotic metabolites depleted by neuronal activation (Kaufman and Driscoll, 1993). Following stimulation, neurons release excitatory and inhibitory amino acids, glutamate and GABA (derived from α-ketoglutarate) and aspartate (derived from oxaloacetate) (Shank and Campbell, 1984). This process depletes neuronal supplies of tricarboxylic acid (TCA) cycle intermediates (Shank *et al.*, 1985). Glia also synthesize glutamine from glutamate and ammonia for neuronal use (Butterworth, 1993). Glutamine is considered to be the primary precursor from which glutamate is synthesized (Schousboe and Westergaard, 1993), though other substances such as the TCA cycle substrate α-ketoglutarate can act as alternative precursors (for GABA as well) (Shank and Campbell, 1984).

Pyruvate carboxylase, which catalyzes pyruvate derived from glycolysis, is localized primarily in astroglial cells (Shank and Aprison, 1981). Pyruvate carboxylase catalyzes the reaction combining pyruvate with carbon dioxide to enter the citric acid cycle as the 4-carbon compound, oxaloacetic acid (Shank and Campbell, 1984). This process is called CO_2 fixation. Astrocytic CO_2 fixation rates are much greater than those

found in neurons suggesting that glial cells may function to replenish the citric acid cycle intermediates in neurons as well as in astroglia themselves (Kaufman and Driscoll, 1993).

In brain, free-floating glucose circulating extracellularly can be stored as glycogen (Pentreath *et al.*, 1982). In fact, glycogen is the largest energy reserve (Jones, 1991; and Watanabe and Passonneau, 1973). Glycogen granules, which are comprised of clusters of glycogen molecules, are found in perisynaptic loci predominantly in astrocytes (Murphy, 1993; Lajtha *et al.*, 1981; and Peters *et al.*, 1991). In fact, glycogen presence in astrocytes is so reliable and ubiquitous that it has been used to identify astrocytes at the ultrastructural level (Pfeiffer *et al.*, 1992).

Glycogen turnover in nervous tissue is rapid (Watanabe and Passonneau, 1973) and the enzymes for its synthesis and degradation are strictly regulated. There are several reasons why glycogen constitutes an ideal form of stored energy. First, glycogen can be mobilized rapidly (more rapidly than fat); the transformation of glycogen into glucose simply requires one step (Devlin, 1992; and Barford and Johnson, 1989). In addition, glycogen can be used as a source of energy in the absence of O_2. The branched structure of glycogen has one beginning (the reducing end) with many terminal branches extended with non-reducing glucosyl units. This structure provides numerous sites for enzymatic degradation of glycogen into glucose (Takarama and Graves, 1991).

Noradrenaline (NA) has long been known to activate glycogenolysis. In muscle, where the physiological phenomenon of glycogenolysis was first studied, NA was the first and longest studied chemical activator of glycogen breakdown investigated. In brain, evidence for NA's activational effect on glycogenolysis is rapidly accumulating. There are several specialized neuronal groups, which secrete NA diffusely throughout the CNS (for review see Fillenz, 1990). These cell groups are believed to innervate glial cells as

well as neurons via α and β-adrenergic receptors (ARs). Astrocytes have been found to express functional α and β-ARs (Bowman and Kimelberg, 1987; Cambray-Deakin *et al.*, 1988; Hansson and Ronnback, 1992; Hirata *et al.*, 1983; and Hosli *et al.*, 1982). Astrocytic ARs are functional since their occupation by NA reliably culminated in a physiological event such as the release of second messengers (Agullo and Garcia, 1991; Clark and Perkins, 1971; Ebersolt *et al.*, 1981; Hosli *et al.*, 1982; Korf and Sebens, 1979; McCarthy and Vellis, 1978; Stone and Ariano, 1989; and Stone and John, 1991), alterations in membrane potential (Bowman and Kimelberg, 1987; and Hirata *et al.*, 1983), astrogliosis and cellular proliferation (Hodges-Savola *et al.*, 1996), and/or activation of astrocytic metabolism (Sorg and Magistretti, 1991; Sorg and Magistretti, 1992: Subbarao and Hertz, 1990; and Subbarao and Hertz, 1991).

Are glia targets of NA innervation?

Numerous *in vitro* studies have consistently reported that glia, astrocytes in particular, are viable targets of noradrenergic innervation. NA release in the CNS is known to increase cyclic AMP (cAMP) levels (Hosli *et al.*, 1982; and Stone and John, 1991). The first indication that glial cells might be targets for neuronally-secreted substances came from observations that NA elicited variable cAMP responses in brain slices and homogenates depending on the region, species and developmental age studied (Salm and McCarthy, 1992). This variability was believed to result from the differing contributions of several cell types, such as neurons and glia to these responses. cAMP levels in three glial clonal cells lines and in glioblastoma cells increased in response to NA administration, an increase which could be inhibited by β-AR antagonists (Clark and

Perkins, 1971; and Gilman and Nirenberg, 1971). Later studies using radioligand binding techniques on primary cultures of astrocytes and in brain slices provided additional evidence that glial cells possess β-ARs (Salm and McCarthy, 1992; and Stone and Ariano, 1989). Burgess *et al.* reported that only 2 out of 5 neuronal tumor cell lines demonstrated increases in cAMP levels in response to β-adrenergic stimulation, whereas 9 out of 11 glial cell lines showed this response. Salm and McCarthy (1992) reported that levels of β-AR sensitive adenylate cyclase in mixed primary cultures of mouse cerebral cortex were initially low, but increased as the neurons died out and glial cells proliferated.

Since cultured brain cells and brain slices are not subjected to the same environmental conditions as cells *in vivo*, they would not necessarily express the same genes. The discovery of a compound, fluorocitrate (FC), which selectively inhibits glial metabolism (Swanson and Graham, 1994; and Hassel *et al.*, 1992), eventually led to *in vivo* support for the *in vitro* results. An earlier finding that acute exposure (2h) of forebrain cortical slices from newborn mice to FC blocked the cAMP response to isoproterenol by 80-95% (Paulsen *et al.*, 1987) led Stone and John (1991) to examine whether FC would have a similar effect on cAMP responses *in vivo*. They found that FC abolished 90.6% of the cAMP response to β-AR stimulation.

Noradrenergic activation of glycogenolysis

NA has been directly shown to activate glycogenolysis *in vitro*. Sorg and Magistretti (1991) found that NA exerted a glycogenolytic action on primary cultures of mouse cerebral cortical astrocytes with an EC50 of 20 nM. Using radioligand binding

studies on rat cortical astrocyte cultures, Cambray-Deaken *et al.* (1988) reported evidence of β-adrenergic, serotonergic and muscarinic cholinergic receptor expression. Stimulation of these three neurotransmitter receptors by their respective agonists showed that, under normal conditions, only NA evoked a statistically significant change in glycogen content (33% decrease). Following NA administration, they were able to observe a clear concentration-dependent glycogenolysis. Quach *et al.* (1978) incubated mouse cortical slices in [^{3}H]glucose to generate an accumulation of [^{3}H]glycogen. After administration of NA, they also observed concentration-dependent glycogenolysis (EC_{50} = 0.09 uM). This glycogenolytic effect was mediated by β-ARs since timolol (β-AR antagonist) inhibited the effect, but phentolamine (α1-AR antagonist) was ineffective. Furthermore, NA's activation of glycogenolysis appeared to involve increases in cAMP production since NA's action was facilitated by the addition of 3-isobutyl 1-methylxanthine, a phosphodiesterase inhibitor which was ineffective when administered on its own (Quach *et al.*, 1978).

The contribution of α-ARs cannot be dismissed, however, since Sorg and Magistretti (1991) reported that pindolol, a β-AR antagonist, did not completely inhibit the effect of NA.They also reported that both the α1 and β-AR agonists, methoxamine and isoproterenol, promoted glycogenolysis with EC50s of 20 nM and 600 nM respectively. Subbarao and Hertz (1990) reported that the stimulatory effect of NA on glycogenolysis, in primary cultures of mouse astrocytes, is likely mediated by both α2- and β-ARs. They found that prazosin, an α1-AR antagonist*, did not attenuate noradrenergic activation of glycogenolysis. α2-AR-enhancement of glycogenolysis is

likely mediated by postsynaptic α2-ARs. The finding that activation of α2-ARs may also stimulate glycogen breakdown is somewhat problematic since α2-ARs inhibit adenylyl cyclase, the enzyme responsible for generating cAMP. Consensus regarding the contribution of specific AR subtypes to induction of glycogenolysis remains controversial. Although there appears to be general agreement that β-ARs mediate this effect, the involvement of α-ARs has yet to be unequivocably established.

To date, few studies have demonstrated that NA activates astrocytic ARs using *in vivo* techniques. However, numerous studies using *in vitro* methods report that astrocytes express both α and β-ARs, which display various physiological responses when exposed to noradrenergic agonists, providing fairly conclusive evidence that astrocytes are viable targets of noradrenergic innervation. *In vitro* studies utilize techniques involving the use of isolated cells and tissue and may not reliably reflect cellular responses in the intact system. It is also difficult to localize the effects of noradrenergic innervation to particular brain areas using these techniques. The next step to fully elucidating the function of noradrenergic activation of glycogenolysis and associating its actions to tangible physiological functions, therefore, requires that this phenomenon be demonstrated and investigated *in vivo*.

Evidence from *in vivo* studies

Results from *in vivo* studies are consistent with a glycogenolytic role for NA in the intact system. An *in vivo* study by Harley *et al.* (1995) reported that stimulating in the vicinity of noradrenergic fibers, namely the medial forebrain bundle (MFB), resulted in

---

* Prazosin can act as an α1-AR antagonist if the dosage or concentration is sufficiently high, however, at lower concentrations, its antagonistic effect is more specific to β1-Ars. (Dr. Detlef Bieger, personal communications).

enhanced glycogenolysis in layers 4, 5b and 6 of ipsilateral granular neocortex. Stimulation of MFB could activate several neurotransmitter systems including NA, serotonin, histamine and dopamine. Dopaminergic activation is unlikely to contribute to this effect since previous studies have reported that this neurotransmitter does not have direct glycogenolytic actions (Cambray-Deakin *et al.*, 1988). Although transmitter regulation of this glycogenolytic effect was not addressed, the results suggest that activation of glycogenolysis following neural pathway stimulation may be localized to selected subregions of the neocortex. Similarly, subregions of the hippocampus demonstrate regional glycogenolytic activity. Patches of aGP in the molecular layer of the dentate gyrus were reported in both the mouse (Wallace, 1982) and rat brain (Harley and Bielajew, 1992). Harley and Rusak (1993) found that levels of GP in the molecular layer of the dentate gyrus of the rat were greater during the dark phase when they appeared as intensely reactive patches, reminiscent of Wong-Riley's cytochrome oxidase blobs in the visual cortex. This increase in glycogenolytic activity coincided with times when rats, nocturnal creatures, were more aroused and active (Wallace, 1982). Again, this finding implies the involvement of noradrenergic, serotonergic and histaminergic systems since innervation of the forebrain by these neurotransmitters (Aston-Jones and Bloom, 1981; Trulson and Jacobs, 1979; and Schwartz *et al.*, 1986, respectively) has been reported to be greater during arousal implying increased release during the dark phase in nocturnal rodents such as rats and mice (Harley and Rusak, 1993).

What physiological events or systems are responsible for modulating this regional distribution of glycogenolytic activity? The connection between serotonin, histamine and particularly NA in activating glycogen breakdown has long been established (Quach *et al.*, 1978). NA was specifically implicated in a recent *in vivo* study by Coopersmith and

Leon (1995), which reported that noradrenergic stimulation of glycogenolysis in the olfactory bulb accompanies olfactory stimulation in young rats indicating a role for NA in modulating some of this regional glycogenolytic activity.

While *in vitro* biochemical measurements and the *in vivo* histochemical and biochemical evidence suggest neuronal NA release could mediate glycogenolysis, no study has examined the anatomical patterns of glycogenolysis following selective NA activation. The histochemical studies available suggest that the localization of aGP increases may vary in different brain areas. Such pattern variation is likely to reflect differing neuronal activity patterns, functions and/or differing degrees of neuronal/glial metabolic coupling. Only by identifying these regions, can we begin to make calculated estimations of the possible functions subserved by noradrenergic modulation of glycogenolysis. A wide range of studies using different experimental paradigms have implicated NA in a variety of physiological, psychological and cognitive functions including long-term potentiation of evoked potentials in the hippocampus, enhancement of learning and mnemonic processes; as well as attentional and exploratory behaviours (Devauges and Sara, 1990; and Sara and Devauges, 1988).

Enzymatic control of glycogenolysis

Glycogen is first broken down via glycogenolysis to produce glucose-1-phosphate (G-1-P). Glycogen phosphorylase (GP), the catabolic enzyme that converts glycogen to G-1-P, exists in an active, phosphorylated form (phosphorylase a) and an inactive, dephosphorylated form (phosphorylase b) (Krebs, 1989). Glycogen synthase, the anabolic enzyme that converts G-1-P to glycogen, also exists in phosphorylated and dephosphorylated forms (Lehninger, 1970). In contrast to GP though, the phosphorylated

form of glycogen synthase is inactive and the dephosphorylated form is active (Killilea *et al.*, 1976). Although the breakdown of glycogen requires the involvement of only one enzyme, phosphorylase a (aGP), two enzymes are involved in the sequence of events culminating in the conversion of phosphorylase b to aGP. First, protein kinase activates phosphorylase kinase. Phosphorylase kinase is the enzyme which directly phosphorylates bGP and converts it to an active form, aGP (Paudel *et al.*, 1993). NA stimulates the conversion of phosphorylase b to aGP. See Figure 1.

Modulation by cAMP

The involvement of cAMP in the control of brain glycogenolysis has been demonstrated in numerous experiments using cultured cell, brain slice and *in vivo* techniques (Salm and McCarthy, 1992; and Stone and John, 1991). The phosphorylation sequence begins with the activation of cAMP-dependent protein kinase by cyclic cAMP, the second messenger formed by activation of adenylyl cyclase (Rosenberg and Li, 1995). This protein kinase is normally inactive and consists of two subunits (R and C) (Gilman, 1987). CAMP binds to R, the regulatory subunit, resulting in the dissociation of the complex and the release of the active catalytic subunit, C (Taylor *et al.*, 1990), which activates phosphorylase kinase, the enzyme responsible for phosphorylation of GP. See Figure 1.

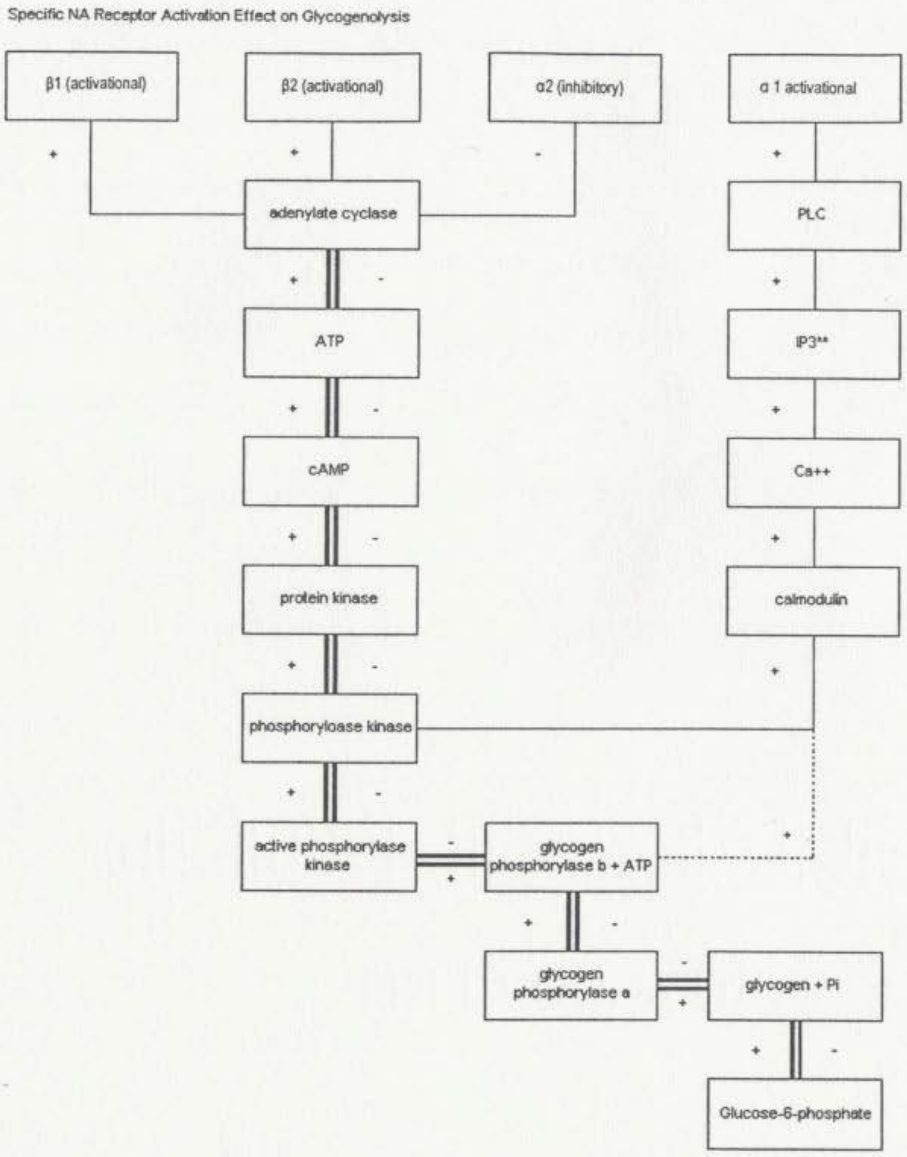

** Note: IP3 is hydrolized into PKC and 1,2 Diacylglycerol

Figure 1

Modulation by Ca^{2+}

It has also been suggested that Ca^{2+} is important in regulating glycogenolysis in nervous tissue (Quach *et al.*, 1982). Using cortical slices of mouse brain, Ververken *et al.* (1982) investigated the relative roles of cAMP and Ca^{2+} as intracellular messengers for the noradrenergic activation of GP. Treatment of slices with 2 mM EGTA to chelate

extracellular Ca^{2+} prevented the activation of GP, but not the early cAMP accumulation. Readdition of Ca^{2+} partially restored enzymatic activation. Similar data were observed with addition of the calcium antagonist La^{3+}.

Ca^{2+} influences the activation of GP via its effects on phosphorylase kinase (Quach *et al.*, 1982; and Ververken *et al.*, 1982). See Figure 1. Phosphorylase kinase is a large enzyme complex consisting of four subunits, α4, β4, γ4, and δ4. Gamma contains the catalytic subunits, α and β which are phosphorylated in the transition from inactive to active form. The γ subunit consists of a Ca^{2+} -binding regulatory protein called calmodulin. The binding of Ca^{2+} to the calmodulin subunit of phosphorylase kinase changes the conformation of the complex, making the enzyme more active with respect to phosphorylation of GP. Maximum activation of phosphorylase kinase likely requires both cAMP and Ca^{2+} stimulation (Devlin, 1992). Takarama *et al.* (1991) reported that a region of DNA coding for GP shows similar homology to the calmodulin subunit of phosphorylase kinase implying that GP might also be activated by Ca^{2+}. They propose that the activation of this region by Ca^{2+} facilitates the allosteric transformations of GP to the active form. Many cell types have two or more functionally distinct ER Ca^{2+} stores which can be distinguished by the intracellular second messenger that induces the release of stored Ca^{2+}. Ca^{2+} is released from one type of ER store by IP_3 (Finch *et al.*, 1991). The relative proportions of IP_3- and Ca^{2+} - sensitive stores vary widely among cell types. Large IP_3 sensitive stores appear to be localized predominantly in glia (Finkbeiner, 1993).

Noradrenergic activation induces the breakdown of glycogen in astrocytes. The characteristics of noradrenergic activation, namely the nature of the second messenger cascades that are initiated by activation of specific ARs, make this neurotransmitter an

ideal glycogenolytic agent. In addition, as will be discussed later, NA effects may involve coupling with other glycogenolytic agents to enhance the overall NA glycogenolytic effect.

There are two classes of ARs, α and β, each of which consist of several subtypes, α1, α2, β1 and β2 (Fillenz, 1990). Studies in the 1960's linked activation of β-ARs to stimulation of adenylyl cyclase which resulted in increased cAMP production (Robison *et al.*, 1965). Initially, it was believed that α-ARs were presynaptic and β-ARs were postsynaptically localized (Kimelberg, 1988). Early studies investigating the mechanism of α-AR-mediated smooth muscle contraction revealed that the effects of α1-AR stimulation were mediated by release of intracellular Ca^{2+}. The sequence of events that is initiated by stimulation of α1-ARs to culminate in Ca^{2+} release is now known to involve the breakdown of phosphatidylinositol 4,5-biphosphate (PIP_2) into two second messengers, diacylglycerol (DAG) and inositol 1,4,5-triphosphate (IP_3) (Fillenz, 1990). α2-ARs have been reported to be negatively coupled to adenylyl cyclase. Activation of β-ARs results in enhancement of cAMP production and activation of α1-ARs results in enhancement of intracellular Ca^{2+} release, both α1- and β-ARs may mediate NA's glycogenolytic actions.The second menssenger cascades mediated by specific AR subtypes are clearly illustrated in Figure 1.

Empirical evidence converges on the conclusion that β-ARs contribute to the cAMP response in glial cells. The connection between β-AR stimulation and cAMP production was so reliable that early researchers initially considered the possibility that adenylyl cyclase and the β-AR were identical (Gilman, 1989). Ligand-binding assay techniques eventually allowed for the resolution of these two proteins as distinct

macromolecules (Gilman, 1989). Noradrenergic activation of adenylyl cyclase appears to be mediated solely by β-ARs since increases in cAMP production are attenuated by administration of β-AR antagonists. Studies investigating the effect of α-AR stimulation on cAMP release in primary cultures of rodent neocortex found that α-AR stimulation alone did not affect cAMP levels (McCarthy and Vellis, 1978; and Van Calker *et al.*, 1978). α-AR blockade did, however, attenuate increases in cAMP elicited by other agonists. Clonidine, an α2-AR antagonist has been shown to effectively reduce increases in cAMP following administration of various drugs (McCarthy and Vellis, 1979).

Although α-ARs did not appear to mediate cAMP responses, they were found to be chiefly responsible for astroglial depolarization (Kimelberg, 1988; and Salm and McCarthy, 1992). Using explant astroglial cultures, Hosli *et al.* (1982) determined the concentration-dependent depolarization in response to NA by recording intracellularly from cells. When NA was replaced with the α1-AR specific agonist, phenylephrine, the authors found that the effects of NA were fully reproduced. Clonidine, an α2-AR specific agonist, also caused depolarization of astroglial cells but not to the same extent as phenylephrine or NA. NA depolarizations were blocked by α-AR antagonists, but not by the β-AR antagonist, atenolol. Propranolol, a β-AR antagonist failed to attenuate the NA depolarization response in astrocytes (Hirata *et al.*, 1983). Bowman and Kimelberg (1983) found that these depolarizations were more sensitive to inhibition by prazosin (α-AR antagonist) than yohimbine (β-AR antagonist). Phenylephrine, furthermore, could elicit these depolarizations while clonidine was ineffectual. These results suggest that NA-induced depolarization is mediated by α1-AR but not α2-AR stimulation.

Amplification of noradrenergic modulation of glycogenolysis

Via stimulation of adenosine release

There are several reasons why NA might be a particularly potent activator of glycogenolysis. Rosenberg and Li (1995) found evidence to suggest that stimulation of β-ARs by NA results in the activation of adenylyl cyclase which causes an accumulation of intracellular cAMP, transport of cAMP into the extracellular space, and degradation of extracellular cAMP to AMP and adenosine. Adenosine accumulation via stimulation of β-ARs appeared to be mediated by extracellular cAMP. Blockade of cAMP transport by probenecid blocked accumulation of both extracellular cAMP and extracellular adenosine. As well, blockade of cyclic nucleotide phosphodiesterase activity also blocked accumulation of extracellular adenosine. Isoproterenol, NA and adrenaline, agents which are known to activate adenylyl cyclase, also stimulate intracellular accumulation of cAMP, transport of cAMP and extracellular accumulation of adenosine with similar potency. The EC50s for isoproterenol, norepinephrine and epinephrine in stimulating cAMP transport were similar to their respective EC50s for stimulating intracellular cAMP accumulation and adenosine accumulation. NA stimulation of β-ARs has been reported to activate adenylyl cyclase which results in extracellular accumulation of adenosine which is also known to stimulate glycogenolysis. Magistretti *et al.* (1986) also reported that adenosine stimulates glycogenolysis. Noradrenergic activation of β-ARs, therefore, stimulates both release of adenosine and production of cAMP, two substances that activate glycogenolysis. Unlike conventional neurochemicals, most of the adenosine in the extracellular space is thought to be derived from sources other than exocytotic release from neuronal vessicles, including transport by a bi-directional adenosine

transporter and degradation of extracellular ATP. In this way, adenosine can act as a signal for low levels of ATP which communicates a need for energy.

Via stimulation of cGMP production

NA has also been reported to stimulate the release of another second messenger, cGMP. Using astrocyte-enriched cultures from rat brain, Agullo and Garcia (1991) found that norepinephrine (EC50 of 1.21 uM) evoked a rapid, concentration-dependent rise in cGMP levels. Prazosin administration significantly inhibited this effect; propranolol administration showed a smaller inhibition; and yohimbine was ineffectual. Therefore, α1-ARs must contribute, at least in part, to this effect.

Agullo and Garcia (1991) reported that NA increases cyclic GMP (a precursor of cGDP and cGTP) in astrocytes. CGTP has been found to amplify the effects of agonistic receptor stimulation. (For review see Gilman, 1989.) Activation of an extracellular receptor (by hormones, neurotransmitters, or sensory stimulation) promotes interaction of the receptor with one or more specific G proteins. This interaction causes a conformational alteration of the G proteins that results in an exchange of tightly bound guanosine diphosphate (GDP), an inactive ligand, for GTP, an activating ligand. The GTP-bound G protein can then interact with the appropriate intracellular effector molecules and influence their functions. The interaction of c-GDP with an agonist-bound receptor facilitates rapid binding of GTP to the complex of agonist, receptor, and G protein. Two consequences result. First, the affinity of the receptor for the agonist is lowered substantially which means that there is more available agonist present in the synaptic cleft to activate more receptors. Second, the ternary complex dissociates which allows the receptor to recycle and catalytically activate several G protein molecules

during the time that one remains active. The overall result, according to Agullo and Garcia (1991), is considerable amplification of the signal.

Sources of NA

Fluorescence histochemical techniques, immunohistochemical techniques and autoradiographic tracing techniques have made possible the elucidation of noradrenergic sources and their projections. (For review see Fillenz, 1990.) The two major noradrenergic cell groups, the locus coeruleus (LC) and the lateral tegmental groups, both have ascending and descending projections. The axon bundles which are comprised in part, but not exclusively, of NA-containing axons include: the MFB, the dorsal tegmental bundle, the central tegmental tract and the medullary catecholamine bundle (Fillenz, 1990). Noradrenergic LC neurons are unique in the brain in that they are unsurpassed in the divergence and ubiquity of their projections throughout the CNS (Jones, 1991).

The LC provides all of the noradrenergic input to the cerebral cortex (Levitt and Moore, 1978). In the rat, noradrenergic axons give off collateral branches in each cortical layer, with extensive collateralization in layers 1, 4, 5 and 6. The LC provides the major noradrenergic input to the thalamus, with the lateral tegmental cell groups providing innervation to isolated thalamic nuclei (Lindvall and Bjorklund, 1974). The hippocampal formation, the main olfactory bulb and most of the amygdala receive noradrenergic innervation exclusively from the LC (Fallon and Moore, 1978). In the pyramidal and molecular layers, there is dense noradrenergic innervation with less dense input to granule cell layers (Swanson and Hartman, 1975). Noradrenergic innervation of the neocortex, hippocampus and thalamus by the LC is further supported by a retrograde fluorescent double labelling study which revealed that injections placed in the cortex,

thalamus and hippocampus resulted in highlighting cells in the dorsal part of the LC (Room *et al.*, 1981). In addition, injections in these areas revealed not only ipsilateral but also contralateral labelling of cells in the LC.

The purpose of the present study

Given the abundance of evidence, both *in vitro* and *in vivo*, implicating noradrenergic involvement in region-specific modulation of glycogenolysis, the present study will attempt to systematically investigate several aspects of noradrenergic activation of glycogenolysis in rats, *in vivo*. The primary purpose of this study is twofold. Visual observations of sections processed for GP histochemistry (both aGP and tGP) reveal a consistent and reliable pattern of staining which has previously been described (Harley and Bielajew, 1992). Statistical analysis of these visual patterns to determine whether particular regions contain significantly more levels of aGP and/or tGP than others has yet to be conducted and was carried out as one component of the present undertaking.

As well, this study explores the effects of NA on glycogenolytic processes *in situ* with particular attention to the neocortical and hippocampal regions, since there is already evidence associating noradrenergic activity to glycogenolysis in these areas. Specifically, the emphasis on neocortical glycogenolytic responses is based on numerous *in vitro* studies showing that NA activates glycogenolysis in this region (Cambray-Deakin *et al.*, 1988; Quach *et al.*, 1978; and Sorg and Magistretti, 1991). *In vivo* evidence shows that stimulation of the MFB (which contain noradrenergic fibers) selectively activates layers of neocortex (Harley *et al.*, 1995). Regional distribution of aGP activity has also been reported for the hippocampus, of which the circadian evidence suggests that

NA may be a viable activator (Aston-Jones and Bloom, 1981; and Wallace, 1982). The noradrenergic projection to the hippocampus has been implicated in many biologically important functions associated with hippocampal processing, including learning and memory. Our study will examine, using histochemical and microcomputer-assisted densitometry techniques, levels of aGP, both under normal and basal conditions and following release of NA. By comparing the two results, levels of basal aGP and enhanced levels of aGP resulting from NA release, the location of regions demonstrating a high sensitivity to noradrenergic modulation of glycogenolysis will be identified.

Some neurotransmitters, like NA, can modulate their own release through inhibitory presynaptic autoreceptors. Evidence supporting the existence of receptors modulating neurotransmitter release was demonstrated for noradrenergic neurons in the CNS (McCormick, 1991; Freedman and Aghajanian, 1984; French *et al.*, 1995; and Raymond *et al.*, 1992). Nerve terminals may also possess presynaptic receptors, called heteroreceptors which are sensitive to endogenous compounds other than the neuron's own neurotransmitter. Heteroreceptors can be either facilitatory or inhibitory and can be activated by co-transmitters such as neuropeptides, neurotransmitters released by adjacent neurons, by locally synthesized substances or those originating from the bloodstream (McCarthy and Vellis, 1979; and Van Velhuizen *et al.*, 1993). The autoreceptor that modulates NA release is of the α2-AR subtype while α-adrenergic heteroreceptors can be either the α1 or α2 subtype (Heal *et al.*, 1995). α2-ARs appear to have a special role in the noradrenergic system which is related to their function as autoreceptors, heteroreceptors and postynaptic receptors (MacDonald and Scheinin, 1995).

Idazoxan has been reported to increase the firing rate of neurons in the LC (Devauges and Sara, 1990) and to produce an increase in NA release in the cortex and hippocampus (French *et al.*, 1995), making idazoxan a potentially valuable tool for investigating the effects of NA on glycogenolytic activity in these two brain regions. While there is little doubt, from the results of numerous microdialysis studies, that idazoxan is a potent enhancer of NA release via its actions on α2-ARs (Van Veldhuizen *et al.*, 1994; and Vanvelhuizen *et al.*, 1993), as previously mentioned, idazoxan also exerts effects on heteroreceptors, postsynaptic receptors and imidazoline receptors, particularly the I2 subtype (Brown *et al.*, 1995; MacKinnon *et al.*, 1995). The possible confounding effects of this labelling, as well as idazoxan's action on α2-postsynaptic receptors and heteroreceptors will be discussed later in the concluding remarks. The role of α2-ARs in mediating NA's glycogenolytic effects is controversial and the use of idazoxan, an α2-AR antagonist, eliminates these questions. In addition, the result of idazoxan administration is to increase NA release so that the effects studied are likely the result of NA activation of α1-, β1- and β2-ARs. Because of the inhibitory effect of α2-ARs on adenylate cyclase (Kimelberg, 1988), and consequently cAMP production, it seems unlikely that α2-ARs would contribute to activation of glycogenolysis. Various AR subtypes mediate different NA effects. The mapping of the anatomical location of the effects on glycogenolysis would improve our knowledge of the function of the central noradrenergic system.

A secondary purpose of the present study, therefore, is to determine the extent to which α1-ARs mediate noradrenergic activation of glycogenolysis by identifying the location of regions that demonstrate increased aGP activity in response to stimulation of

α1-ARs by the α1-AR agonist phenylephrine. There are no known β1-AR agonists that cross the blood brain barrier of the adult rat which eliminates the use of a similar procedure to determine the involvement of β1-ARs in noradrenergic activation of glycogenolysis.

A basal glycogenolytic activity is observed consistently in brain slices processed histochemically for aGP reactivity, which has been described by Harley and Bielajew (1992). Basal aGP levels can probe the contribution, if any, of β-AR activation to baseline glycogenolytic activity. The final purpose of this study is to determine whether basal glycogenolytic activity depends on basal noradrenergic effects mediated by β-ARs. A double-blocker cocktail consisting of prazosin, a specific β1-AR antagonist Yamaguchi *et al.*, 1991), and propranolol, a non-selective β1/β2-AR antagonist (Attia *et al.*, 1995; Mancinelli *et al.*, 1991; and Otani *et al.*, 1991), will be administered to subjects and the resulting changes, if any, to basal glycogenolytic activity will be examined.

For each aGP histochemistry there will be a corresponding tGP histochemistry performed. TGP histochemistry labels both phosphorylase a (aGP) and phosphorylase b, to give an indication of all the GP present in the area. By comparing the values obtained from aGP histochemistry with those obtained from tGP it will be possible to determine the degree of activation (by idazoxan-induced NA release or phenylephrine administration) or inhibition (by prazosin and propranolol administration) relative to the maximal activity that can possibly be induced. In addition, it will provide an opportunity to examine tonic patterns of activity in a more quantitative manner than has previously been described.

As comparisons to the neocortex and hippocampus, which derive exclusive innervation from the LC, it would be interesting to note aGP effects of our drug manipulations in the thalamus, which derives most, but not all noradrenergic innervation from the LC, and in the striatum, particularly in areas where there is no noradrenergic projection.

METHODS

Subjects

Subjects were 35 albino, male, Sprague-Dawley rats weighing approximately 250 g from Memorial University Vivarium. Animals were maintained on a 12:12 light/dark cycle and provided with Purina Rat Chow and water ad libitum.

Procedure

Drugs were administered to half the animals and the appropriate vehicle was injected into the remaining half, the control animals. To examine the changes in glycogenolytic activity resulting from increased NA release, idazoxan (5 mg/kg) was dissolved in physiological saline (0.9% NaCl) and injected at a volume of 5 mg/ml intraperitoneally (i.p.) into seven subjects. Corresponding volumes of the vehicle, saline, were administered i.p. to seven control rats. To selectively probe the role of the α1-AR subtype, phenylephrine (3 mg/kg) was dissolved in a solution containing 25% ethanol (95%) and 75% physiological saline (0.9% NaCl) and injected at a volume of (3 mg/8ml) i.p. into six subjects. Prazosin, a á1-AR antagonist, (3mg/kg) was dissolved in a solution containing 25% ethanol (95%) and 75% physiological saline (0.9% NaCl). Propranolol, a â1/β2-AR antagonist, (5 mg/kg) was dissolved into a solution with the exact composition

described for prazosin. To assess the noradrenergic contribution to daytime levels of aGP, prazosin and propranolol were then co-administered i.p. at volumes of 3 mg/4ml and 5 mg/4ml respectively. Corresponding volumes of the vehicle solutions were administered i.p. to ten subjects to be used as control animals for both the phenylephrine- and double blocker-treated animals.**

All subjects injected with idazoxan were paired with subjects injected with vehicle so that both animals could be sacrificed at approximately the same time. Phenylephrine, prazosin and propranolol and vehicle injections were initially conducted in triplets (one for each manipulation) to ensure that animals could be sacrificed simultaneously and to allow for the use of one vehicle animal as the control for both drug manipulations. Half of the vehicle brain was used as control for the phenylephrine brain and the other half was used as control for the prazosin and propranolol. After the first two triplets, however, it became evident that it was preferable to use one control for each drug manipulation to optimize matching. As well, to ensure optimal matching of chimeric brains, subjects were matched for age and weight.

All injections were performed between 11:30 am and 2:30 p.m. to minimize potentially confounding circadian effects. Forty-five minutes (pilot studies suggested this time interval was adequate for idazoxan to produce changes in noradrenergic activity) after idazoxan/saline administration, rats were injected with chloral hydrate (0.5 ml/100

** Note: Rationale for dose selection is as follows. For the idazoxan dose, many studies used 2 mg/kg and a 30 minute time interval. Devauges and Sara (1990) found that i.p. administration of idazoxan (2 mg/kg) was effective in facilitating an attentional shift in rats. However, although we also found glycogenolytic effects at 2 mg/kg, the effects were more reliable at 5 mg/kg and after a longer time interval, 45 minutes. Current literature regarding the use of phenylephrine in various *in vivo* paradigms showed that doses ranging between 2 and 5 mg/kg were found to be effective in peripheral and central experiments (Lopez-Sanudo and Arilla, 1994; and Peter *et al.*, 1995). Consequently, a dose of 3 mg/kg was selected for phenylephrine. I.p. administration of prazosin at 1 and 5 mg/kg was found to suppress IL-1 mRNA in the rat hypothalamus (Yamaguchi et al, 1991). The midpoint of these two values, 3 mg/kg was cautiously selected as a viable dose for prazosin. A dose at the higher level was avoided as prazosin loses its α1-AR specificity at higher concentrations. (Dr. Detlef Bieger, personal communications.) The propranolol dose of 5 mg/kg was selected since a dose of either 2.5 or 5 mg/kg was found to exert central effects affecting rat performance in the forced swimming task (Mancinelli *et al.*, 1991).

g, 80 mg/ml) and decapitated rapidly after losing consciousness, which typically occurred within two minutes. In the phenylephrine and the prazosin and propranolol treatment conditions, rats were injected with chloral hydrate (0.5 ml/100 g, 80 mg/ml) thirty minutes after administration of drug(s)/vehicle. Brains were immediately fresh-frozen by immersion in methyl butane cooled to 70°C to preserve enzymatic activity prior to sectioning and histochemical processing.

Sectioning

Fresh frozen tissue was necessary because fixatives denature GP. Brains were wrapped in foil and stored in the Forma Scientific -86° freezer at a temperature of 70°C until sectioning. Prior to sectioning in a cryostat, chimeric brains were constructed by cutting a drug-treated brain and a control brain along the midsagittal axis and joining complementary halves together. Coronal sections 30 uM thick were cut of the resulting whole chimeric brain at temperatures ranging from minus 12 °C to minus 14°C, using a Jung Frigocut 2800 E cryostat. Three consecutive sections were mounted on three slide sets for aGP histochemistry, tGP histochemistry and Nissl staining (cresyl violet). Each slide contained at least 4 "chimeric brain" slices, which were separated by approximately seven consecutive slices. As well, an additional 5 slices, each taken roughly after a slide set was completed, were placed on a slide for analysis of unincubated, baseline staining intensity, in the absence of either aGP or tGP reactivity. All slides were refrigerated until sectioning was complete. After sectioning, brains were allowed to warm at room temperature for approximately 10 minutes prior to histochemical processing which followed immediately after the warm up period. This precaution was necessary to minimize fluctuations in the water bath temperature (37°C) following immersion of

slides.

Histochemical procedures

AGP histochemistry

Incubation medium for aGP histochemistry was always prepared fresh for maximum effectiveness (not stored longer than one day in the refrigerator). It consisted of 0.1 M sodium acetate buffer (pH 5.6, which contained 2.97 g sodium acetate, 0.22 ml glacial acetic acid, 400 ml distilled water; either HCl or NaOH was added until the pH of the buffer reached 5.6). Into 45 mL of buffer solution, 100 mg disodium ethylenediaminetetra-acetate, 80 mg sodium fluoride, 2 g dextran and 400 mg α-d-glucose-1-phosphate (disodium salt) were added. The resulting solution was well mixed and either HCl or NaOH was added until the mixture reached a pH of 6.0. Distilled H_20 was then added to the solution to bring the volume of liquid to 50 mL. The medium was placed in a water bath at a temperature of 37°C for at least 1 hour prior to incubation of slides. Samples were immersed in the following solutions consecutively: incubation medium (30 minutes), 95% ethanol (3 minutes) Lugol's iodine (4 minutes) and physiological saline (5 seconds). Slices were allowed to air dry for at least 15 minutes following immersion in incubation medium and ethanol. Following immersion in Lugol's iodine slices were immediately placed in physiological saline to remove excess iodine. Slices were subsequently allowed to air dry overnight prior to coverslipping with Microkit. This protocol is a minor variation of that described in Woolf *et al.*, (1985).

TGP histochemistry

The procedure for histochemical assessment of tGP followed that of aGP. The

only difference between the two methods is that the incubation medium for tGP histochemistry contains 40 mg AMP to activate all GP enzyme present. Otherwise the two procedures were identical.

Nissl staining (cresyl violet)

Nissl-stained slides were used for reference in situations when accurate judgements of anatomical distinctions were difficult to make during the relative optical density (ROD) measurements. Slides undergoing Nissl staining were immersed in the following solutions in consecutive order:

Cresyl violet staining procedures

1.	110 mL glacial acetic acid and 110 mL acetone	(5 min)
2.	distilled H_2O	(1 min)
3.	cresyl violet	(8 min)
4.	25 mL glacial acetic acid and 225 mL H_2O	(2 min)
5.	acetone	(15 sec)
6.	acetone	(30 sec)
7.	xylene	(1 min)
8.	xylene	(1 min)

Unincubated staining

The procedure for histochemical assessment of unincubated slides to be used as an index of basal staining in the absence of aGP or tGP reactivity, consisted of the same general processes as those involved in aGP and tGP histochemistry. The only difference

in the two procedures is that in the unincubated staining, the incubation step is omitted. Unincubated slides were placed in all other solutions (40% ethanol solution, Lugol's iodine, and physiological saline) in the same order, for the same duration and with the same drying times.

Chimeric brains were used to reduce if not eliminate many of the variables which can affect aGP histochemistry. In some instances, in the vertical slides holders, a gradient of reactivity was seen with upper sections exhibiting lighter staining. Temperature and humidity variation also impinge on overall staining. These sources of variation can be minimized by chimeric preparations.

Relative optical density measurements

Apparatus

The neuroimaging apparatus consisted of an IBM-compatible microcomputer, software (M4 version of MCID software from Imaging Research Inc.), a solid state video camera (VSP Inc.) with a lens (Nikon), a light box (Northern Light), an image monitor (Electrohome Ltd.) and a mouse (Mouse Systems Corp.) The camera was mounted on an adjustable stand and the light box was situated directly under the camera.

Precautionary measures

Illumination effects

ROD measurements are influenced by fluxes in lighting conditions. To minimize such fluctuations, all densitometry work was conducted in a small inner room where all light sources were under manual control (overhead lights, computer screen and light box). The light box used was specifically designed for densitometry. Unlike microscope

illuminators, it has a digital readout that allows for precise setting of illumination level which remains fairly consistent with a variation within $\pm$ 0.5% over a 12 hour period.

Location effects

All video densitometry image systems exhibit density variability over the field of view so that variability in density measures may result from differences in location of target sample on the screen. In order to correct for this potential confound, shading error correction, which makes the blank field of view (no object being sampled) homogeneous, was performed prior to measurement of samples. This correction involves the system scanning a blank field of view and storing a pixel by pixel matrix of deviation values. The deviation matrix contains a density value (in gray levels) for each pixel in the image. After correcting for shading error, the system reports an average density value (in gray levels) for the entire field of view, which is essentially the average intensity of the overall image. This average intensity is a reflection of the intensity of light entering the camera that is digitized by the image analysis system. It varied insignificantly throughout the duration of the first experiment indicating that lighting conditions did not vary much between measurement-taking days. As an added precaution, slices were placed so that the image projected was centered.

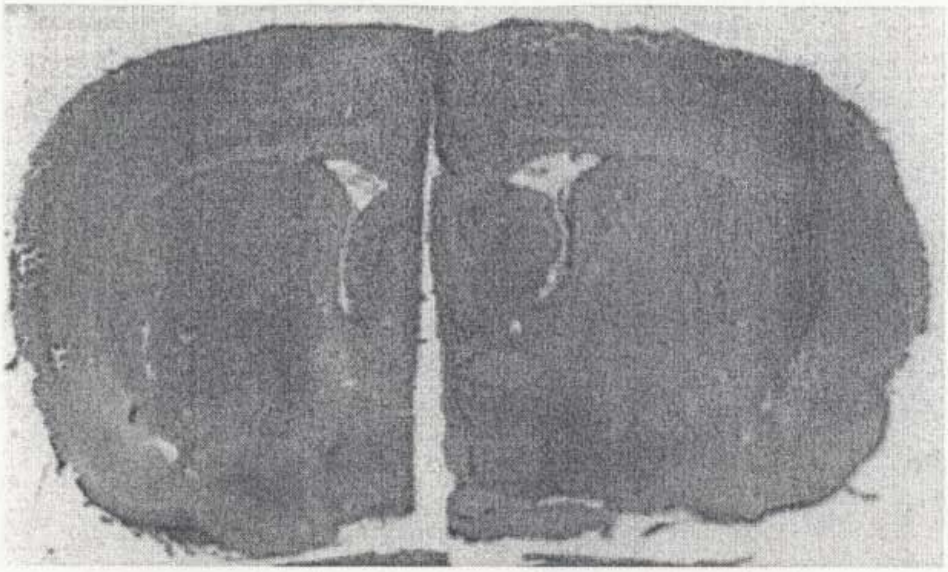

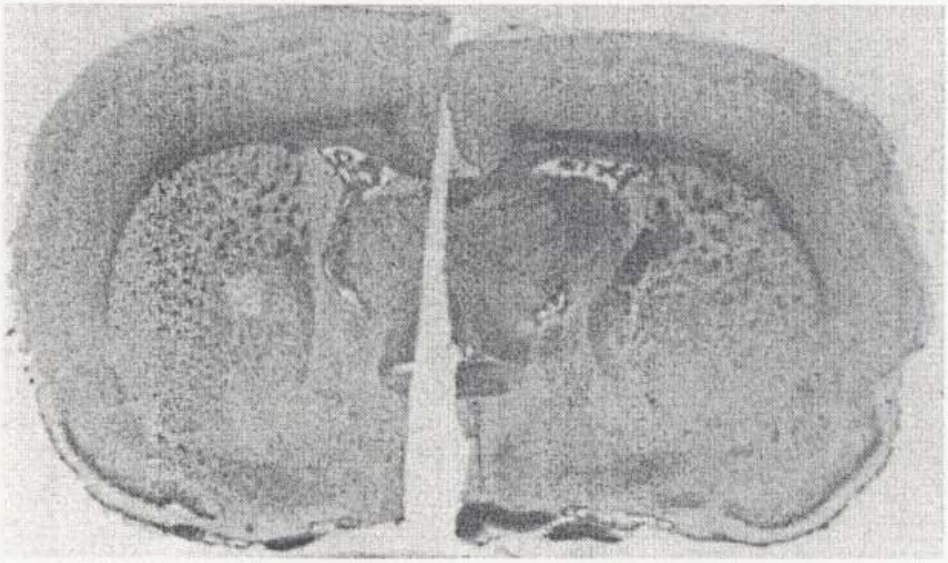

Images 1 & 2. Chimeric aGP-stained brain showing the neocortical layers studied (**Image 1 – top**) and a corresponding Nissl-stained chimeric brain (**Image 2 – bottom**). See Image 7 to view placement and size of boxes used to select regions of neocortex for ROD analysis.

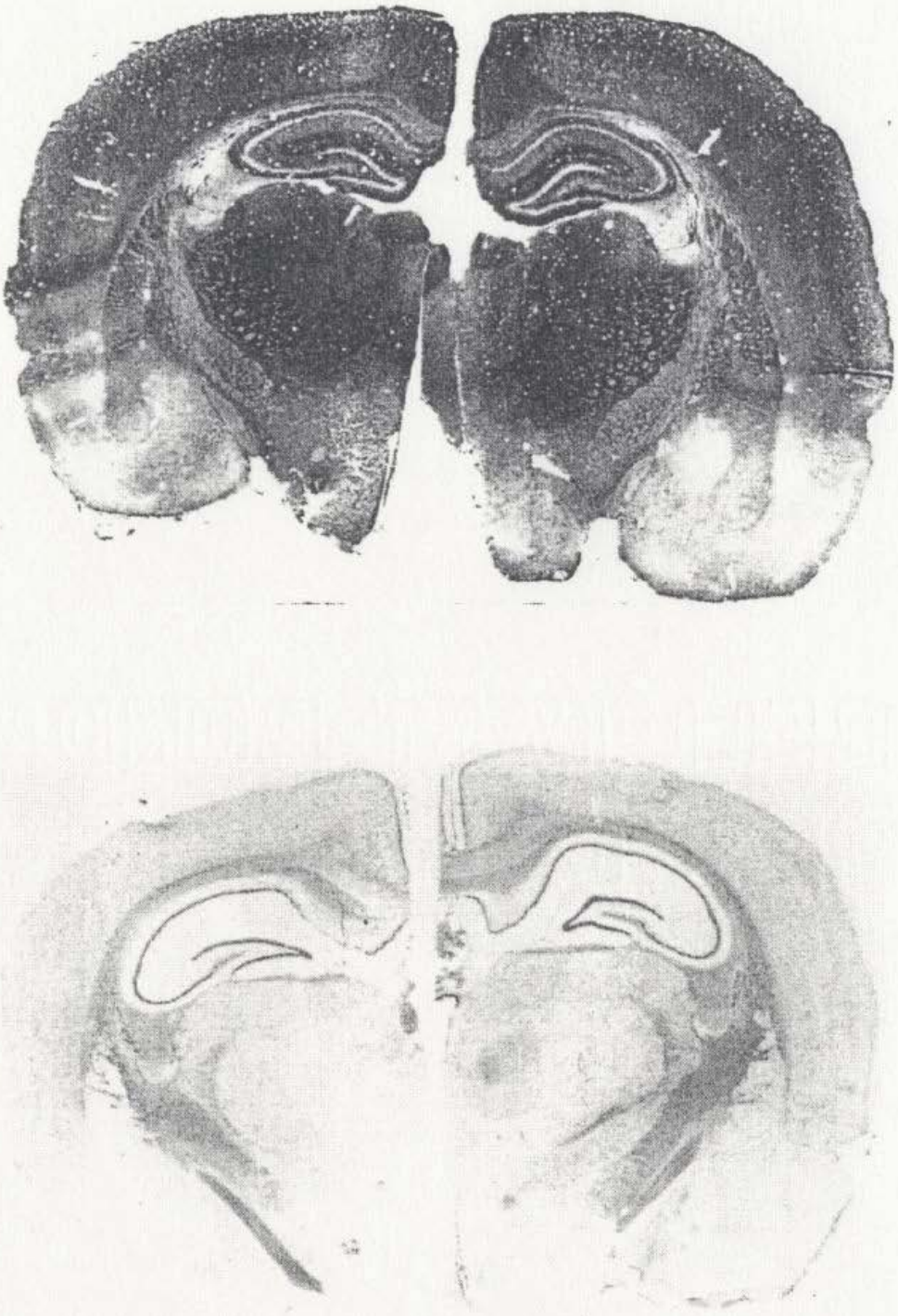

Images 3 & 4. Chimeric aGP-stained brain showing the hippocampal layers studied (**Image 3 – top**) and the corresponding Nissl-stained chimeric brain (**Image 4 –bottom**). See **Image 8** to view placement and size of boxes used to select regions of hippocampus for ROD analysis.

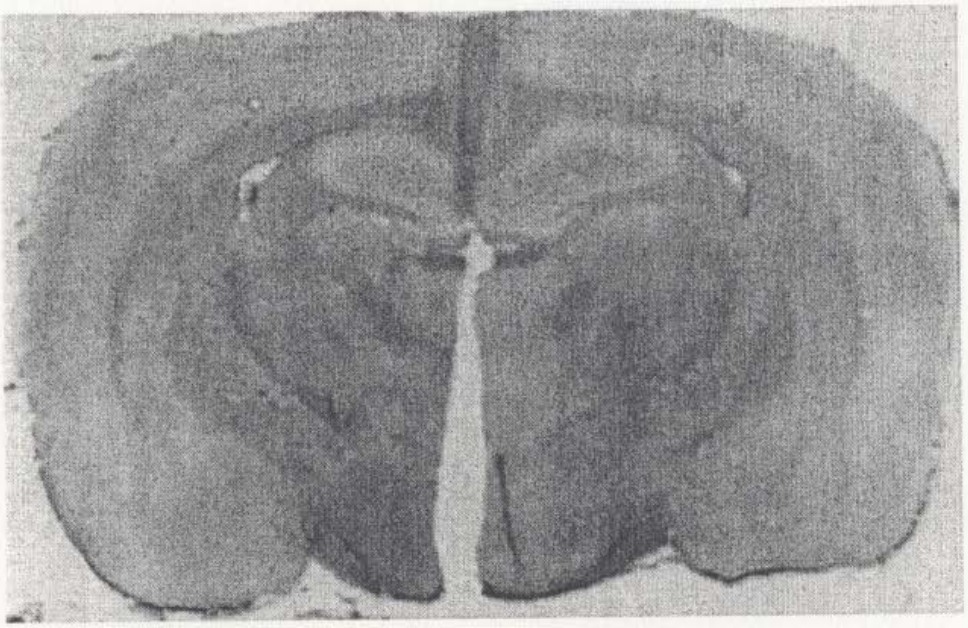

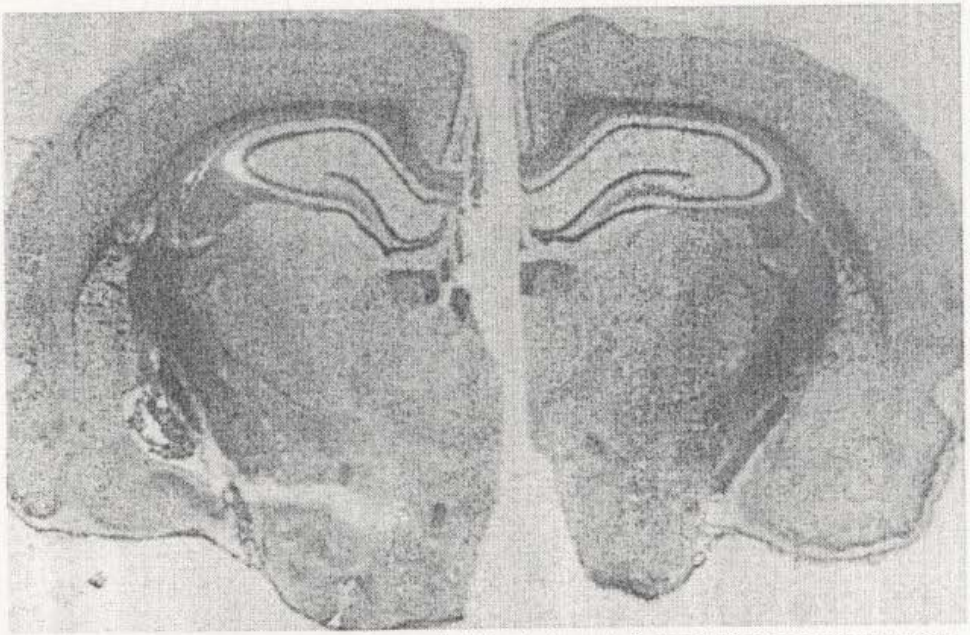

Images 5 & 6. Chimeric aGP-stained brain showing the thalamic, diencephalic and striatal regions studied (**Image 5 – top**) and the corresponding Nissl-stained chimeric brain (**Image 6 – top**). See **Image 9** to view placement and size of boxes used to select thalamic, diencephalic and striatal sites for ROD analysis.

Sampling bias

The "chimeric" brain construction of the slices allowed for simultaneous measurement of drug-treated and vehicle-treated sites which further decreased the amount of variability due to fluxes in lighting conditions. In addition, it assisted in the selection of regions to measure. The location of corresponding drug and vehicle brain areas were sampled as symmetrically as possible with the aim of measuring the anatomical regions that were as similar as possible. All brain sites sampled were sampled in similar locations. To facilitate the identification of particular brain areas, corresponding aGP-stained and Nissl-stained sections were also employed. See Images 2, 4 and 6.

Relative optical density measurement procedure

Background parameters

As recommended by MCID operating instructions, a background of pinkish/blue was first obtained by adjusting the F-stop on the Nikon lens and relative light intensity values of the light-box. The F-stop was 5.6 and relative light intensity varied between 643 and 681. Finally, prior to taking ROD measurements of samples, it was necessary to determine the appropriate magnification for samples and to perform several calibration steps.

Magnification

Lens magnification was kept constant at 68 mm (36 mm + 20 mm + 12 mm). For neocortical measurements magnification, which was adjusted by moving the camera position up or down on the arm on which it was attached, was selected to allow for viewing of the entire chimeric brain so that the neocortex of both hemispheres was maximally visible. For hippocampal measurements, magnification was selected to allow for reasonable enlargement of hippocampal areas of both halves of the chimeric brain.

Magnification for thalamic, diencephalic and striatal sites was the same as that for hippocampal sites. At this magnification relevant sites were clearly visible and storage of brain images was simplified. See Images 1, 3 and 5 above.

Measurement boxes were predetermined for cortical and hippocampal slices but not for thalamic and striatal nuclei. For cortical sites and hippocampal measurements, the dimensions of the measurement box were 4 pixels in width and 25 pixels in length. This size was found to best fit the thinnest layers of the hippocampus - the pyramidal and granular layers. When measuring thalamic, diencephalic, striatal and fiber tract regions the largest possible box that would fit the target site on both hemispheres was used. See Images 7, 8 and 9 below.

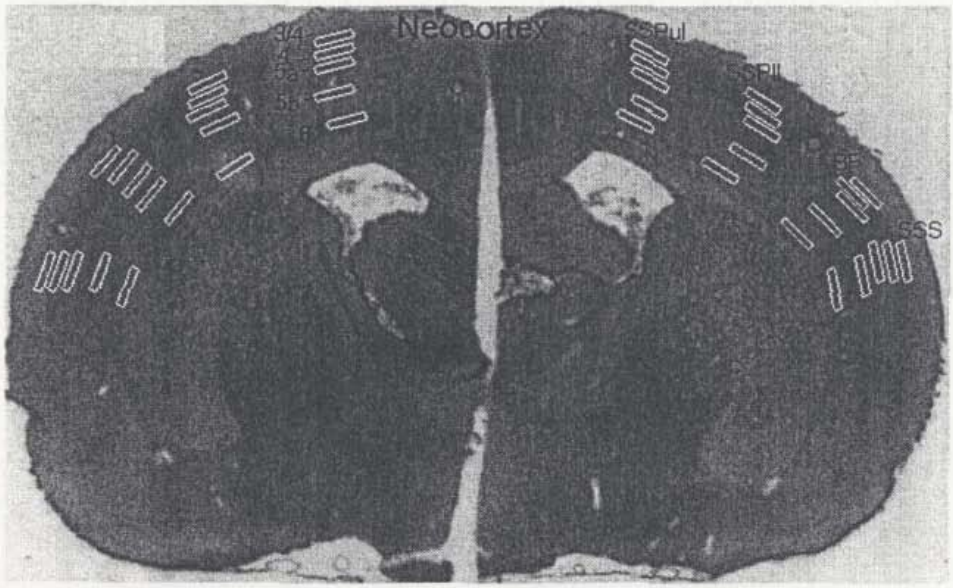

Image 7. A tGP-stained chimeric brain showing the neocortical layers studied and the dimensions of the measurement box size used. See **Image 2** to view Nissl-stained neocortex.

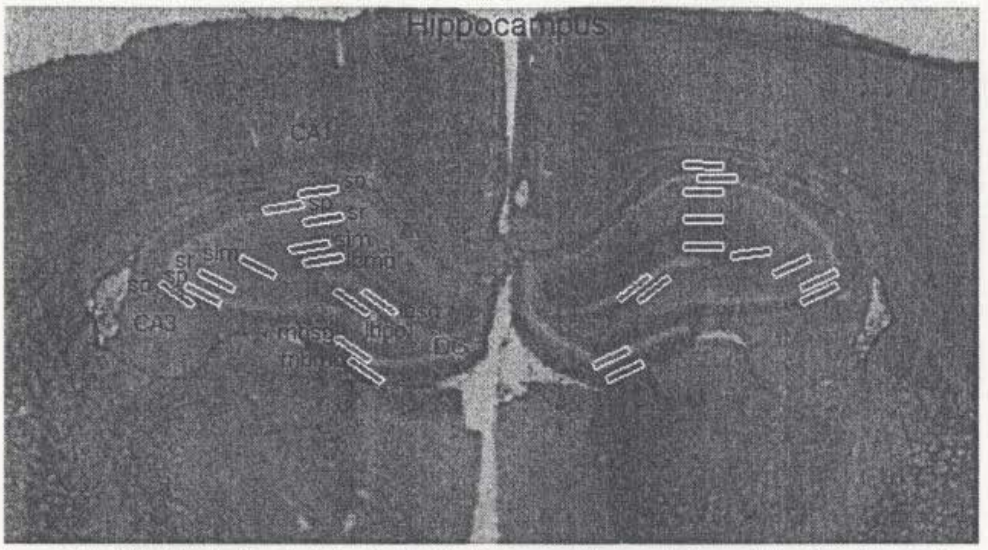

Image 8. A tGP-stained chimeric brain showing the hippocampal layers studied and the dimensions of the measurement box size used. See **Image 4** to view Nissl-stained hippocampus.

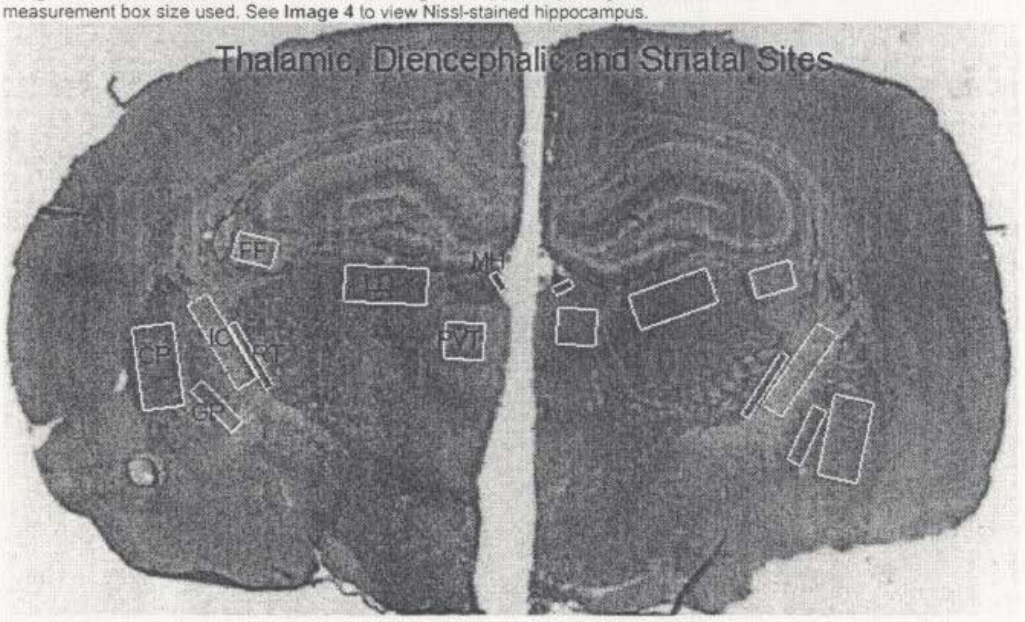

Image 9. A tGP-stained chimeric brain showing thalamic, diencephalic and striatal sites studied and the dimensions of the measurement box sizes used. See **Image 6** to view these sites in a Nissl-stained slice.

Calibration

After completion of the idazoxan measurements, an additional calibration step was introduced. Because the densitometric measurement procedure contains many variables which, if altered, can affect the ROD values obtained, calibration of the system was performed by measuring steps 1-8 of Kodak Step Tablet No. 705ST801. Calibration

allows for relatively accurate comparison of ROD values measured at different times. By comparing ROD values obtained for Kodak steps measured, it will be possible to compare these calibration values with values obtained at other times by other investigators. If ROD values obtained for similar sites by other investigators are higher than what we report and the calibration values for the same Kodak steps are also higher to a similar degree, then the ROD values are similar.

Prior to taking ROD measurements of samples the shading error corrections and average intensity values were recorded. An average of all average intensity values was then determined. ROD values were measured for the first eight steps of Kodak Step Tablet No. 705ST801 since these steps contained the range of ROD values found in the tissue samples to be measured. Although Kodak Step Tablet No. 705ST801 values were not recorded prior to densitometric analysis of idazoxan-treated slices, they were taken prior to densitometric analysis of the phenylephrine and the prazosin and propranolol treatment conditions. A comparison of the ROD values obtained for the idazoxan group for sites selected randomly after Kodak Step Tablet No. 705ST801 values were taken were fairly consistent with previously taken values. Therefore these Kodak step values can also be applied to the samples in idazoxan experimental condition.

The values corresponding to K1, K2, K3, K4, K5, K6 and K7 were the calibration values obtained in the process of analyzing and storing section images of the phenylephrine group and for the prazosin and propranolol group. The ROD values corresponding to K8 were obtained when the reliability of the measurements for the idazoxan group was examined for consistency in relation to Kodak Step calibrations taken for the other two treatment conditions. ROD values for random slices and sections were examined and compared to previously obtained ROD values. These raw calibration

values are listed on Table 1.

Table 1

ROD Values for Steps 1-8 of Kodak Step Tablet No. 705ST801

Step #	K1	K2	K3	K4	K5	K6	K7	K8	K9	Mean
1	0.0629	0.0605	0.0669	0.0593	0.0616	0.0609	0.0834	0.0670	0.0637	0.0651
2	0.1792	0.1752	0.1928	0.1777	0.1793	0.1775	0.1928	0.1749	0.1804	0.1811
3	0.2895	0.2855	0.2954	0.2897	0.2915	0.2879	0.2945	0.2805	0.2948	0.2899
4	0.3650	0.3612	0.3660	0.3601	0.3676	0.3627	0.3670	0.3537	0.3748	0.3642
5	0.4502	0.4476	0.4546	0.4498	0.4535	0.4483	0.4426	0.4338	0.4303	0.4456
6	0.5248	0.5205	0.5305	0.5288	0.5301	0.5238	0.5172	0.5074	0.5121	0.5217
7	0.5961	0.5920	0.6007	0.6000	0.6033	0.5970	0.6033	0.5799	0.6030	0.5973
8	0.6650	0.6590	0.6681	0.6663	0.6712	0.6655	0.6574	0.6506	0.6651	0.6631

K values showing ROD values taken for Kokak Step Table No. 705ST801, steps 1-8. K1 to K7 values were obtained prior to performing ROD analysis of the phenylephrine- and prazosin and propranolol-treated chimeric brains. No K measurements were taken prior to ROD analysis of idazoxan-treated chimeric brains. K8 values represent the calibration of the idazoxan-treated brains. ROD measurements of the idazoxan-treated sections following K8 calibration did not vary markedly from the values taken initially prior to calibration. K9 values represent calibration for the range of ROD values for each drug treatment condition listed on Table 3.

The range of values obtained under these conditions was similar to those previously obtained, but not exactly the same. It would be impossible to obtain exactly the same values because it is not possible to measure exactly the same area just the same general area. Other factors already mentioned previously also contribute to the variation. The calibration values for steps K1-K8 also varied slightly. The minimum and maximum values, along with the mean values are shown on Table 2.

Table 2

Range of ROD Values for Kodak Step Tablet No. 705ST801

Step#	Lowest Value	Highest Value	Mean Value
1	0.0593	0.0834	0.0670
2	0.1749	0.1928	0.1839
3	0.2805	0.2948	0.2877
4	0.3537	0.3748	0.3643
5	0.4303	0.4546	0.4425
6	0.5074	0.5301	0.5188
7	0.5799	0.6033	0.5916
8	0.6506	0.6712	0.6609

Range of and mean ROD values for Kodak Step Tablet No. 705ST801. The lowest and highest ROD calibration values obtained, along with their means, are listed to demonstrate that variation was not substantial.

Our analysis provided satisfactory evidence to conclude that Kodak Step No. 705ST801 calibrations determined for the phenylephrine and prazosin and propranolol groups could also apply to the idazoxan group. The last set of Kodak Step calibration values, K9 were taken towards the end of the ROD analysis procedure when new ROD measurements were obtained to show the range of ROD values for some sites found to be significant in each of the treatment conditions. These ranges are shown on Table 3.

Table 3

ROD Range Samples of Sites Demonstrating Significant Drug-Induced Effects

Drug Treatment	Site	Drug Min	Drug Max	Veh Min	Veh Max
Double blocker*	BF3	0.2096	0.7227	0.1789	0.6025
Phenylephrine	SSS3	0.4014	0.4170	0.3366	0.3476
Phenylephrine	SSPul3	0.3983	0.4919	0.3097	0.3399
Phenylephrine	SSPul5b	0.3625	0.4254	0.3086	0.3754
Phenylephrine	SSPul6	0.4059	0.5218	0.3403	0.4542
Idazoxan	CA3so	0.5902	0.6248	0.4601	0.5896
Idazoxan	CA3sr	0.5144	0.6067	0.4076	0.5533
Idazoxan	CA3slm	0.5942	0.6823	0.4442	0.6437

Table 3. Minimum and maximum ROD values for drug- and vehicle-treated sites are listed to show the variation observed under each treatment condition. These values were derived by visually selecting two samples showing the lightest and darkest aGP staining. The values were obtained from two different chimeric trial groups and not the same chimeric pair. *Please note that the double blocker refers to the prazosin and propranolol treatment condition.

After taking all the ROD measurements for the idazoxan-treated animals, it became possible to store all images of chimeric brain slices into our computer mainframe, allowing for increased standardization of lighting conditions since images could be stored rapidly under identical conditions and measured at a later time.

Replications

ROD measurements for cortex, hippocampus and selected thalamic and striatal nuclei for aGP-stained, tGP-stained and unincubated slices were recorded. Three ROD measurement replications were taken of each site within both drug-treated and control-treated halves of the chimeric brain using consecutive slices so that each site was

measured six times per chimeric brain (three replications per hemisphere times two hemispheres). Replications were used to increase the representative accuracy of the ROD values obtained.

Cortical regions examined

ROD measurements were confined to the following regions. In the neocortex, we measured staining intensities of layers 3/4, 4, 5a, 5b and 6. See Image 7. Layers 1 and 2 were not examined because these layers, being the most superficially located, were frequently damaged. They were also more vulnerable to fluctuations in sectioning thickness because of their superficial location. In hippocampus, we assessed staining intensities in the following sites. Within the CA1 and CA3 regions, we examined the stratum oriens, stratum pyramidale, stratum radiatum, stratum lacunosum moleculare. Within the dentate gyrus we looked at the molecular and granular layers of medial and lateral blades and the hilar region. See Image 8. Other areas examined included the reticular, laterodorsal and paraventricular nuclei of the thalamus; one diencephalic region, the medial habenula; two fiber tract regions, the fornia fimbrix and the internal capsule and two striatal regions, the caudate putamen and the globus pallidus. See Image 9. Thalamic, diencephalic and fiber tract regions which were clear and which allowed for three measurement replications were selected. The sites in this latter grouping were chosen to include regions which either did not receive noradrenergic innervation exclusively from the LC or which received no direct projections from noradrenergic fibers (striatum).

Statistical analysis

To assess the basal pattern of aGP, a rank ordering of ROD values for each site in the vehicle portion of the chimeric brains of the idazoxan study was determined and statistically analyzed using the Wilcoxon Signed Ranks Test. Only the vehicle-treated sites in the idazoxan treatment condition were used in this study. Data from the vehicle halves of the phenylephrine and double blocker (prazosin and propranolol) groups were not included in this analysis for several reasons which are discussed in the RESULTS section ("*Differences in variability*" p. 98).

To assess which sites, if any, were significantly affected by drug treatment statistical analyses of dependent samples were conducted. Sites were matched histologically by their staining and were treated as matched samples. The statistical procedure involved calculating the difference between the means of the ROD measurements for each drug-treated and vehicle-treated site and then using the difference scores as if they were the original data in a one-sample test. The means were analyzed using one-way ANOVAs to determine whether a site main effect existed for tissue assessed histochemically for aGP and tGP. As a follow-up, to determine where these significant differences occurred, t-test analyses of dependent samples were performed. This method of analysis was selected to eliminate the batch effect variation observed in the measurements introduced by our histochemical procedure. The batch effect is the variability due to the batch processing of the samples. Because the samples of each batch consisted of slices from one chimeric brain, batch was confounded with subject and replication, making removal of this variation impossible using conventional statistical methods.

To facilitate comparison of the ROD values obtained from our histochemical assessment of aGP levels with those obtained through other techniques such as biochemical assays, aGP levels of aGP were further calculated as percent of tGP by subtracting unincubated staining ROD values from drug/control aGP ROD values, deriving 'corrected' means for each condition and expressing the resulting value as a percent of the corrected tGP ROD values measured for each site. To obtain basal aGP levels, the following formula was used:

$$\left[\frac{\text{corrected mean vehicle treated aGP ROD value}}{\text{corrected mean tGP ROD value}}\right](100)$$

To obtain the percent increase/decrease of aGP levels induced by administration of drug(s), the following formula was used:

$$\left[\frac{\text{corrected mean drug-treated aGP ROD value} - \text{corrected mean vehicle treated ROD value}}{\text{corrected mean tGP ROD value}}\right](100)$$

RESULTS

Calibration

Calibration information, including varibility analysis, is found on Tables 1, 2 & 3 previously. The values we obtained indicate that our ROD measurement procedures did not exhibit sufficient variation to significantly affect our results

.

Measurements of basal aGP and tGP activity

Basal aGP activity

Wilcoxon Signed Rank Test statistical analysis of the aGP patterns demonstrated by the sites that received vehicle in the idazoxan treatment condition was conducted to determine whether there were any significant differences in aGP levels among the sites investigated. These aGP differences would represent site variations in glycogenolytic metabolic activity under basal conditions.

Neocortical sites

In general the barrel fields region was the most highly reactive for aGP histochemistry, significantly more so than other neocortical areas examined. Layer 5a and 5b of the barrel fields, in particular, are more reactive than both layer 3/4 of upper limb and layer 6 of lower limb of the primary somatosensory cortex. Barrel field layer 5b is also more reactive than layer 5b of lower limb. Barrel field layer 4 is more reactive than layer 4 of upper limb. Outside the barrel fields region, only two layers demonstrated notable aGP reactivity. Layer 4 of the secondary somatosensory cortex and layer 3/4 of

lower limb were significantly more reactive than layer 4 and layer 5a of upper limb respectively. See Table 4.

Table 4

A Comparison of Basal Active Glycogen Phosphoryalse (aGP) Levels in the Neocortex Using Wilcoxon Signed Ranks Test Statistical Analysis

Site	Significance	Site	Significance
BF5b-SSPll5b	p<0.0468	SSS4-SSpul4	p<0.0468
BF5b-SSPll6	p<0.0468	SSPll3-SSPul5a	p<0.0312
BF5b-SSPul3	p<0.0468		
BF5a-SSPll6	p<0.0468		
BF5a-SSPul3	p<0.0312		
BF4-SSPul4	p<0.0468		

The first site listed is significantly more reactive for aGP than the second site. Significant site differences in levels of aGP within the layers of the neocortex were analyzed using a Wilcoxon Signed Ranks Test statistical analysis. N=6. df=2.

Hippocampal sites

A clear and consistent pattern of aGP reactivity was observed in the hippocampus. Overall, the stratum lacunosum moleculare of CA1 and CA3 exhibited the highest levels of aGP histochemical reactivity in the hippocampus, significantly greater than all other layers. The stratum oriens of CA3 and CA1 demonstrated significantly higher aGP reactivity than respective stratum radiatum. CA3 stratum oriens and stratum radiatum were significantly more reactive than corresponding layers in CA1. The basal level of aGP within the polymorphic layer of the lateral blade (which corresponds to the hilar region) was significantly more reactive than the stratum oriens and stratum radiatum of CA1. The molecular layer of the medial blade (ventral or exposed blade) was significantly more reactive than CA1 stratum radiatum. The granular and pyramidal layers demonstrated the least aGP reactivity and were significantly less reactive than all other layers within the hippocampus. As with the neocortex, differences across sites were more salient than across layers. The CA3 region was significantly more reactive than the CA1. For instance, CA3 stratum radiatum demonstrated significantly higher aGP reactivity than CA1 stratum oriens and stratum radiatum. As well, CA3 stratum oriens was significantly more reactive than CA1 stratum radiatum. See Table 5.

Table 5

A Comparison of Basal Active Glycogen Phosphorylase (aGP) Levels in the Hippocampus
Using Wilcoxon Signed Ranks Test Statistical Analysis

Site	Significance	Site	Significance
CA1so-CA1sp	p<0.0156	CA3so-CA1sp	p<0.0156
CA1so-CA1sr	p<0.0156	CA3so-CA1sr	p<0.0468
CA1so-CA3sp	p<0.0156	CA3so-CA3sp	p<0.0156
CA1so-Dglbsg	p<0.0156	CA3so-CA3sr	p<0.0156
CA1so-Dgmbsg	p<0.0156	CA3so-Dglbsg	p<0.0156
CA1sr-CA1sp	p<0.0156	CA3so-Dgmbsg	p<0.0156
CA1sr-CA3sp	p<0.0156	CA3sp-Dgmbsg	p<0.0156
CA1sr-Dglbsg	p<0.0156	CA3slm-CA3so	p<0.0312
CA1sr-Dgmbsg	p<0.0156	CA3slm-CA3sp	p<0.0156
CA1slm-CA1so	p<0.0156	CA3slm-CA3sr	p<0.0156
CA1slm-CA1sp	p<0.0156	CA3slm-CA1so	p<0.0156
CA1slm-CA1sr	p<0.0156	CA3slm-CA1sp	p<0.0156
CA1slm-CA3so	p<0.0312	CA3slm-CA1sr	p<0.0156
CA1slm-CA3sp	p<0.0156	CA3slm-Dglbmo	p<0.0156
CA1slm-CA3sr	p<0.0312	CA3slm-Dglbsg	p<0.0156
CA1slm-Dglbmo	p<0.0156	CA3slm-Dglbpo	p<0.0156
CA1slm-Dglbsg	p<0.0156	CA3slm-Dgmbsg	p<0.0156
CA1slm-Dglbpo	p<0.0156	CA3slm-Dgmbmo	p<0.0156
CA1slm-Dgmbsg	p<0.0156	CA3sr-CA1so	p<0.0156
CA1slm-Dgmbmo	p<0.0156	CA3sr-CA1sp	p<0.0156
Dglbpo-CA1so	p<0.0156	CA3sr-CA1sr	p<0.0156
Dglbpo-CA1sp	p<0.0156	CA3sr-CA3sp	p<0.0156
Dglbpo-CA3sp	p<0.0156	CA3sr-Dglbsg	p<0.0156
Dglbpo-CA1sr	p<0.0468	CA3sr-Dgmbsg	p<0.0156
Dglbpo-Dglbsg	p<0.0156	Dgmbmo-CA1sp	p<0.0156
Dglbpo-Dgmbsg	p<0.0156	Dgmbmo-CA1sr	p<0.0156
Dglbsg-Dgmbsg	p<0.0156	Dgmbmo-CA3sp	p<0.0156
Dgmbmo-Dglbsg	p<0.0156		
Dgmbmo-Dgmbsg	p<0.0156		

The first site listed is significantly more reactive for aGP than the second site. Significant site differences in levels of aGP among hippocampal sites investigated were analyzed using a Wilcoxon signed Ranks Test statistical analysis. N=6, df=2.

Thalamic, diencephalic, striatal and fiber tract regions

Of the sites examined in the thalamus, diencephalon, and striatum, the medial habenula was significantly more reactive for aGP histochemistry than all other sites measured in this grouping, followed by the reticular nucleus of the thalamus and the globus pallidus. See Table 6.

Table 6

A Comparison of Basal Active Glycogen Phosphorylase (aGP) Levels in the Thalamus, Diencephalon and Striatum Using Wilcoxon Signed Ranks Test Statistical Analysis

Site	Significance	Site	Significance
GP-CP	p<0.0468	MH-CP	p<0.0468
GP-FF	p<0.0468	MH-FF	p<0.0468
GP-PVT	p<0.0468	MH-GP	p<0.0468
GP-IC	p<0.0468	MH-LD	p<0.0468
RT-CP	p<0.0468	MH-PVT	p<0.0468
RT-FF	p<0.0468	MH-IC	p<0.0468
RT-GP	p<0.0468	MH-RT	p<0.0468
RT-LD	p<0.0468		
RT-PVT	p<0.0468		
RT-IC	p<0.0468		

The first site listed is significantly more reactive for aGP than the second site. Significant site differences in levels of aGP in the thalamic, diencephalic and striatal sites were analyzed using a Wilcoxon Signed Ranks Test statistical analysis. N=6, df=2.

Overall comparison of sites

A comparison of sites within the three groupings: neocortical; hippocampal; and diencephalic, thalamic and striatal and fiber tract regions revealed that all sites measured (in the neocortex, hippocampus, thalamus, diencephalon and striatum) were significantly more reactive than the strata pyramidale and granulare of the hippocampus and the fiber tracts, the fornia fimbrix and the internal capsule. In addition, the stratum lacunosum moleculare of CA3 was found to demonstrate significantly higher levels of aGP reactivity than all layers of the upper limb region of primary somatosensory cortex except layer 3/4. CA1 stratum lacunosum moleculare was found to show significantly higher levels of aGP than layers 5b and 6 of upper limb of primary somatosensory cortex. The molecular layer of the dentate gyrus medial blade showed significantly greater aGP reactivity than layer 3/4 of the barrel fields. The medial habenula of the diencephalon was more reactive than all layers of upper limb neocortex, layer 6 of lower limb and barrel fields and layer 5b of lower limb. The reticular nucleus of the thalamus was also significantly more reactive than layer 6 of upper limb somatosensory neocortex and layer 3 of the neocortical barrel fields. See Table 7.

Table 7

A Comparison of Basal Active Glycogen Phosphorylase (aGP) Levels in the Neocortex, Hippocampus, Thalamus, Diencephalon and Striatum Using Wilcoxon Signed Ranks Test Statistical Analysis

Site	Significance	Site	Significance
BF3-CA1sp	p<0.0156	SSS3-CA1sp	p<0.0156
BF3-CA1sr	p<0.0312	SSS3-CA1sr	p<0.0312
BF3-CA3sp	p<0.0156	SSS3-CA3sp	p<0.0156
BF3-Dglbsg	p<0.0156	SSS3-Dglbsg	p<0.0156
BF3-Dgmbsg	p<0.0156	SSS3-Dgmbsg	p<0.0156
BF3-CP	p<0.0468	SSS3-FF	p<0.0468
BF3-FF	p<0.0468	SSS3-IC	p<0.0468
BF3-IC	p<0.0468	SSS4-CA1sp	p<0.0156
BF4-CA1sp	p<0.0156	SSS4-CA1sr	p<0.0312
BF4-CA1sr	p<0.0312	SSS4-CA3sp	p<0.0156
BF4-CA3sp	p<0.0156	SSS4-Dglbsg	p<0.0156
BF4-Dglbsg	p<0.0156	SSS4-Dgmbsg	p<0.0156
BF4-Dgmbsg	p<0.0156	SSS4-FF	p<0.0468
BF4-FF	p<0.0468	SSS4-IC	p<0.0468
BF4-IC	p<0.0468	SSS5a-CA1sp	p<0.0156
BF5a-CA1sp	p<0.0156	SSS5a-CA1sr	p<0.0312
BF5a-CA1sr	p<0.0312	SSS5a-CA3sp	p<0.0156
BF5a-CA3sp	p<0.0156	SSS5a-Dglbsg	p<0.0156
BF5a-Dglbsg	p<0.0156	SSS5a-Dgmbsg	p<0.0156
BF5a-Dgmbsg	p<0.0156	SSS5a-FF	p<0.0468
BF5a-FF	p<0.0468	SSS5a-IC	p<0.0468
BF5a-IC	p<0.0468	SSS5b-CA1sp	p<0.0156
BF5b-CA1sp	p<0.0156	SSS5b-CA1sr	p<0.0312
BF5b-CA1sr	p<0.0468	SSS5b-CA3sp	p<0.0156
BF5b-CA3sp	p<0.0156	SSS5b-Dglbsg	p<0.0156
BF5b-Dglbsg	p<0.0156	SSS5b-Dgmbsg	p<0.0156
BF5b-Dgmbsg	p<0.0156	SSS5b-FF	p<0.0468
BF5b-FF	p<0.0468	SSS5b-IC	p<0.0468
BF5b-IC	p<0.0468	SSS6-CA1sp	p<0.0156
BF6-CA1sp	p<0.0156	SSS6-CA1sr	p<0.0312
BF6-CA1sr	p<0.0468	SSS6-CA3sp	p<0.0156
BF6-CA3sp	p<0.0156	SSS6-Dglbsg	p<0.0156
BF6-Dglbsg	p<0.0156	SSS6-Dgmbsg	p<0.0156
BF6-Dgmbsg	p<0.0156	SSS6-FF	p<0.0468
BF6-FF	p<0.0468	SSS6-IC	p<0.0468
BF6-IC	p<0.0468	SSPul3-CA1sp	p<0.0156
SSPll3-CA1sp	p<0.0156	SSPul3-CA1sr	p<0.0468
SSPll3-CA1sr	p<0.0156	SSPul3-CA3sp	p<0.0156
SSPll3-CA3sp	p<0.0156	SSPul3-Dglbsg	p<0.0156
SSPll3-Dglbsg	p<0.0156	SSPul3-Dgmbsg	p<0.0156
SSPll3-Dgmbsg	p<0.0156	SSPul3-FF	p<0.0468
SSPll3-FF	p<0.0468	SSPul3-IC	p<0.0468
SSPll3-IC	p<0.0468	SSPul4-CA1sp	p<0.0156
SSPll4-CA1sp	p<0.0156	SSPul4-CA1sr	p<0.0156
SSPll4-CA1sr	p<0.0156	SSPul4-CA3sp	p<0.0156
SSPll4-CA3sp	p<0.0156	SSPul4-Dglbsg	p<0.0468
SSPll4-Dglbsg	p<0.0156	SSPul4-Dgmbsg	p<0.0156
SSPll4-Dgmbsg	p<0.0156	SSPul4-FF	p<0.0468
SSPll4-FF	p<0.0468	SSPul4-IC	p<0.0468
SSPll4-IC	p<0.0468	SSPul5a-CA1sp	p<0.0156
SSPll5a-CA1sp	p<0.0156	SSPul5a-CA1sr	p<0.0156
SSPll5a-CA1sr	p<0.0468	SSPul5a-CA3sp	p<0.0312
SSPll5a-CA3sp	p<0.0156	SSPul5a-Dglbsg	p<0.0156
SSPll5a-Dglbsg	p<0.0156	SSPul5a-Dgmbsg	p<0.0312
SSPll5a-Dgmbsg	p<0.0156	SSPul5a-FF	p<0.0468
SSPll5a-FF	p<0.0468	SSPul5a-IC	p<0.0468
SSPll5a-IC	p<0.0468	SSPul5b-CA1sp	p<0.0156
SSPll5b-CA1sp	p<0.0312	SSPul5b-CA1sr	p<0.0156
SSPll5b-CA1sr	p<0.0156	SSPul5b-CA3sp	p<0.0156
SSPll5b-CA3sp	p<0.0156	SSPul5b-Dglbsg	p<0.0312
SSPll5b-Dglbsg	p<0.0312	SSPul5b-Dgmbsg	p<0.0156
SSPll5b-Dgmbsg	p<0.0156	SSPul5b-FF	p<0.0468
SSPll5b-FF	p<0.0468	SSPul5b-IC	p<0.0468

(Table 7 continued)

Site	Significance	Site	Significance
SSPll5b-IC	p<0.0468	SSPul6-CA1sp	p<0.0156
SSPll6-CA1sr	p<0.0156	SSPul6-CA1sr	p<0.0156
SSPll6-CA1sp	p<0.0156	SSPul6-CA3sp	p<0.0156
SSPll6-CA3sp	p<0.0156	SSPul6-Dglbsg	p<0.0156
SSPll6-Dglbsg	p<0.0156	SSPul6-Dgmbsg	p<0.0312
SSPll6-Dgmbsg	p<0.0156	SSPul6-FF	p<0.0468
SSPll6-FF	p<0.0468	SSPul6-IC	p<0.0468
SSPll6-IC	p<0.0468	CA1so-FF	p<0.0468
CA3so-FF	p<0.0468	CA1so-IC	p<0.0468
CA3so-IC	p<0.0468	CA1sr-FF	p<0.0468
CA3sr-FF	p<0.0468	CA1sr-IC	p<0.0468
CA3sr-IC	p<0.0468	CA1slm-SSPul5b	p<0.0156
CA3slm-SSPul4	p<0.0156	CA1slm-SSPul6	p<0.0156
CA3slm-SSPul5a	p<0.0156	CA1slm-FF	p<0.0468
CA3slm-SSPul5b	p<0.0156	CA1slm-IC	p<0.0468
CA3slm-SSPul6	p<0.0156	Dgmbmo-BF3	p<0.0312
CA3slm-FF	p<0.0468	Dglbpo-FF	p<0.0468
CA3slm-IC	p<0.0468	Dglbpo-IC	p<0.0468
GP-CA1sp	p<0.0468	MH-SSPul3	p<0.0468
GP-CA1sr	p<0.0468	MH-SSPul4	p<0.0468
GP-CA3sp	p<0.0468	MH-SSPul5a	p<0.0468
GP-CA3sr	p<0.0468	MH-SSPul5b	p<0.0468
GP-Dglbsg	p<0.0468	MH-SSPul6	p<0.0468
GP-Dgmbsg	p<0.0468	MH-SSPll5a	p<0.0468
RT-SSPul6	p<0.0468	MH-SSPll6	p<0.0468
RT- BF3	p<0.0468	MH-BF6	p<0.0468
RT-CA1sp	p<0.0468	MH-CA1sp	p<0.0468
RT-CA1sr	p<0.0468	MH-CA1sr	p<0.0468
RT-CA3sp	p<0.0468	MH-CA3sp	p<0.0468
RT-CA3sr	p<0.0468	MH-CA3sr	p<0.0468
RT-Dglbsg	p<0.0468	MH-Dglbsg	p<0.0468
RT-Dgmbsg	p<0.0468	MH-Dgmbsg	p<0.0468

The first site listed is significantly more reactive for aGP than the second site. Significant site differences in levels of aGP between the three groupings: neocortical, hippocampal, and thalamic, diencephalic and striatal sites were analyzed using a Wilcoxon Signed Ranks Test statistical analysis. N=6, df=2.

Thus, hippocampal stratum lacunosum moleculare, dentate gyrus molecular layer, medial habenula and reticualr nucleus of the thalamus were all more reactive than at least some layers of somatosensory neocortex, but did not differ from each other, while the cell layers of the hippocampus and the fiber tracts were the least reactive areas measured.

TGP activity

There were no significant differences between drug versus vehicle sites when assessed for tGP activity in the idazoxan condition. As we predicted, one acute administration of drug was not sufficient to affect normal levels of available GP or tGP, only levels of phosphorylase a or aGP. There was insufficient time between the single

administration of the drug treatment and the sacrifice to produce visible changes in protein synthesis. Consequently, tGP ROD values between drug and vehicle-treated groups were averaged.

Neocortical sites

Barrel fields layers 3/4, 4 and 5a were significantly more reactive than all layers of the secondary somatosensory cortex. Layer 5b of the barrel fields was significantly more reactive than all other layers of secondary somatosensory cortex except layer 3/4. Barrel fields layer 3/4, 4 and 5a were significantly more reactive than layer 5b and 6 of barrel fields. Barrel fields layer 6 was significantly less reactive than barrel fields layer 5b and all layers of the secondary somatosensory cortex. Layer 6 of lower limb somatosensory cortex was the most reactive in this region, more reactive than all other lower limb layers except layer 4. Lower limb layers 3/4, 4 and 6 were found to be significantly more reactive than all secondary somatosensory cortex layers and layers 5b and 6 of the barrel fields. Layer 5a and 5b of lower limb somatosensory cortex were not as reactive as the other layers in the area and were only significantly more reactive than layers 5a and 5b of barrel fields and layer 6 of the secondary somatosensory cortex.

Of the neocortical sites examined, the most reactive region was found to be the upper limb. Layer 4 of upper limb was the most reactive of all the neocortical sites analyzed and was significantly more reactive than all other layers in the upper limb, barrel fields and lower limb regions of the primary somatosensory cortex and the secondary somatosensory cortex. Layers 3/4, 5a and 5b of upper limb were also significantly more reactive than all layers of barrel fields and the secondary somatosensory cortex, but unlike, layer 4, they were only more reactive than layers 3/4,

5a and 5b of lower limbs. Layer 6 was the least reactive layer in the upper limb region. It was only more reactive than layers 5b and 6 of the barrel fields and secondary somatosensory cortex and layer 3/4, 5a and 5b of lower limb. See Table 8.

Table 8

A Comparison of Total Glycogen Phosphorylase (tGP) Levels in the Neocortex Using Wilcoxon Signed Ranks Test Statistical Analsysis

Site	Significance	Site	Significance
BF3-BF5a	p<0.0156	SSPul3-BF3	p<0.0468
BF3-BF5b	p<0.0156	SSPul3-BF4	p<0.0468
BF3-BF6	p<0.0156	SSPul3-BF5a	p<0.0468
BF3-SSS3	p<0.0156	SSPul3-BF5b	p<0.0156
BF3-SSS4	p<0.0156	SSPul3-BF6	p<0.0156
BF3-SSS5a	p<0.0312	SSPul3-SSS3	p<0.0156
BF3-SSS5b	p<0.0156	SSPul3-SSS4	p<0.0312
BF3-SSS6	p<0.0156	SSPul3-SSS5a	p<0.0312
BF3- SSPll5a	p<0.0156	SSPul3-SSS5b	p<0.0156
BF4-BF5b	p<0.0156	SSPul3-SSS6	p<0.0156
BF4-BF6	p<0.0156	SSPul3-SSPll3	p<0.0156
BF4-SSS3	p<0.0156	SSPul3-SSPll5a	p<0.0156
BF4-SSS4	p<0.0468	SSPul3-SSPll5b	p<0.0156
BF4-SSS5a	p<0.0468	SSPul4-BF3	p<0.0156
BF4-SSS5b	p<0.0312	SSPul4-BF4	p<0.0156
BF4-SSS6	p<0.0156	SSPul4-BF5a	p<0.0156
BF5a-BF5b	p<0.0156	SSPul4-BF5b	p<0.0156
BF5a-BF6	p<0.0156	SSPul4-BF6	p<0.0156
BF5a-SSS3	p<0.0312	SSPul4-SSS3	p<0.0156
BF5a-SSS4	p<0.0312	SSPul4-SSS4	p<0.0156
BF5a-SSS5a	p<0.0312	SSPul4-SSS5a	p<0.0156
BF5a-SSS5b	p<0.0156	SSPul4-SSS5b	p<0.0156
BF5a-SSS6	p<0.0156	SSPul4-SSS6	p<0.0156
BF5a-SSPll5a	p<0.0312	SSPul4-SSPll3	p<0.0156
BF5b-BF6	p<0.0468	SSPul4-SSPll4	p<0.0156
BF5b-SSS4	p<0.0312	SSPul4-SSPll5a	p<0.0156
BF5b-SSS5a	p<0.0468	SSPul4-SSPll5b	p<0.0156
BF5b-SSS5b	p<0.0312	SSPul4-SSPll6	p<0.0156
BF5b-SSS6	p<0.0156	SSPul4-SSPul3	p<0.0156
SSS3-BF6	p<0.0156	SSPul4-SSPul5a	p<0.0156
SSS3-SSS6	p<0.0156	SSPul4-SSPul5b	p<0.0156
SSS4-BF6	p<0.0156	SSPul4-SSPul6	p<0.0156
SSS4-SSS6	p<0.0156	SSPul5a-BF3	p<0.0468
SSS5a-BF6	p<0.0156	SSPul5a-BF4	p<0.0468
SSS5a-SSS6	p<0.0156	SSPul5a-BF5a	p<0.0468
SSS5b-BF6	p<0.0156	SSPul5a-BF5b	p<0.0156
SSS5b-SSS6	p<0.0156	SSPul5a-BF6	p<0.0156
SSS6-BF6	p<0.0156	SSPul5a-SSS3	p<0.0156
SSPll3-BF5b	p<0.0156	SSPul5a-SSS4	p<0.0312
SSPll3-BF6	p<0.0156	SSPul5a-SSS5a	p<0.0156
SSPll3-SSS3	p<0.0468	SSPul5a-SSS5b	p<0.0312
SSPll3-SSS5b	p<0.0468	SSPul5a-SSS6	p<0.0156
SSPll3-SSS6	p<0.0156	SSPul5a-SSPll3	p<0.0312
SSPll3-SSPll5a	p<0.0312	SSPul5a-SSPll5a	p<0.0156
SSPll3-SSPul3	p<0.0156	SSPul5a-SSPll5b	p<0.0156
SSPll4-BF5b	p<0.0156	SSPul5b-BF4	p<0.0468
SSPll4-BF6	p<0.0156	SSPul5b-BF5a	p<0.0468
SSPll4-SSS3	p<0.0156	SSPul5b-BF5b	p<0.0156
SSPll4-SSS4	p<0.0312	SSPul5b-BF6	p<0.0156
SSPll4-SSS5a	p<0.0312	SSPul5b-SSS3	p<0.0468
SSPll4-SSS5b	p<0.0156	SSPul5b-SSS4	p<0.0468

(Table 8 continued)

Site	Significance	Site	Significance
SSPll4-SSS6	p<0.0156	SSPul5b-SSS5a	p<0.0468
SSPll4-SSPll3	p<0.0312	SSPul5b-SSS5b	p<0.0468
SSPll4-SSPll5a	p<0.0156	SSPul5b-SSS6	p<0.0156
SSPll4-SSPll5b	p<0.0312	SSPul5b-SSPll3	p<0.0468
SSPll5a-BF5b	p<0.0468	SSPul5b-SSPll5a	p<0.0156
SSPll5a-BF6	p<0.0156	SSPul5b-SSPll5b	p<0.0156
SSPll5a-SSS6	p<0.0156	SSPul6-BF5b	p<0.0156
SSPll5b-BF5b	p<0.0312	SSPul6-BF6	p<0.0156
SSPll5b-BF6	p<0.0156	SSPul6-SSS5b	p<0.0156
SSPll5b-SSS6	p<0.0156	SSPul6-SSS6	p<0.0156
SSPll5b-SSPll5a	p<0.0312	SSPul6-SSPll3	p<0.0468
SSPll6-BF5a	p<0.0468	SSPul6-SSPll5a	p<0.0156
SSPll6-BF5b	p<0.0156	SSPul6-SSPll5b	p<0.0156
SSPll6-BF6	p<0.0156	SSPll6-SSS3	p<0.0312
SSPll6-SSS4	p<0.0468	SSPll6-SSS5a	p<0.0468
SSPll6-SSS5b	p<0.0156		
SSPll6-SSS6	p<0.0156		
SSPll6-SSPll5a	p<0.0312		
SSPll6-SSPll5b	p<0.0156		
SSPll6-SSPll3	p<0.0468		

The first site listed is significantly more reactive for tGP than the second site. Significant site differences in levels of tGP within the layers of the neocortex were analyzed using a Wilcoxon Signed Ranks Test statistical analysis. N=12, df=2.

Hippocampal sites

In the hippocampus, the stratum laconosum moleculare of CA1 demonstrated the highest levels of available GP, followed by the stratum lacunosum moleculare of CA3. The stratum oriens of CA3, the polymorphic layer and the stratum moleculare of the dentate gyrus, both medial and lateral blades were also fairly reactive. The layers of both lateral and medial blades in the dentate gyrus except the granular layer were significantly more reactive than the stratum oriens of CA1 and CA3. Of these layers, the lateral blade molecular layer was the most reactive, more so than the molecular layer of the medial blade and the polymorphic layer. The stratum oriens of CA3 was significantly more reactive than CA1 stratum oriens and the stratum radiatum of both CA1 and CA3. CA1 stratum radiatum was significantly more reactive than CA3 stratum radiatum. As with the basal aGP results, the granular and pyramidal layers showed the least tGP reactivity, significantly less than all other layers within the hippocampus. CA1sr was also relatively unreactive, more reactive than the granular and pyramidal layers but less so than all other

sites examined in the hippocampus. Wilcoxon Signed Ranks Test results for the hippocampus are listed on Table 9.

Table 9

A Comparison of Total Glycogen Phosphorylase (tGP) Levels in the Hippocampus Using Wilcoxon Signed Ranks Test Statistical Analysis

Site	Significance	Site	Significance
CA1so-CA1sp	p<0.0156	CA3so-CA1so	p<0.0312
CA1so-CA1sr	p<0.0156	CA3so-CA1sp	p<0.0156
CA1so-Dglbsg	p<0.0156	CA3so-CA1sr	p<0.0156
CA1so-Dgmbsg	p<0.0156	CA3so-CA3sp	p<0.0156
CA1sr-CA1sp	p<0.0156	CA3so-CA3sr	p<0.0312
CA1sr- CA3sp	p<0.0156	CA3so-Dglbsg	p<0.0156
CA1sr- Dglbsg	p<0.0156	CA3so-Dgmbsg	p<0.0156
CA1sr- Dgmbsg	p<0.0156	CA3sr-CA1sp	p<0.0156
CA1slm-CA1so	p<0.0156	CA3sr-CA1sr	p<0.0156
CA1slm-CA1sp	p<0.0156	CA3sr-CA3sp	p<0.0156
CA1slm-CA1sr	p<0.0156	CA3sr-DGlbsg	p<0.0156
CA1slm-CA3so	p<0.0156	CA3sr-DGmbsg	p<0.0156
CA1slm-CA3sp	p<0.0156	CA3slm-CA1so	p<0.0156
CA1slm-CA3sr	p<0.0156	CA3slm-CA1sp	p<0.0156
CA1slm-CA3slm	p<0.0468	CA3slm-CA1sr	p<0.0156
CA1slm-Dglbmo	p<0.0312	CA3slm-CA3so	p<0.0156
CA1slm-Dglbsg	p<0.0156	CA3slm-CA3sp	p<0.0156
CA1slm-Dglbpo	p<0.0156	CA3slm-CA3sr	p<0.0156
CA1slm-Dgmgsg	p<0.0156	CA3slm-DGlbsg	p<0.0156
CA1slm-Dgmbmo	p<0.0156	CA3slm-DGlbpo	p<0.0156
Dglbmo-CA1so	p<0.0156	CA3slm-DGmbsg	p<0.0156
Dglbmo-CA1sp	p<0.0156	CA3slm-DGmbmo	p<0.0156
Dglbmo-CA1sr	p<0.0156	Dgmbmo-CA1so	p<0.0156
Dglbmo-CA3so	p<0.0156	Dgmbmo-CA1sp	p<0.0156
Dglbmo-CA3sp	p<0.0156	Dgmbmo-CA1sr	p<0.0156
Dglbmo-CA3sr	p<0.0156	Dgmbmo-CA3so	p<0.0312
Dglbmo-Dglbpo	p<0.0156	Dgmbmo-CA3sp	p<0.0156
Dglbmo-Dgmbsg	p<0.0156	Dgmbmo-CA3sr	p<0.0156
Dglbmo-Dmbmo	p<0.0156	Dgmbmo-Dglbsg	p<0.0156
DGlbsg-Dgmbsg	p<0.0312	Dgmbmo-Dglbpo	p<0.0468
Dglbpo-CA1so	p<0.0156	Dgmbmo-Dgmbsg	p<0.0156
Dglbpo-CA1sp	p<0.0156	Dglbpo-CA1sr	p<0.0156
Dglbpo-CA3so	p<0.0468	Dglbpo-CA3sp	p<0.0156
Dglbpo-CA3sr	p<0.0156	Dglbpo-Dglbsg	p<0.0156
Dglbpo-Dgmgsg	p<0.0156		

The first site listed is significantly more reactive for tGP than the second site. Significant site differences in levels of tGP within the layers of the hippocampus were analyzed using a Wilcoxon Signed Ranks Test statistical analysis. N=12, df=2.

Thalamic, diencephalic, striatal and fiber tract regions

Observations within the striatal, diencephalic and thalamic sites investigated for tGP staining were also similar to results found for aGP histochemistry. The medial habenula demonstrated the highest tGP reactivity, followed by the reticular nucleus of the

thalamus and the globus pallidus. These sites were significantly more reactive than all other sites in this grouping. The medial habenula was significantly more reactive than the reticular nucleus and the globus pallidus and the reticular nucleus was more reactive than the globus pallidus. The fornia fimbrix and the internal capsule were the least reactive sites. Even the laterodorsal and paraventricular nuclei of the thalamus and the caudate putamen, which were not found to be significantly more reactive than any other sites for aGP histochemistry were found to be more reactive for tGP staining than the internal capsule and fornia fimbrix. See Table 10.

Table 10

A Comparison of Total Glycogen Phosphorylase Levels in the Thalamus, Diencephalon and Striatum Using Wilcoxon Signed Ranks Test Statistical Analysis

Site	Significance	Site	Significance
CP-FF	p<0.0156	RT-CP	p<0.0156
CP-IC	p<0.0156	RT-FF	p<0.0156
GP-CP	p<0.0156	RT-GP	p<0.0156
GP-FF	p<0.0156	RT-LD	p<0.0156
GP-LD	p<0.0156	RT-PV	p<0.0156
GP-PVT	p<0.0156	RT-IC	p<0.0156
GP-IC	p<0.0156	MH-CP	p<0.0156
LD-FF	p<0.0156	MH-FF	p<0.0156
LD-IC	p<0.0156	MH-GP	p<0.0468
PVT-FF	p<0.0156	MH-LD	p<0.0312
PVT-IC	p<0.0156	MH-PV	p<0.0156
MH-IC	p<0.0156	MH-RT	p<0.0468

The first site is significantly more reactive for tGP than the second site. Significant site differences in levels of tGP within the thalamic, diencephalic and striatal sites investigated were analyzed using a Wilcoxon Signed Ranks Test statistical analysis. N=12, df=2.

Overall comparison of sites

A comparison of the neocortical, hippocampal, and thalamic, diencephalic, and striatal sites found that all neocortical sites were significantly more reactive than most hippocampal, thalamic, diencephalic and striatal sites except for the most reactive of these sites, namely the stratum lacunosum moleculare of CA1 and CA3, the medial habenula, globus pallidus and the reticular nucleus. All neocortical sites except layer 6 of

the secondary somatosensory cortex, for instance were significantly more reactive than the strata oriens, pyramidale and radiatum of CA1 and CA3 and the granular layer of both blades of the dentate gyrus. Most, if not all neocortical sites except layer 6 of the secondary somatosensory cortex were also significantly more reactive than the caudate putamen, the laterodorsal and paraventricular nucleus of the thalamus, the fornia fimbrix and the internal capsule.

Some neocortical sites such as lower limb layers 3/4 and 4 and all upper limb layers except 5b (3/4, 4, 5a and 6) were significantly more reactive than the polymorphic layer and the molecular layer of the medial and lateral blades of the dentate gyrus. Other neocortical sites such as all barrel fields layers except 5b, secondary somatosensory cortex layer 4 and lower limb layers 5b and 6 were only significantly darker than the polymorphic layer and the molecular layer of the medial blade of the dentate gyrus. As well, a few neocortical sites were only more reactive than the polymorphic layer (layers 5a and 5b of secondary somatosensory cortex and the polymorphic layer and the molecular layer of the medial blade of the dentate gyrus layer 5a of lower limb). None of the neocortical sites were more reactive than the stratum lacunosum moleculare, however, some neocortical sites were more reactive than the globus pallidus (all barrel fields layers except 5b, lower limb layers 4 and 6 and all upper limb layers).

The stratum lacunosum moleculare of CA1 and CA3 were signficantly more reactive than most layers of the secondary somatosensory cortex. The reticular nucleus of the thalamus, globus pallidus and medial habenula were significantly more reactive than most hippocampal sites (except the stratum lacunosum moleculare). The medial habenula was significantly darker than all neocortical and hippocampal sites except for the stratum lacunosum moleculare of CA1 and CA3. Most, if not all thalamic, diencephalic and

striatal sites were significantly more reactive than most strata within the hippocampus, including, oriens, pyramidale, radiatum, granulare, moleculare and even the polymorphic layer of the dentate gyrus. See Table 11. Thus, the neocortical regions appear to have a large residual capacity for GP activity that is reflected in the differences between basal and tGP activity.

Table 11

Basal Total Glycogen Phosphorylase (tGP) Wilcoxon Signed Rank Test Comparison of Neocortical, Hippocampal, Thalamic, Striatal and Diencephalic Sites

Site	Significance	Site	Significance
BF3-CA1so	p<0.0156	BF5b-CA1so	p<0.0156
BF3-CA1sp	p<0.0156	BF5b-CA1sp	p<0.0156
BF3-CA1sr	p<0.0156	BF5b-CA1sr	p<0.0156
BF3-CA3so	p<0.0156	BF5b-CA3sp	p<0.0156
BF3-CA3sp	p<0.0156	BF5b-CA3sr	p<0.0312
BF3-CA3sr	p<0.0156	BF5b-Dglbsg	p<0.0156
BF3-Dglbsg	p<0.0156	BF5b-Dgmbsg	p<0.0156
BF3-Dglbpo	p<0.0156	BF5b-CP	p<0.0156
BF3-Dgmbsg	p<0.0156	BF5b-FF	p<0.0156
BF3-Dgmbmo	p<0.0468	BF5b-IC	p<0.0156
BF3-CP	p<0.0156	BF6-CA1sp	p<0.0156
BF3-FF	p<0.0156	BF6-CA1sr	p<0.0468
BF3-GP	p<0.0468	BF6-CA3sp	p<0.0156
BF3-LD	p<0.0156	BF6-Dglbsg	p<0.0156
BF3-PVT	p<0.0156	BF6-Dgmbsg	p<0.0156
BF3-IC	p<0.0156	BF6-CP	p<0.0468
BF4-CA1so	p<0.0156	BF6-FF	p<0.0156
BF4-CA1sp	p<0.0156	BF6-GP	p<0.0312
BF4-CA1sr	p<0.0156	BF6-IC	p<0.0156
BF4-CA3so	p<0.0156	SSS3-CA1so	p<0.0156
BF4-CA3sp	p<0.0156	SSS3-CA1sp	p<0.0156
BF4-CA3sr	p<0.0156	SSS3-CA1sr	p<0.0156
BF4-Dglbsg	p<0.0156	SSS3-CA3so	p<0.0312
BF4-Dglbpo	p<0.0156	SSS3-CA3sp	p<0.0156
BF4-Dgmbsg	p<0.0156	SSS3-CA3sr	p<0.0156
BF4-Dgmbmo	p<0.0468	SSS3-Dglbsg	p<0.0156
BF4-CP	p<0.0156	SSS3-Dgmbsg	p<0.0156
BF4-FF	p<0.0156	SSS3-FF	p<0.0156
BF4-GP	p<0.0156	SSS3-LD	p<0.0468
BF4-LD	p<0.0156	SSS3-PVT	p<0.0312
BF4-PVT	p<0.0156	SSS3-IC	p<0.0156
BF4-IC	p<0.0156	SSS4-CA1so	p<0.0156
BF5a-CA1so	p<0.0156	SSS4-CA1sp	p<0.0156
BF5a-CA1sp	p<0.0156	SSS4-CA1sr	p<0.0156
BF5a-CA1sr	p<0.0156	SSS4-CA3so	p<0.0156
BF5a-CA3so	p<0.0156	SSS4-CA3sp	p<0.0156
BF5a-CA3sp	p<0.0156	SSS4-CA3sr	p<0.0156
BF5a-CA3sr	p<0.0156	SSS4-Dglbsg	p<0.0156
BF5a-Dglbsg	p<0.0156	SSS4-Dglbpo	p<0.0312
BF5a-Dglbpo	p<0.0156	SSS4-Dgmbsg	p<0.0156
BF5a-Dgmbsg	p<0.0156	SSS4-Dgmbmo	p<0.0312
BF5a-Dgmbmo	p<0.0312	SSS4-CP	p<0.0468
BF5a-CP	p<0.0156	SSS4-FF	p<0.0156
BF5a-FF	p<0.0156	SSS4-LD	p<0.0156
BF5a-GP	p<0.0156	SSS4-PVT	p<0.0156

(Table 11 continued)

Site	Significance	Site	Significance
BF5a-LD	p<0.0156	SSS4-IC	p<0.0156
BF5a-PVT	p<0.0156	SSS5a-CA1so	p<0.0156
BF5a-IC	p<0.0156	SSS5a-CA1sp	p<0.0156
SSS5b-CA1so	p<0.0156	SSS5a-CA1sr	p<0.0156
SSS5b-CA1sp	p<0.0156	SSS5a-CA3so	p<0.0156
SSS5b-CA1sr	p<0.0156	SSS5a-CA3sp	p<0.0156
SSS5b-CA3so	p<0.0156	SSS5a-CA3sr	p<0.0156
SSS5b-CA3sp	p<0.0156	SSS5a-Dglbsg	p<0.0156
SSS5b-CA3sr	p<0.0156	SSS5a-Dglbpo	p<0.0156
SSS5b-Dglbsg	p<0.0156	SSS5a-Dgmbsg	p<0.0156
SSS5b-Dglbpo	p<0.0156	SSS5a-CP	p<0.0312
SSS5b-Dgmbsg	p<0.0156	SSS5a-FF	p<0.0156
SSS5b-FF	p<0.0156	SSS5a-LD	p<0.0156
SSS5b-LD	p<0.0156	SSS5a-PVT	p<0.0156
SSS5b-PVT	p<0.0156	SSS5a-IC	p<0.0156
SSS5b-IC	p<0.0156	SSS6-CA1sp	p<0.0156
SSPII3-CA1so	p<0.0156	SSS6-CA1sr	p<0.0156
SSPII3-CA1sp	p<0.0156	SSS6-CA3sp	p<0.0156
SSPII3-CA1sr	p<0.0156	SSS6-Dglbsg	p<0.0156
SSPII3-CA3so	p<0.0156	SSS6-Dgmbsg	p<0.0156
SSPII3-CA3sp	p<0.0156	SSS6-FF	p<0.0156
SSPII3-CA3sr	p<0.0156	SSS6-IC	p<0.0156
SSPII3-Dglbmo	p<0.0468	SSPII4-CA1so	p<0.0156
SSPII3-Dglbsg	p<0.0156	SSPII4-CA1sp	p<0.0156
SSPII3-Dglbpo	p<0.0156	SSPII4-CA1sr	p<0.0156
SSPII3-Dgmbsg	p<0.0156	SSPII4-CA3so	p<0.0156
SSPII3-Dgmbmo	p<0.0156	SSPII4-CA3sp	p<0.0156
SSPII3-CP	p<0.0156	SSPII4-CA3sr	p<0.0156
SSPII3-FF	p<0.0156	SSPII4-Dglbmo	p<0.0156
SSPII3-LD	p<0.0156	SSPII4-Dglbsg	p<0.0156
SSPII3-PVT	p<0.0156	SSPII4-Dglbpo	p<0.0156
SSPII3-IC	p<0.0156	SSPII4-Dgmbsg	p<0.0156
SSPII5a-CA1so	p<0.0156	SSPII4-Dgmbmo	p<0.0156
SSPII5a-CA1sp	p<0.0156	SSPII4-CP	p<0.0156
SSPII5a-CA1sr	p<0.0156	SSPII4-FF	p<0.0156
SSPII5a-CA3so	p<0.0156	SSPII4-GP	p<0.0156
SSPII5a-CA3sp	p<0.0156	SSPII4-LD	p<0.0156
SSPII5a-CA3sr	p<0.0156	SSPII4-PVT	p<0.0156
SSPII5a-Dglbsg	p<0.0156	SSPII4-IC	p<0.0156
SSPII5a-Dglbpo	p<0.0156	SSPII5b-CA1so	p<0.0156
SSPII5a-Dgmbsg	p<0.0156	SSPII5b-CA1sp	p<0.0156
SSPII5a-CP	p<0.0312	SSPII5b-CA1sr	p<0.0156
SSPII5a-FF	p<0.0156	SSPII5b-CA3so	p<0.0156
SSPII5a-LD	p<0.0312	SSPII5b-CA3sp	p<0.0156
SSPII5a-PVT	p<0.0312	SSPII5b-CA3sr	p<0.0156
SSPII5a-IC	p<0.0156	SSPII5b-Dglbsg	p<0.0156
SSPII6-CA1so	p<0.0156	SSPII5b-Dglbpo	p<0.0156
SSPII6-CA1sp	p<0.0156	SSPII5b-IC	p<0.0156
SSPII6-CA1sr	p<0.0156	SSPII5b-Dgmbsg	p<0.0156
SSPII6-CA3so	p<0.0156	SSPII5b-Dgmbmo	p<0.0468
SSPII6-CA3sp	p<0.0156	SSPII5b-CP	p<0.0156
SSPII6-CA3sr	p<0.0156	SSPII5b-FF	p<0.0156
SSPII6-Dglbmo	p<0.0312	SSPII5b-LD	p<0.0312
SSPII6-Dglbsg	p<0.0156	SSPII5b-PVT	p<0.0156
SSPII6-Dglbpo	p<0.0156	SSPul3-CA1so	p<0.0156
SSPII6-Dgmbsg	p<0.0156	SSPul3-CA1sp	p<0.0156
SSPII6-Dgmbmo	p<0.0156	SSPul3-CA1sr	p<0.0156
SSPII6-CP	p<0.0156	SSPul3-CA3so	p<0.0156
SSPII6-FF	p<0.0156	SSPul3-CA3sp	p<0.0156
SSPII6-GP	p<0.0156	SSPul3-CA3sr	p<0.0156
SSPII6-LD	p<0.0156	SSPul3-Dglbmo	p<0.0156
SSPII6-PVT	p<0.0156	SSPul3-Dglbsg	p<0.0156
SSPII6-IC	p<0.0156	SSPul3-Dglbpo	p<0.0156
SSPul4-CA1so	p<0.0156	SSPul3-Dgmbsg	p<0.0156
SSPul4-CA1sp	p<0.0156	SSPul3-Dgmbmo	p<0.0156
SSPul4-CA1sr	p<0.0156	SSPul3-CP	p<0.0156
SSPul4-CA3so	p<0.0156	SSPul3-FF	p<0.0156
SSPul4-CA3sp	p<0.0156	SSPul3-GP	p<0.0156

(Table 11 continued)

Site	Significance	Site	Significance
SSPul4-CA3sr	p<0.0156	SSPul3-LD	p<0.0156
SSPul4-Dglbmo	p<0.0156	SSPul3-PVT	p<0.0156
SSPul4-Dglbsg	p<0.0156	SSPul3-IC	p<0.0156
SSPul4-Dglbpo	p<0.0156	SSPul5a-CA1so	p<0.0156
SSPul4-Dgmbsg	p<0.0156	SSPul5a-CA1sp	p<0.0156
SSPul4-Dgmbmo	p<0.0156	SSPul5a-CA1sr	p<0.0156
SSPul4-CP	p<0.0156	SSPul5a-CA3so	p<0.0156
SSPul4-FF	p<0.0156	SSPul5a-CA3sp	p<0.0156
SSPul4-GP	p<0.0156	SSPul5a-CA3sr	p<0.0156
SSPul4-LD	p<0.0156	SSPul5a-Dglbmo	p<0.0312
SSPul4-PVT	p<0.0156	SSPul5a-Dglbsg	p<0.0156
SSPul4-IC	p<0.0156	SSPul5a-Dglbpo	p<0.0156
SSPul5b-CA1so	p<0.0156	SSPul5a-Dgmbsg	p<0.0156
SSPul5b-CA1sp	p<0.0156	SSPul5a-Dgmbmo	p<0.0156
SSPul5b-CA1sr	p<0.0156	SSPul5a-CP	p<0.0156
SSPul5b-CA3so	p<0.0156	SSPul5a-FF	p<0.0156
SSPul5b-CA3sp	p<0.0156	SSPul5a-GP	p<0.0312
SSPul5b-CA3sr	p<0.0156	SSPul5a-LD	p<0.0156
SSPul5b-Dglbsg	p<0.0156	SSPul5a-PVT	p<0.0156
SSPul5b-Dglbpo	p<0.0156	SSPul5a-IC	p<0.0156
SSPul5b-Dgmbsg	p<0.0156	SSPul6-CA1so	p<0.0156
SSPul5b-Dgmbmo	p<0.0156	SSPul6-CA1sp	p<0.0156
SSPul5b-CP	p<0.0156	SSPul6-CA1sr	p<0.0156
SSPul5b-FF	p<0.0156	SSPul6-CA3so	p<0.0156
SSPul5b-GP	p<0.0312	SSPul6-CA3sp	p<0.0156
SSPul5b-LD	p<0.0156	SSPul6-CA3sr	p<0.0156
SSPul5b-PVT	p<0.0156	SSPul6-Dglbmo	p<0.0468
SSPul5b-IC	p<0.0156	SSPul6-Dglbsg	p<0.0156
CA1slm-BF5b	p<0.0156	SSPul6-Dglbpo	p<0.0156
CA1slm-SSS3	p<0.0156	SSPul6-Dgmbsg	p<0.0156
CA1slm-SSS4	p<0.015	SSPul6-Dgmbmo	p<0.0156
CA1slm-SSS5a	p<0.0156	SSPul6-CP	p<0.0156
CA1slm-SSS5b	p<0.0156	SSPul6-FF	p<0.0156
CA1slm-SSS6	p<0.0156	SSPul6-GP	p<0.0312
CA3slm-SSS3	p<0.0312	SSPul6-LD	p<0.0156
CA3slm-SSS4	p<0.0468	SSPul6-PVT	p<0.0156
CA3slm-SSS5b	p<0.0156	SSPul6-IC	p<0.0156
CA3slm-SSS6	p<0.0156	Dglbmo-SSS3	p<0.0468
CP-CA1so	p<0.0468	Dglbmo-SSS4	p<0.0468
CP-CA1sp	p<0.0156	Dglbmo-SSS5b	p<0.0312
CP-CA1sr	p<0.0156	Dglbmo-SSS6	p<0.0156
CP-CA3so	p<0.0156	Dglbpo-SSS3	p<0.0312
CP-CA3sp	p<0.0156	Dglbpo-SSS6	p<0.0312
CP-CA3sr	p<0.0468	Dgmbmo-SSS6	p<0.0156
CP-Dglbmo	p<0.0468	FF-Dglbsg	p<0.0468
CP-DGlbsg	p<0.0156	FF-Dgmbsg	p<0.0468
CP-DGmbsg	p<0.0156	GP-SSS6	p<0.0312
LD-CA1sp	p<0.0156	GP-CA1so	p<0.0156
LD-CA3sp	p<0.0156	GP-CA1sp	p<0.0156
LD-Dglbsg	p<0.0156	GP-CA1sr	p<0.0156
LD-Dgmbsg	p<0.0156	GP-CA3so	p<0.0156
PVT-CA1so	p<0.0468	GP-CA3sp	p<0.0156
PVT-CA1sp	p<0.0156	GP-CA3sr	p<0.0156
PVT-CA1sr	p<0.0156	GP-Dglbpo	p<0.0312
PVT-CA3sp	p<0.0156	GP-Dglbsg	p<0.0156
PVT-Dglbsg	p<0.0156	GP-Dgmbsg	p<0.0156
PVT-Dgmbsg	p<0.0156	GP-Dgmbmo	p<0.0468
MH-BF3	p<0.0312	RT-BF6	p<0.0312
MH-BF4	p<0.0312	RT-SSS4	p<0.0312
MH-BF5a	p<0.0156	RT-SSS5b	p<0.0156
MH-BF5b	p<0.0156	RT-SSS6	p<0.0156
MH-BF6	p<0.0156	RT-SSPul4	p<0.0468
MH-SSS3	p<0.0312	RT-CA1so	p<0.0156
MH-SSS4	p<0.0312	RT-CA1sp	p<0.0156
MH-SSS5a	p<0.0156	RT-CA1sr	p<0.0156
MH-SSS5b	p<0.0156	RT-CA3so	p<0.0156
MH-SSS6	p<0.0156	RT-CA3sp	p<0.0156
MH-SSPll3	p<0.0312	RT-CA3sr	p<0.0156

(Table 11 continued)

Site	Significance	Site	Significance	
MH-SSPll4		p<0.0312	RT-Dglbsg	p<0.0156
MH-SSPll5a		p<0.0312	RT-Dglbpo	p<0.0468
MH-SSPll5b		p<0.0468	RT-Dgmbsg	p<0.0156
MH-SSPll6		p<0.0312	RT-Dgmbmo	p<0.0468
MH-SSPul3		p<0.0312	MH-CA1so	p<0.0156
MH-SSPul4		p<0.0468	MH-CA1sp	p<0.0156
MH-SSPul5a		p<0.0312	MH-CA1sr	p<0.0156
MH-SSPul5b		p<0.0312	MH-CA3so	p<0.0156
MH-SSPul6		p<0.0312	MH-CA3sp	p<0.0156
MH-Dglbmo		p<0.0156	MH-CA3sr	p<0.0156
MH-Dglbpo		p<0.0156	MH-Dglbsg	p<0.0156
MH-Dgmbsg		p<0.0156	MH-Dgmbmo	p<0.0156

The first site listed is significantly more reactive for tGP than the second site. Significant site differences in levels of tGP between the three groupings: neocortical, hippocampal, and thalamic, diencephalic and striatal sites were analyzed using a Wilcoxon Signed Ranks Test statistical analysis. N=12, df=2.

Differences in aGP activity in response to experimental condition

Idazoxan treatment condition

Neocortical regions

T-test analysis of mean differences ($\alpha \leq 0.05$, df = 6, one-tailed t(crit) ≤ 1.943) revealed that idazoxan significantly increased levels of aGP fairly consistently in the lower layers of the neocortex. In the barrel field, layers 5a and 5b were significantly darker in the idazoxan hemisphere of the chimeric brain. In the lower limb portion of primary somatosensory cortex only layer 5a of was significantly darker. All layers of the upper limb portion of the primary somatosensory cortex (layers 3, 4, 5a, 5b and 6) were significantly darker on the idazoxan treated site. See Tables 12 and 13; Graph 1 and 2; and Images 10 and 11.

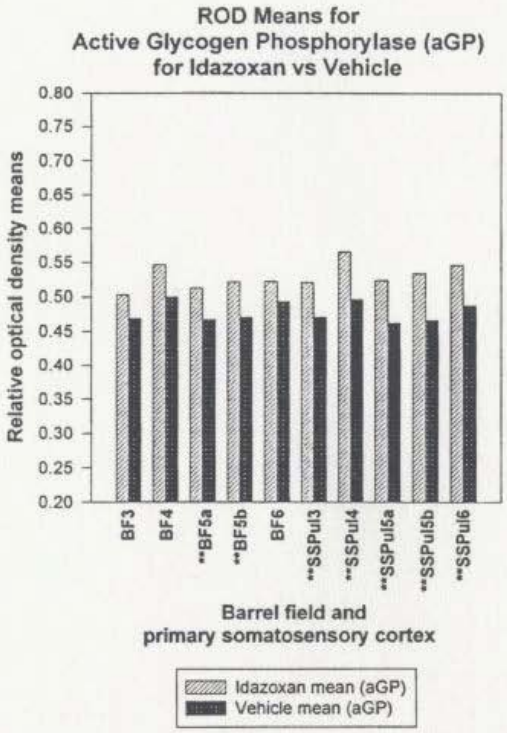

Graph 1. AGP levels for idazoxan- and vehicle-treated sites in the barrel fields and the upper limb portion of the primary somatosensory cortex. The double asterisks denote significant differences between the two groups. See Table 13 for α levels.

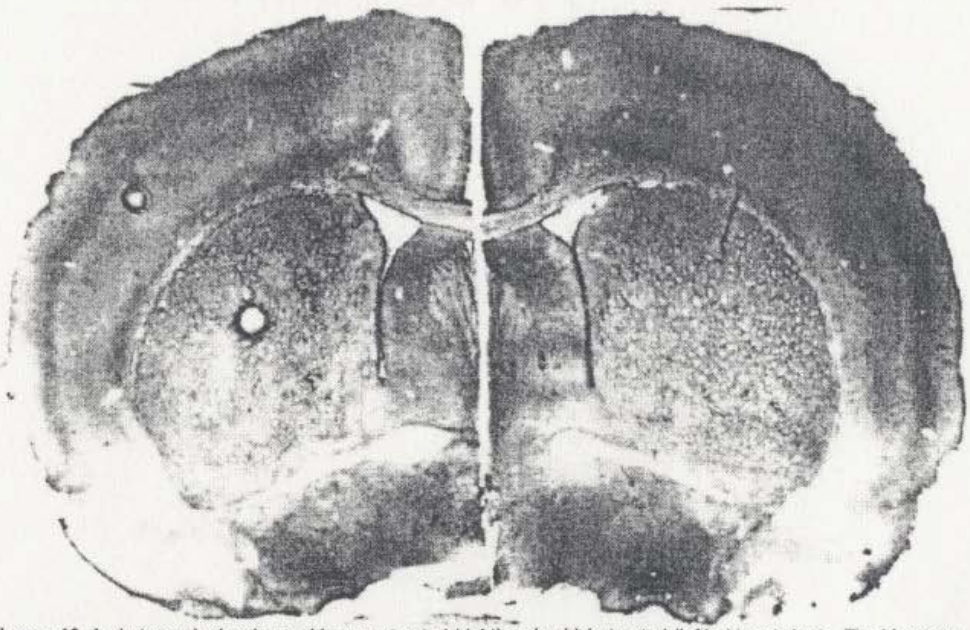

Image 10. A photograph showing an idazoxan-treated (right) and vehicle-treated (left) chimeric brain. The idazoxan half clearly demonstrates more intense aGP reactivity in various parts of the neocortex than the corresponding vehicle half. The corresponding tGP-stained section is provided in **Image 19**.

Table 12

A Comparison of Levels of Active Glycogen Phosphorylase Between Idazoxan-Treated and Vehicle-Treated Sites Using T-Test Statistical Analysis

Site	Mean Diff	Std Dev	SE	T-Test	Alpha (Sig)
BF3	0.035	0.066	0.025	1.403	
BF4	0.047	0.067	0.025	1.856	
BF5a	0.046	0.044	0.017	2.766	p<0.025
BF5b	0.051	0.042	0.016	3.213	p<0.001
BF6	0.029	0.061	0.023	1.258	
SSS3	0.019	0.075	0.028	0.670	
SSS4	0.026	0.084	0.032	0.819	
SSS5a	0.029	0.075	0.028	1.023	
SSS5b	0.039	0.062	0.023	1.664	
SSS6	0.030	0.072	0.027	1.103	
SSPll3	0.043	0.069	0.026	1.649	
SSPll4	0.033	0.066	0.025	1.323	
SSPll5a	0.032	0.051	0.019	1.660	
SSPll5b	0.037	0.041	0.015	2.388	p<0.050
SSPll6	0.032	0.048	0.018	1.764	
SSPul3	0.050	0.051	0.019	2.594	p<0.025
SSPul4	0.069	0.059	0.022	3.094	p<0.025
SSPul5a	0.062	0.049	0.019	3.348	p<0.010
SSPul5b	0.067	0.047	0.018	3.772	p<0.010
SSPul6	0.058	0.053	0.020	2.896	p<0.025
CA1so	0.062	0.052	0.020	3.155	p<0.010
CA1sp	0.039	0.039	0.015	2.646	p<0.025
CA1sr	0.043	0.036	0.014	3.161	p<0.010
CA1slm	0.071	0.063	0.024	2.982	p<0.025
CA3so	0.035	0.038	0.014	2.437	p<0.050
CA3sp	0.006	0.040	0.015	0.397	
CA3sr	0.046	0.030	0.011	4.057	p<0.005
CA3slm	0.074	0.066	0.025	2.967	p<0.025
Dglbmo	0.041	0.053	0.020	2.047	p<0.050
Dglbsg	0.023	0.042	0.016	1.449	
Dglbpo	0.041	0.051	0.019	2.127	p<0.050
Dgmbsg	0.022	0.024	0.009	2.426	p<0.050
Dgmbmo	-0.009	0.060	0.023	-0.397	
CP	0.022	0.022	0.008	2.646	p<0.025
FF	0.006	0.012	0.005	1.323	
GP	0.017	0.030	0.011	1.499	
LD	0.031	0.022	0.008	3.728	p<0.005
PVT	0.024	0.011	0.004	5.773	p<0.005
IC	0.005	0.035	0.013	0.378	
RT	0.038	0.033	0.012	3.047	p<0.025
MH	0.004	0.018	0.007	0.588	

One-tailed t-test of the difference between the idazoxan group means and the vehicle group means for aGP reactivity. α=0.050, df=6, t(crit)=1.943, SE(avr)=0.018.

Table 13

Summary of Active Glycogen Phosphorylase T-Test Results

Site	Ida aGP	Phe aGP	P&P aGP	Ida tGP	Phe tGP	P&P tGP
BF3			p<0.05			
BF4						
BF5a	p<0.025					
BF5b	p<0.001					
BF6						
SSS3		p<0.050				
SSS4						
SSS5a						
SSS5b						
SSS6						
SSPil3						
SSPil4						
SSPil5a						
SSPil5b	p<0.050					
SSPil6						
SSPui3	p<0.025	p<0.050				
SSPui4	p<0.025					
SSPui5a	p<0.010					
SSPui5b	p<0.010	p<0.050				
SSPui6	p<0.025	p<0.050				
CA1so	p<0.010					
CA1sp	p<0.025					
CA1sr	p<0.010					
CA1slm	p<0.025					
CA3so	p<0.050					
CA3sp					p<0.020	
CA3sr	p<0.005					
CA3slm	p<0.025					
Dgibmo	p<0.050					
Dgibsg						p<0.050
Dgibpo	p<0.050					p<0.050
Dgmbsg	p<0.050					
Dgmbmo						
CP	p<0.025					
FF						
GP						
LD	p<0.005					
PVT	p<0.005					
IC						
RT	p<0.025					
MH						

Sites showing significant drug-related effects for any of the three treatment conditions using a one-tailed t-test of the difference between the drug group means and the vehicle group means are listed. $\alpha = 0.050$, df = 6. T(cnt) = 1.943, SE(avr) = 0.018

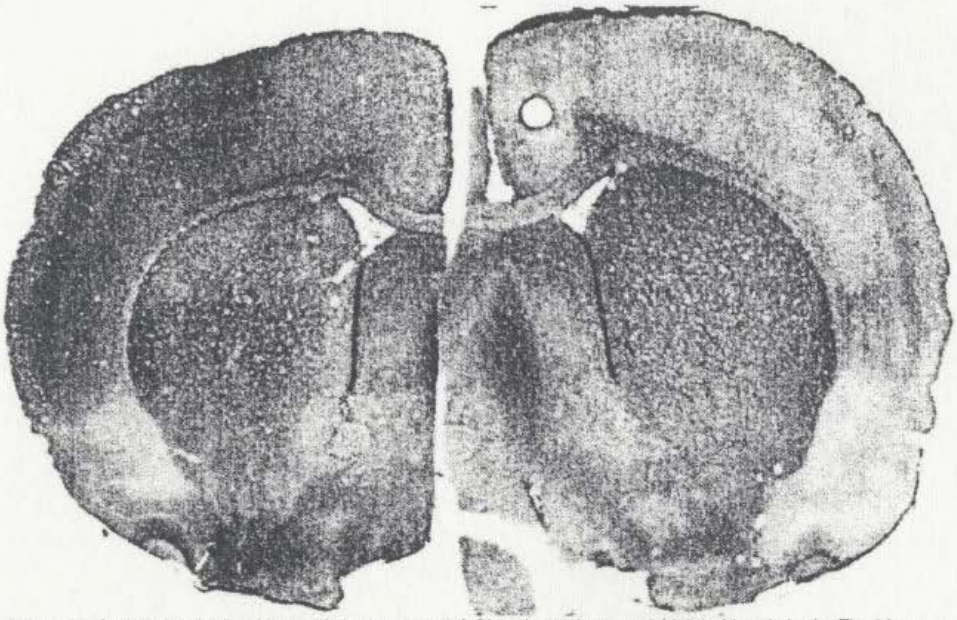

Image 11. A photograph showing an idazoxan-treated (left) and vehicle-treated (right) chimeric brain. The idazoxan half clearly demonstrates more intense aGP reactivity in various parts of the neocortex than the corresponding vehicle half. The corresponding tGP-stained section is provided in **Image 20**.

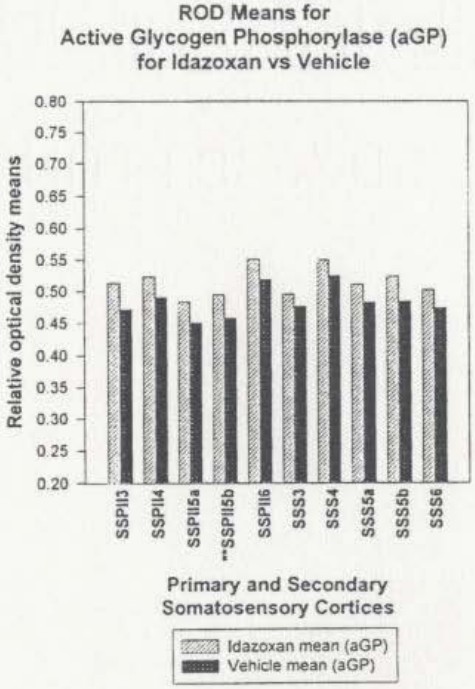

Graph 2. AGP levels for idazoxan- and vehicle-treated sites in the lower limb portion of the primary somatosensory cortex and in the secondary somatosensory cortex. The double asterisks denote significant differences between the two groups. See Table 13 for α levels.

Hippocampal regions

T-test analysis ($\alpha \leq 0.05$, df = 6, one-tailed t(crit) ≤ 1.943) of mean differences revealed that the effect of idazoxan was widespread in the hippocampus. All layers of CA1 demonstrated significantly darker ROD values on the idazoxan-treated site than corresponding vehicle sites. Similarly, all layers of CA3, with the exception of stratum pyramidale, were significantly darker on the idazoxan-treated site. In the dentate gyrus, the molecular layer and the polymorphic layer (this area corresponds roughly to the hilar region) of the lateral blade and granular layer of the medial blade showed significant enhancement of aGP activity by idazoxan administration. See Tables 12 and 13; Graph 3; and Images 12 and 13.

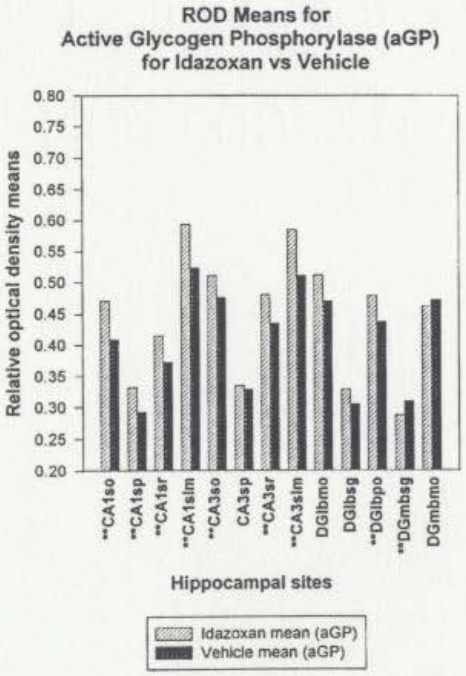

Graph 3. AGP levels for idazoxan- and vehicle-treated sites in the hippocampus. The double asterisks denote significant differences between the two groups. See Table 13 for α levels.

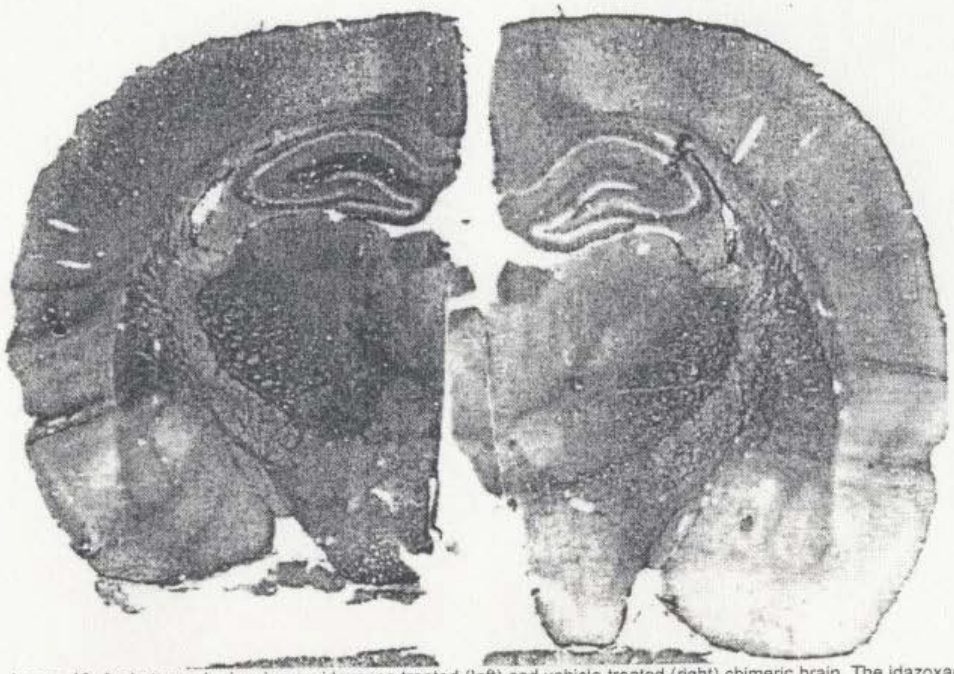

Image 12. A photograph showing an idazoxan-treated (left) and vehicle-treated (right) chimeric brain. The idazoxan half clearly demonstrates more intense aGP reactivity in the hippocampus and various parts of the thalamus, diencephalon and striatum than the corresponding vehicle half. The corresponding tGP-stained section is provided in **Image 21**.

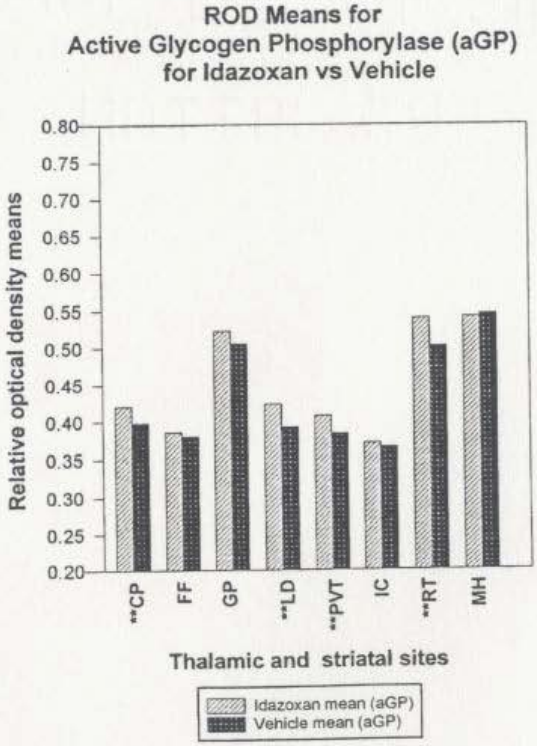

Graph 4. AGP levels for idazoxan- and vehicle-treated sites in thalamus, diencephalon and striatum. The double asterisks denote significant differences between the two groups. See Table 13 for α levels.

Thalamic and striatal regions

T-test analysis ($\alpha \leq 0.05$, df = 5, one-tailed t(crit) ≤ 2.015) of mean differences revealed that all thalamic sites measured showed significantly increased levels of aGP in response to idazoxan administration. One of the striatal sites measured also demonstrated significant GP activation, the caudate putamen. See Tables 12 and 13, Graph 4 and Images 12 and 13.

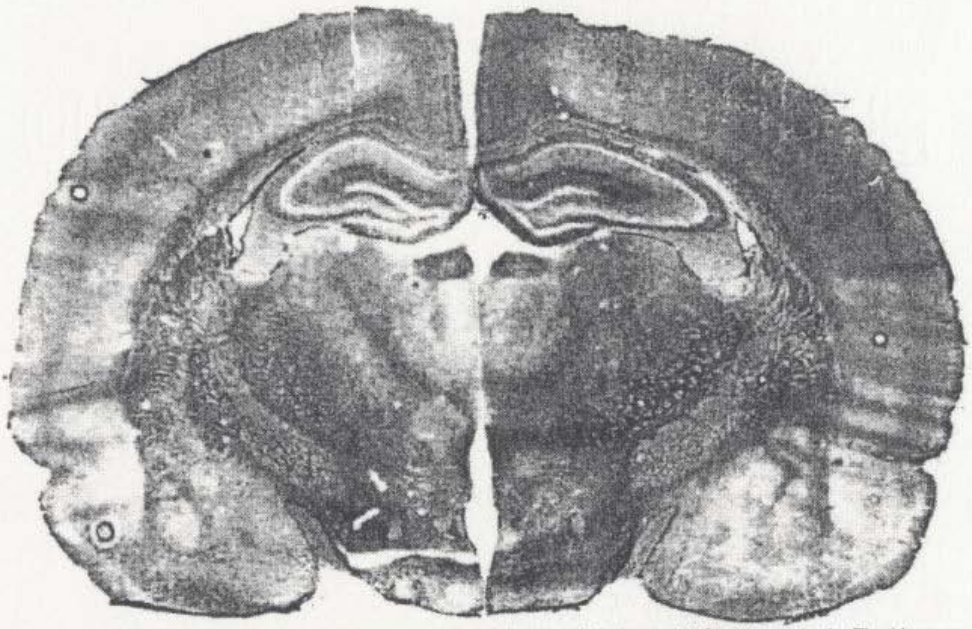

Image 13. A photograph showing an idazoxan-treated (right) and vehicle-treated (left) chimeric brain. The idazoxan half clearly demonstrates more intense aGP reactivity in the hippocampus and various parts of the thalamus, diencephalon and striatum than the corresponding vehicle half. The corresponding tGP-stained section is provided in **Image 22**.

Phenylephrine treatment condition

Neocortical and hippocampal sites

T-test analysis ($\alpha \leq 0.05$, df = 5, one-tailed t(crit) ≤ 2.015) of mean differences for neocortical sites found that layer 3 of the secondary somatosensory cortex, and layers 3, 5b and 6 of the upper limb portion of the primary somatosensory cortex showed increases in aGP levels in response to phenylephrine administration. No hippocampal sites showed significant differences in aGP in response to phenylephrine administration. Thalamic and striatal ROD measurements were not possible for this group because the sections were not sufficiently symmetrical to allow such measurements. See Tables 13 and 14; Graphs 5-7; and Images 14, 15 and 16.

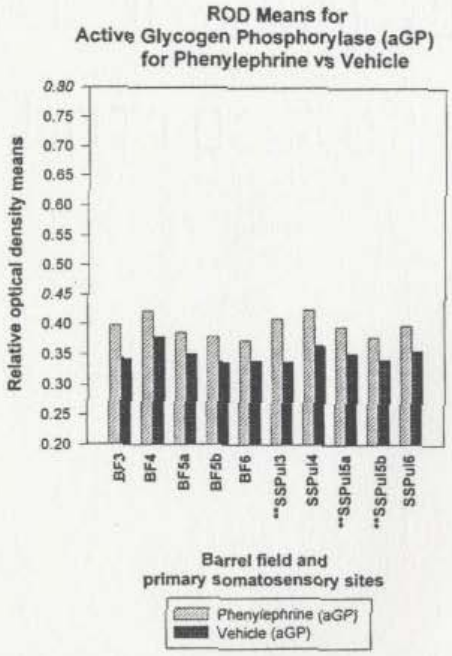

Graph 5. AGP levels for phenylephrine- and vehicle-treated sites in the barrel fields and lower limb portion of the primary somatosensory cortex. The double asterisks denote significant differences between the two groups. See Table 13 for α levels.

Table 14

A Comparison of Levels of Active Glycogen Phosphorylase Between Phenylephrine-Treated and Vehicle-Treated Sites Using T-Test Statistical Analysis

Site	Mean Diff	Std Dev	SE	T-Test	Alpha (Sig)
BF3	0.054	0.078	0.032	1.695	
BF4	0.044	0.071	0.029	1.518	
BF5a	0.035	0.064	0.026	1.339	
BF5b	0.040	0.056	0.023	1.749	
BF6	0.034	0.062	0.025	1.343	
SSS3	0.066	0.076	0.031	2.127	p<0.050
SSS4	0.051	0.074	0.030	1.688	
SSS5a	0.046	0.070	0.029	1.609	
SSS5b	0.033	0.069	0.028	1.171	
SSS6	0.022	0.063	0.026	0.855	
SSPll3	0.036	0.060	0.024	1.469	
SSPll4	0.019	0.051	0.021	0.912	
SSPll5a	0.006	0.040	0.016	0.367	
SSPll5b	0.007	0.030	0.012	0.571	
SSPll6	0.028	0.035	0.014	1.959	
SSPul3	0.072	0.075	0.031	2.351	p<0.050
SSPul4	0.060	0.075	0.031	1.959	
SSPul5a	0.044	0.065	0.027	1.658	
SSPul5b	0.037	0.042	0.017	2.157	p<0.050
SSPul6	0.042	0.050	0.020	2.057	p<0.050
CA1so	0.015	0.048	0.020	0.765	
CA1sp	0.005	0.062	0.025	0.198	
CA1sr	0.028	0.059	0.024	1.162	
CA1slm	0.051	0.095	0.039	1.315	
CA3so	0.055	0.099	0.040	1.361	
CA3sp	0.024	0.043	0.018	1.367	
CA3sr	0.038	0.073	0.030	1.275	
CA3slm	0.032	0.076	0.031	1.031	
Dglbmo	0.041	0.099	0.040	1.014	
Dglbsg	0.018	0.064	0.026	0.689	
Dglbpo	0.015	0.075	0.031	0.490	
Dgmbsg	0.027	0.067	0.027	0.987	
Dgmbmo	0.046	0.108	0.044	1.043	

One-tailed t-test of the difference between the phenylephrine group means and the vehicle group means for aGP reactivity. $\alpha = 0.050$, df = 5, t(cnt) = 2.015, SE(avr) = 0.027

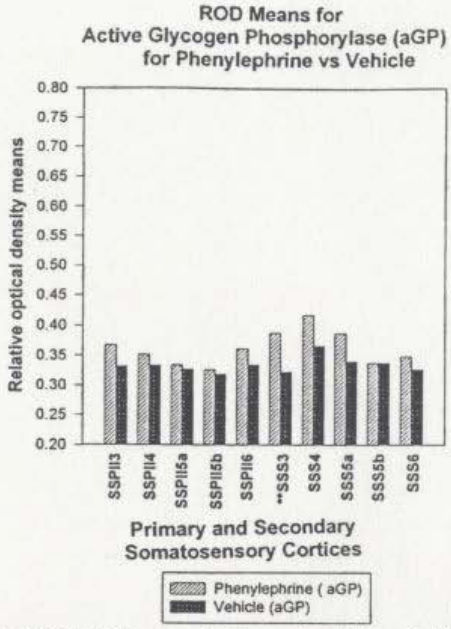

Graph 6. AGP levels for phenylephrine- and vehicle-treated sites in the lower limb portion of the primary somatosensory cortex and in the secondary somatosensory cortex. The double asterisks denote significant differences between the two groups. See Table 13 for α levels.

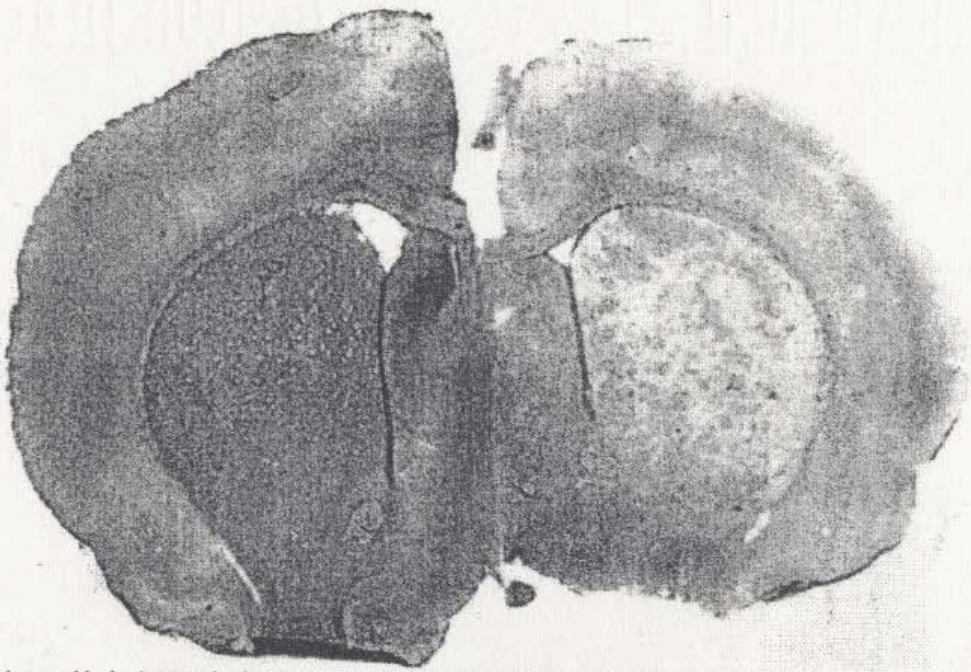

Image 14. A photograph showing a phenylephrine-treated (left) and vehicle-treated (right) chimeric brain. The phenylephrine half demonstrates more intense aGP reactivity in various parts of the neocortex than the corresponding vehicle half. The corresponding tGP-stained section is provided in **Image 23.**

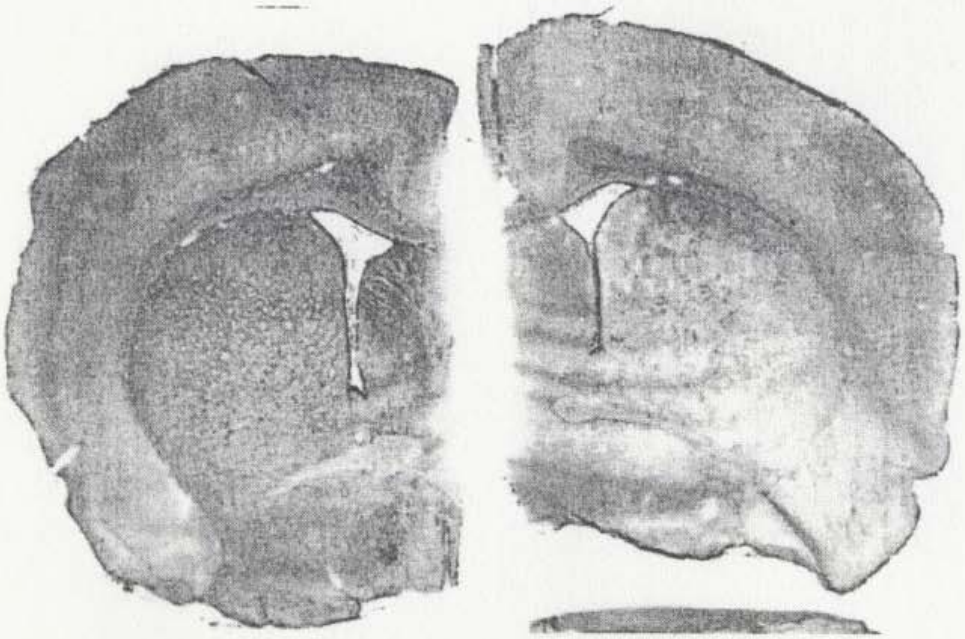

Image 15. A photograph showing a phenylephrine-treated (left) and vehicle-treated (right) chimeric brain. The phenylephrine half demonstrates more intense aGP reactivity in various parts of the neocortex than the corresponding vehicle half. The corresponding tGP-stained section is provided in **Image 24**.

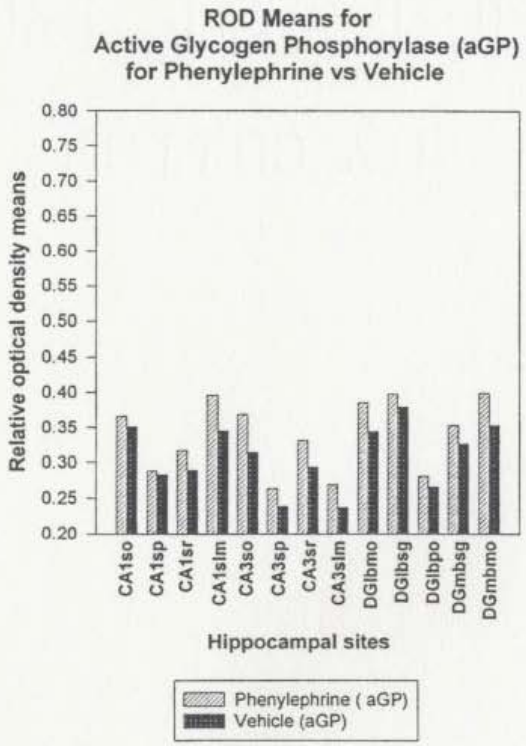

Graph 7. AGP levels for idazoxan- and vehicle-treated sites in the hippocampus. There were no significant differences found between the two groups.

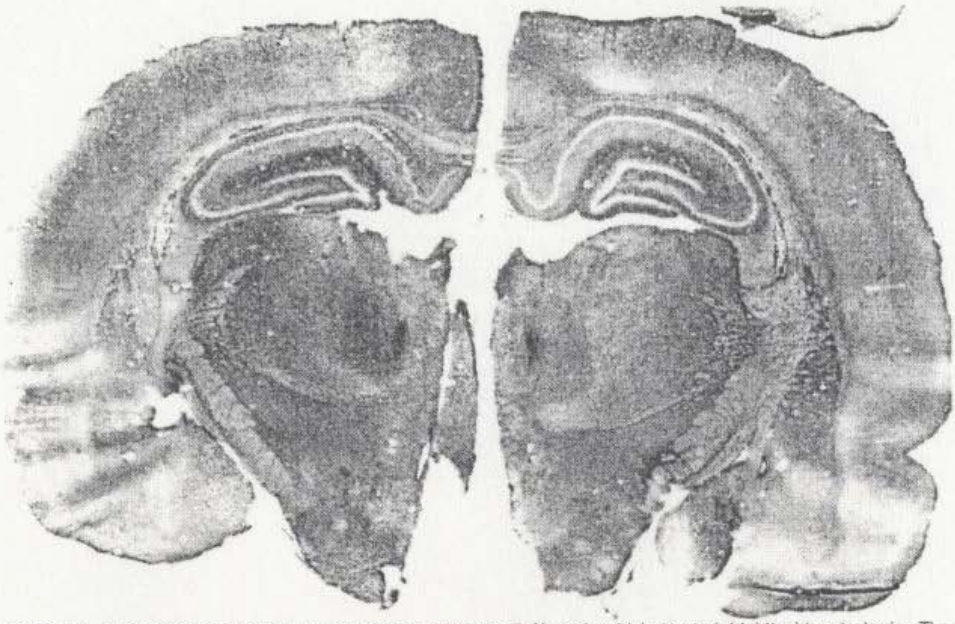

Image 16. A photograph showing a phenylephrine-treated (left) and vehicle-treated (right) chimeric brain. The phenylephrine half demonstrates more intense aGP reactivity in various parts of the hippocampus than the corresponding vehicle half, though no significant differences were found. The corresponding tGP-stained section is provided in **Image 25**.

Prazosin and propranolol treatment condition

Neocortical and hippocampal sites

T-test analysis ($\alpha \leq 0.05$, df = 5, one-tailed t(crit) ≤ 2.015) of mean differences for neocortical sites found only layer 3 of the barrel field showed significantly decreased aGP activity in response to prazosin and propranolol administration. No hippocampal sites showed a similar response to the application of the α1- and β-adrenergic antagonists.

See Tables 13 and 15; Graphs 8-10; and Images 17 and 18.

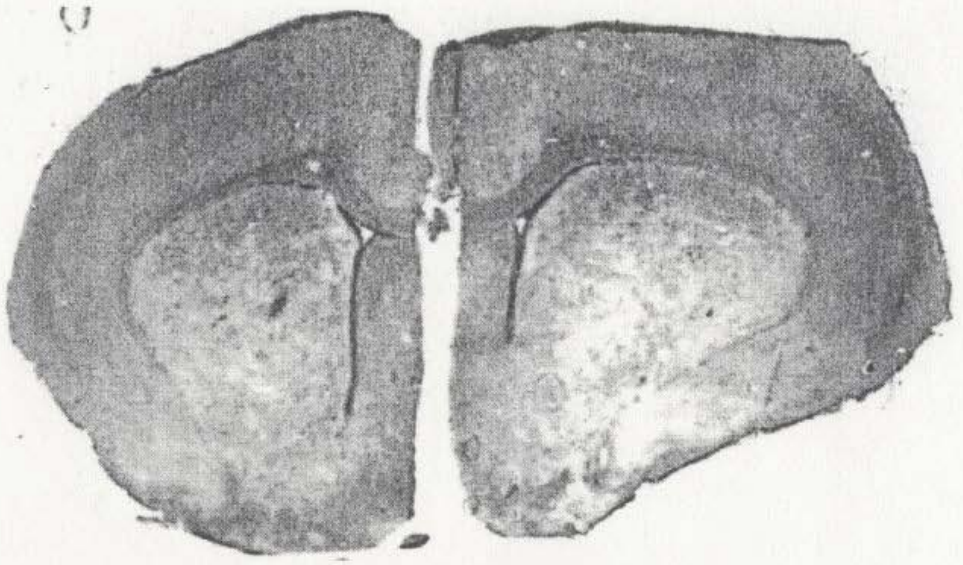

Image 17. A photograph showing a prazosin and propranolol-treated (left) and vehicle-treated (right) chimeric brain. The prazosin and propranolol half demonstrates less intense aGP reactivity in various parts of the neocortex than the corresponding vehicle half. The corresponding tGP-stained section is provided in **Image 26**.

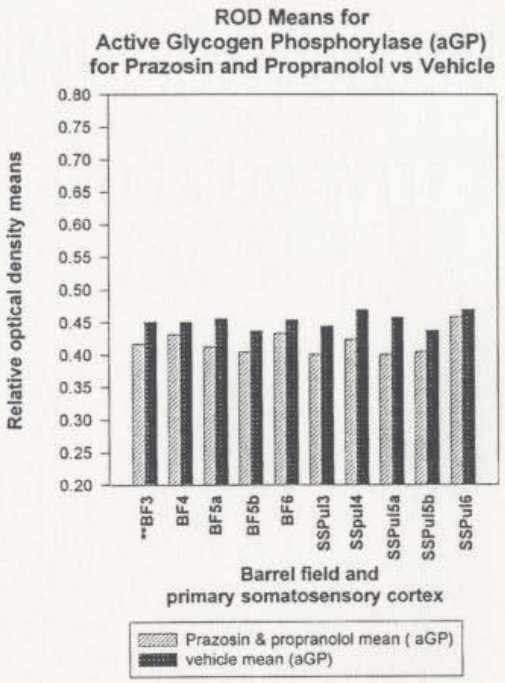

Graph 8. AGP levels for prazosin and propranolol- and vehicle-treated sites in the barrel fields and upper limb portion of the primary somatosensory cortex. The double asterisks denote significant differences between the two groups. See Table 13 for α levels.

Table 15

A Comparison of Levels of Active Glycogen Phosphorylase Between Prazosin and Propranolol-Treated and Vehicle-Treated Sites Using T-Test Statistical Analysis

Site	Mean Diff	Std Dev	SE	T-Test	Alpha (Sig)
BF3	-0.042	0.051	0.021	-2.017	p<0.05
BF4	-0.015	0.088	0.036	-0.417	
BF5a	-0.050	0.085	0.035	-1.441	
BF5b	-0.029	0.095	0.039	-0.748	
BF6	-0.034	0.074	0.030	-1.125	
SSS3	-0.033	0.066	0.027	-1.225	
SSS4	-0.026	0.117	0.048	-0.544	
SSS5a	-0.070	0.122	0.050	-1.405	
SSS5b	-0.061	0.118	0.048	-1.266	
SSS6	-0.049	0.086	0.035	-1.395	
SSPll3	0.015	0.082	0.033	0.448	
SSPll4	-0.008	0.065	0.027	-0.301	
SSPll5a	-0.008	0.062	0.025	-0.316	
SSPll5b	-0.015	0.051	0.021	-0.720	
SSPll6	0.025	0.074	0.030	0.827	
SSPul3	-0.014	0.090	0.037	-0.381	
SSPul4	-0.035	0.099	0.040	-0.866	
SSPul5a	-0.053	0.109	0.045	-1.191	
SSPul5b	-0.026	0.099	0.040	-0.643	
SSPul6	0.001	0.068	0.028	0.036	
CA1so	-0.032	0.083	0.034	-0.944	
CA1sp	-0.006	0.058	0.024	-0.253	
CA1sr	-0.010	0.055	0.022	-0.445	
CA1slm	-0.005	0.075	0.031	-0.163	
CA3so	-0.030	0.093	0.038	-0.790	
CA3sp	-0.020	0.072	0.029	-0.680	
CA3sr	-0.001	0.071	0.029	-0.034	
CA3slm	0.001	0.072	0.029	0.034	
Dglbmo	0.002	0.090	0.037	0.054	
Dglbsg	-0.008	0.063	0.026	-0.311	
Dglbpo	-0.002	0.048	0.020	-0.102	
Dgmbsg	0.006	0.061	0.025	0.241	
Dgmbmo	0.001	0.082	0.033	0.030	

One-tailed t-test of the difference between the prazosin and propranolol group means and the vehicle group means for aGP reactivity. $\alpha = 0.050$, df = 5, t(crit) = 2.015, SE(avr) = 0.032

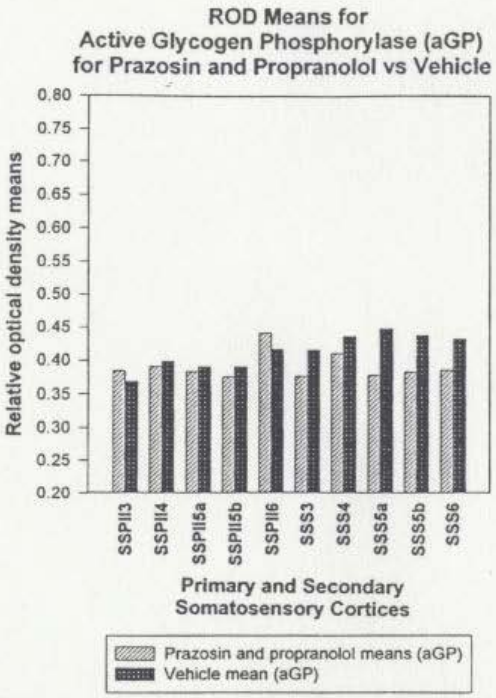

Graph 9. AGP levels for prazosin and propranolol- and vehicle-treated sites in the lower limb portion of the primary somatosensory cortex and the secondary somatosensory cortex. There were no significant differences between the two groups.

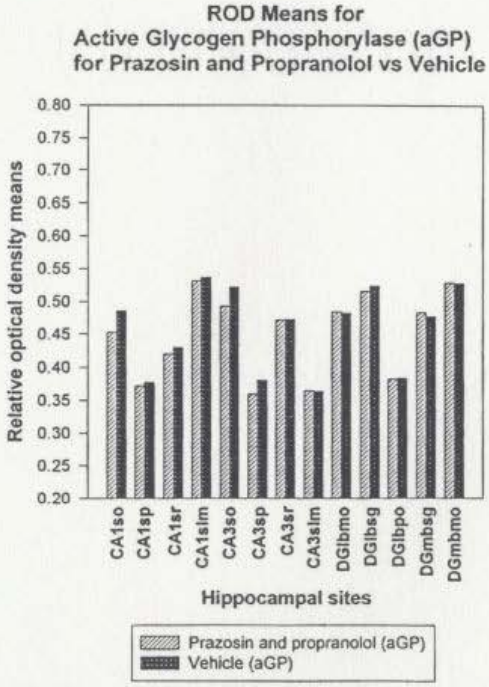

Graph 10. AGP levels for prazosin and propranolol- and vehicle-treated sites in the hippocampus. There were no significant differences between the two groups.

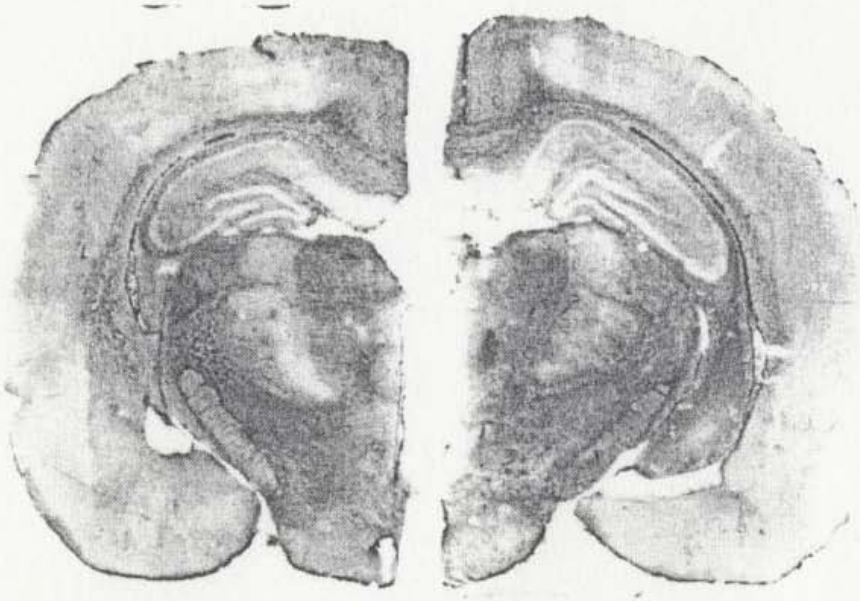

Image 18. A photograph showing a prazosin and propranolol-treated (right) and vehicle-treated (left) chimeric brain. The prazosin and propranolol half demonstrates less intense aGP reactivity in various parts of the *hippocampus than the corresponding vehicle half, though no significant differences were found.* The corresponding tGP-stained section is provided in **Image 27**.

Differences in tGP activity in response to experimental condition

Idazoxan treatment condition

Neocortical, hippocampal striatal and thalamic sites

T-test analysis ($\alpha \leq 0.05$, df = 6, two-tailed t(crit) ≤ 2.447) of mean differences for neocortical, hippocampal, thalamic and striatal sites showed no significant differences in levels of tGP between idazoxan-treated and vehicle-treated groups. See Table 16; Graphs 11 – 14; and Images 19 - 22.

Image 19. A photograph showing an idazoxan-treated (right) and vehicle-treated (left) chimeric brain. The difference in tGP staining intensity within the neocortex is not as salient as the difference in aGP staining for this chimeric brain (See **Image 10**). In fact no significant difference between the sites in the two halves was found for tGP reactivity.

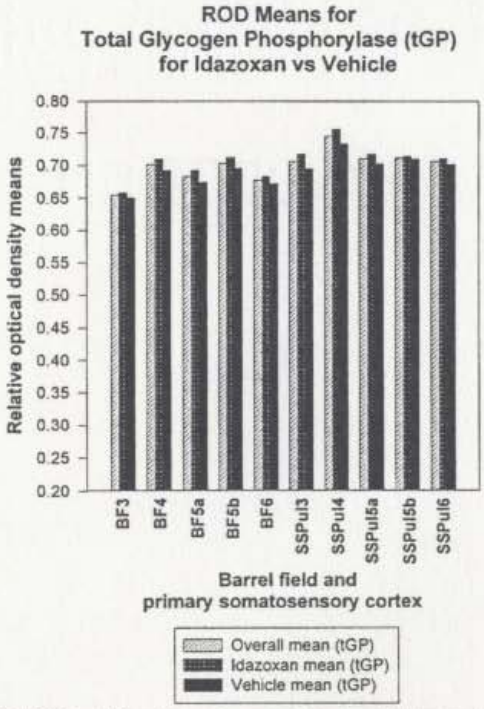

Graph 11. TGP levels for idazoxan- and vehicle-treated sites in the barrel field and lower limb portion of the primary somatosensory cortex. The mean of the idazoxan and vehicle tGP levels is also included since there were no significant differences between the two groups.

Table 16

A Comparison of Levels of Total Glycogen Phosphorylase Between Idazoxan-Treated and Vehicle-Treated Sites Using T-Test Statistical Analysis

Site	Mean Diff	Std Dev	SE	T-Test	Alpha (Sig)
BF3	0.008	0.040	0.015	0.529	
BF4	0.017	0.052	0.020	0.865	
BF5a	0.018	0.047	0.018	1.013	
BF5b	0.017	0.060	0.023	0.750	
BF6	0.011	0.045	0.017	0.647	
SSS3	0.018	0.043	0.016	1.108	
SSS4	0.016	0.043	0.016	0.985	
SSS5a	0.015	0.039	0.015	1.018	
SSS5b	0.013	0.039	0.015	0.882	
SSS6	0.008	0.038	0.014	0.557	
SSPll3	0.022	0.028	0.011	2.079	
SSPll4	0.011	0.037	0.014	0.787	
SSPll5a	0.006	0.039	0.015	0.407	
SSPll5b	0.006	0.030	0.011	0.529	
SSPll6	0.005	0.026	0.010	0.509	
SSPul3	0.023	0.037	0.014	1.645	
SSPul4	0.022	0.041	0.015	1.420	
SSPul5a	0.015	0.040	0.015	0.992	
SSPul5b	0.004	0.033	0.012	0.321	
SSPul6	0.009	0.034	0.013	0.700	
CA1so	0.009	0.026	0.010	0.916	
CA1sp	0.002	0.017	0.006	0.311	
CA1sr	0.009	0.032	0.012	0.744	
CA1slm	0.010	0.043	0.016	0.615	
CA3so	0.004	0.045	0.017	0.235	
CA3sp	0.006	0.048	0.018	0.331	
CA3sr	0.017	0.034	0.013	1.323	
CA3slm	0.011	0.044	0.017	0.662	
Dglbmo	0.007	0.027	0.010	0.686	
Dglbsg	0.002	0.026	0.010	0.204	
Dglbpo	0.002	0.025	0.009	0.212	
Dgmbsg	0	0.046	0.017	0.000	
Dgmbmo	-0.009	0.043	0.016	-0.554	
CP	0.012	0.076	0.029	0.418	
FF	0.002	0.043	0.016	0.123	
GP	0.004	0.051	0.019	0.208	
LD	0.008	0.045	0.017	0.470	
PVT	0.009	0.029	0.011	0.821	
IC	0.008	0.062	0.023	0.341	
RT	0.009	0.047	0.018	0.507	
MH	0.005	0.026	0.010	0.509	

Two-tailed t-test of the difference between the idazoxan group means and the vehicle group means for tGP reactivity. α=0.050, df = 6, t(crit) = 2.447, SE(avr) = 0.015

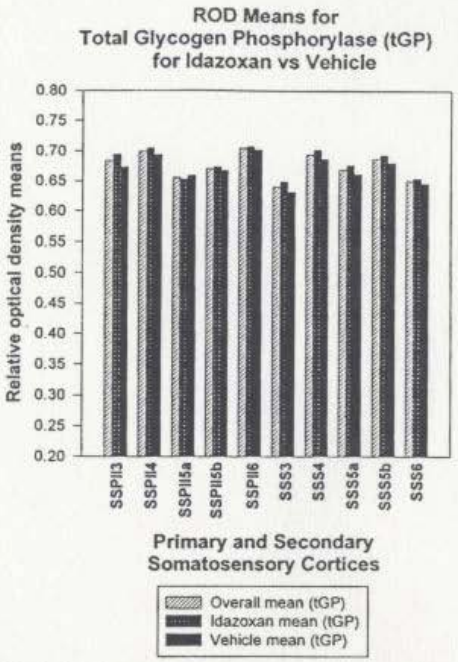

Graph 12. TGP levels for idazoxan- and vehicle-treated sites in the upper limb portion of the primary somatosensory cortex and the secondary somatosensory cortex. The mean of the idazoxan and vehicle tGP levels is also included since there were no significant differences between the two groups.

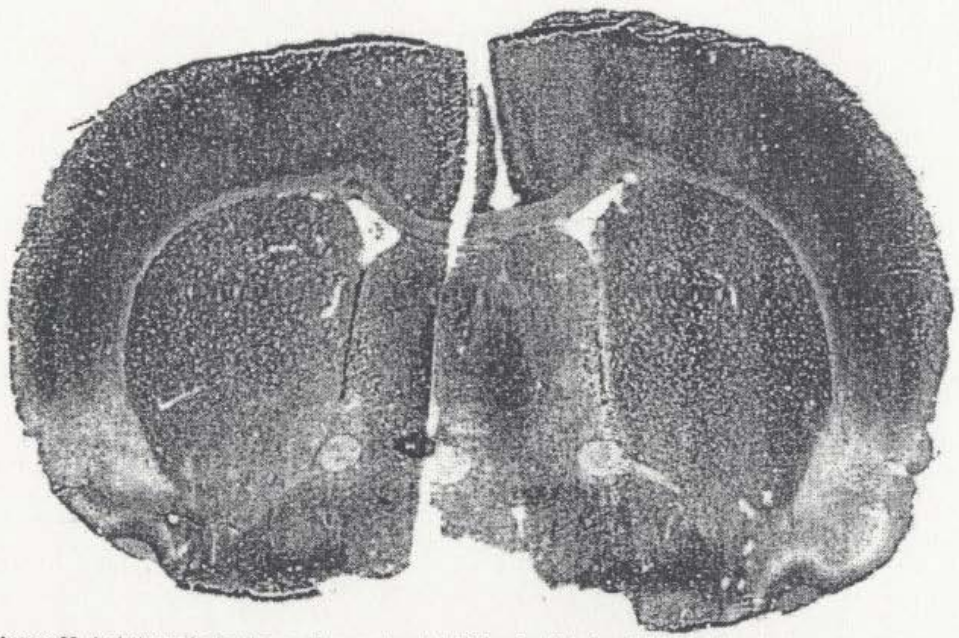

Image 20. A photograph showing an idazoxan-treated (left) and vehicle-treated (right) chimeric brain. The difference in tGP staining intensity within the neocortex for the two halves is not as visibly obvious as the difference in aGP staining for this chimeric brain (See **Image 11**).

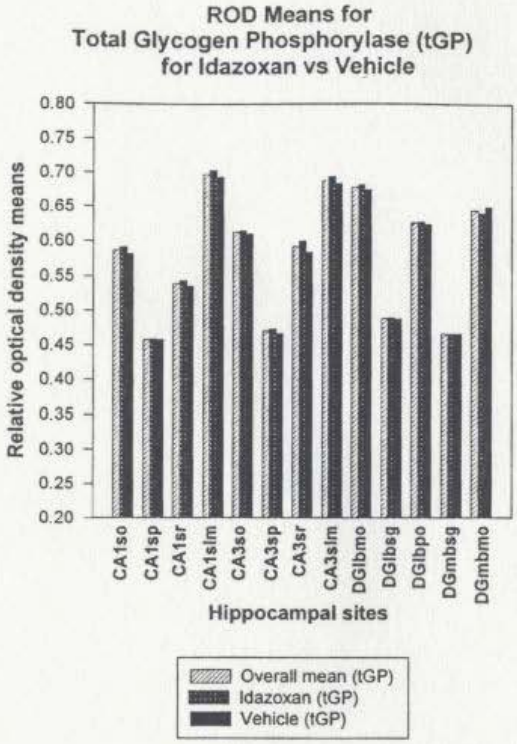

Graph 13. TGP levels for idazoxan- and vehicle-treated sites in the hippocampus. The mean of the idazoxan and vehicle tGP levels is also included since there were no significant differences between the two groups.

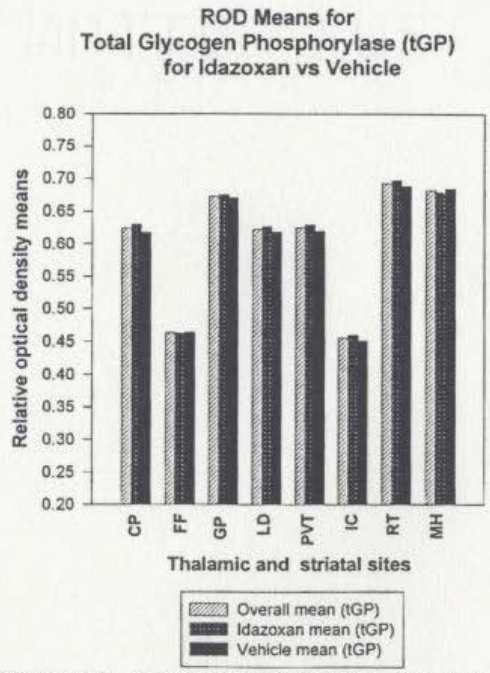

Graph 14. TGP levels for idazoxan- and vehicle-treated sites in the thalamus, diencephalon and striatum. The mean of the idazoxan and vehicle tGP levels is also included since there were no significant differences between the two groups.

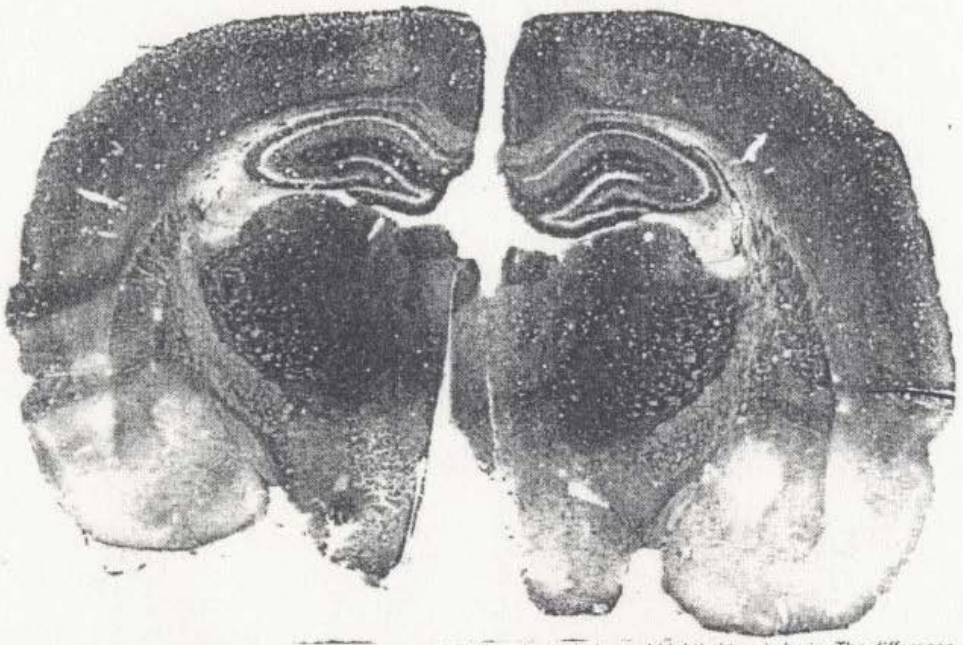

Image 21. A photograph showing an idazoxan-treated (left) and vehicle-treated (right) chimeric brain. The difference in tGP staining intensity within the hippocampus is not as visibly obvious to the naked eye as the difference in aGP staining for this chimeric brain (See **Image 12**).

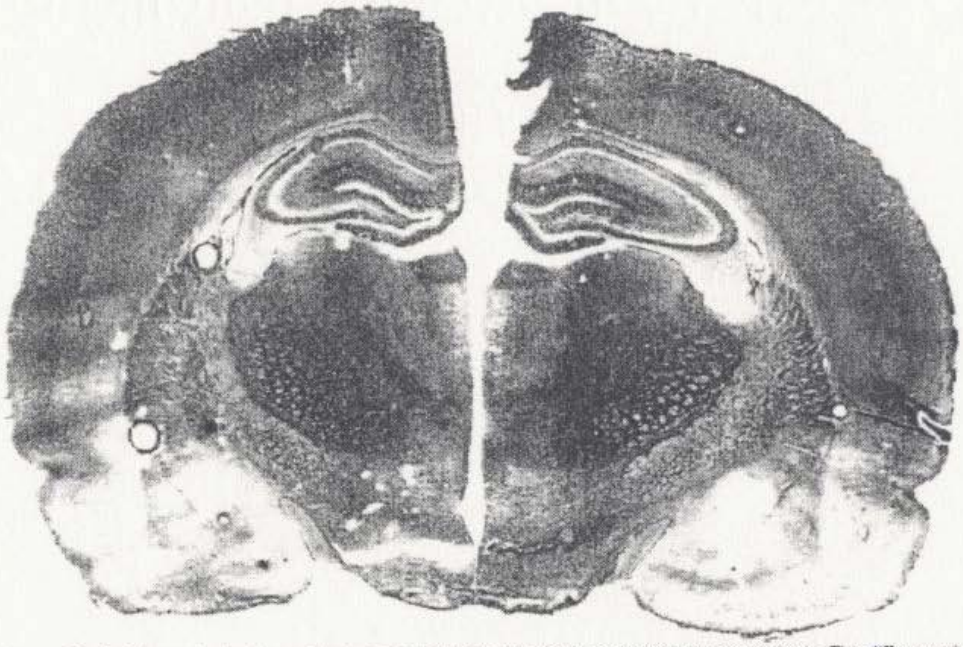

Image 22. A photograph showing an idazoxan-treated (left) and vehicle-treated (right) chimeric brain. The difference in tGP staining intensity within the hippocampus is not as salient as the difference in aGP staining for this chimeric brain (See **Image 13**).

Phenylephrine treatment condition

Neocortical and hippocampal sites

T-test analysis ($\alpha \leq 0.05$, df = 6, two-tailed t(crit) ≤ 2.447) of mean differences for neocortical, hippocampal, thalamic and striatal sites showed significant increases in levels of tGP in the phenylephrine-treated section of the chimeric brain only in the stratum pyramidale of CA3. In the phenylephrine group, no significant differences in levels of tGP were found in any of the sites examined except for the pyramidal layer of CA3. See Table 17; Graphs 15-17; and Images 23 – 25. Since this area contains little GP in the first place, it is likely that the pyramidal layer and the granular layer became significant because of the bleeding of the staining from surrounding areas which may have been measured by the standard box we used to record relative optical density. Our box size was at times too large and encompassed small sections of neighbouring tissue. See Image 11.

Table 17

A Comparison of Levels of Total Glycogen Phosphorylase Between Phenylephrine-Treated and Vehicle-Treated Sites Using T-Test Statistical Analysis

Site	Mean Diff	Std Dev	SE	T-Test	Alpha (Sig)
BF3	0.006	0.096	0.039	0.153	
BF4	0.018	0.082	0.033	0.538	
BF5a	0.022	0.066	0.027	0.816	
BF5b	0.012	0.071	0.029	0.414	
BF6	0.006	0.047	0.019	0.313	
SSS3	-0.006	0.084	0.034	-0.175	
SSS4	0.009	0.089	0.036	0.248	
SSS5a	0.008	0.079	0.032	0.248	
SSS5b	0.019	0.074	0.030	0.629	
SSS6	0.007	0.071	0.029	0.241	
SSPll3	0.004	0.049	0.020	0.200	
SSPll4	0.040	0.074	0.030	1.324	
SSPll5a	0.027	0.055	0.022	1.202	
SSPll5b	0.026	0.054	0.022	1.179	
SSPll6	0.007	0.041	0.017	0.418	
SSPul3	0.006	0.073	0.030	0.201	
SSPul4	0.003	0.072	0.029	0.102	
SSPul5a	0.009	0.063	0.026	0.350	
SSPul5b	0.012	0.042	0.017	0.700	
SSPul6	0.005	0.045	0.018	0.272	
CA1so	0.003	0.044	0.018	0.167	
CA1sp	0	0.036	0.015	0.000	
CA1sr	0.014	0.027	0.011	1.270	
CA1slm	-0.001	0.023	0.009	-0.106	
CA3so	0.017	0.023	0.009	1.810	
CA3sp	0.011	0.007	0.003	3.848	p<0.020
CA3sr	0.012	0.019	0.008	1.547	
CA3slm	0.023	0.022	0.009	2.560	
Dglbmo	0.019	0.041	0.017	1.135	
Dglbsg	0	0.037	0.015	0.000	
Dglbpo	0.019	0.032	0.013	1.454	
Dgmbsg	0.014	0.029	0.012	1.182	
Dgmbmo	0.008	0.038	0.016	0.516	

Two-tailed t-test of the difference between the phenylephrine group means and the vehicle group means for tGP reactivity. $\alpha = 0.050$, df = 5, t(cnt) = 2.571, SE(avr) = 0.021

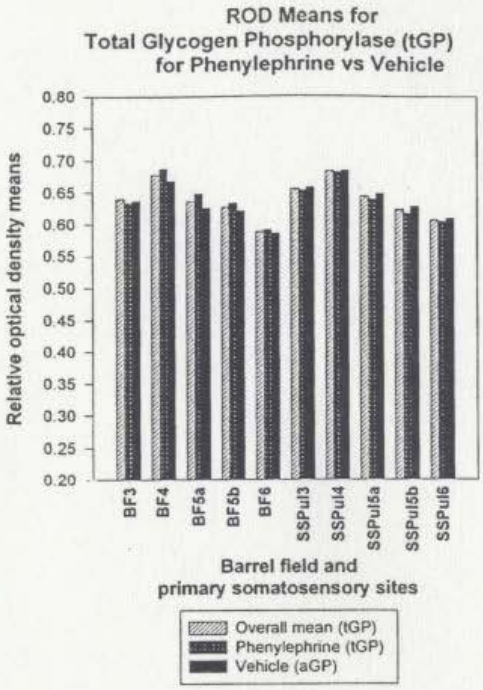

Graph 15. TGP levels for phenylephrine- and vehicle-treated sites in the barrel field and lower limb portion of the primary somatosensory cortex. The mean of the phenylephrine and vehicle tGP levels is also included since there were no significant differences between the two groups.

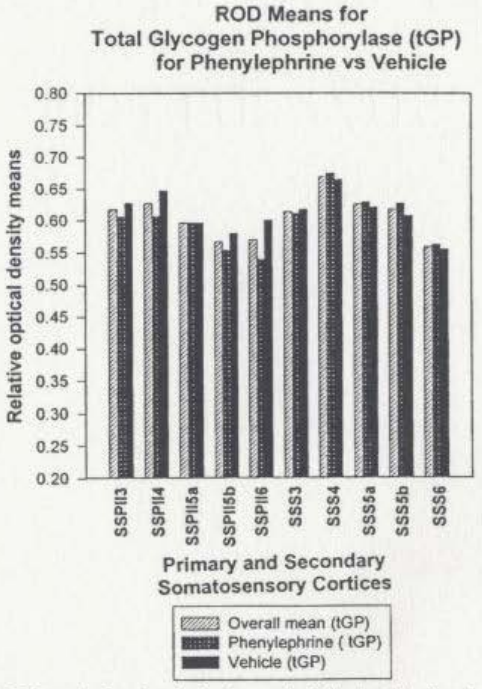

Graph 16. TGP levels for phenylephrine- and vehicle-treated sites in the upper limb portion of the primary somatosensory cortex and the secondary somatosensory cortex. The mean of the phenylephrine and vehicle tGP levels is also included since there were no significant differences between the two groups.

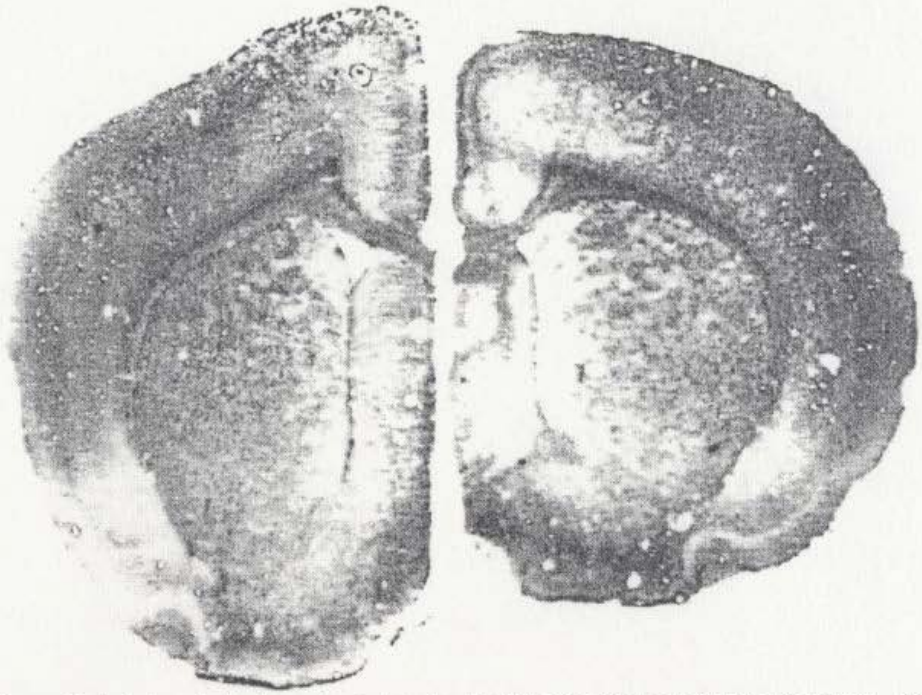

Image 23. A photograph showing a phenylephrine-treated (left) and vehicle-treated (right) chimeric brain. The difference in tGP staining intensity within the neocortex is not as salient as the difference in aGP staining for this same chimeric brain (See **Image 14**).

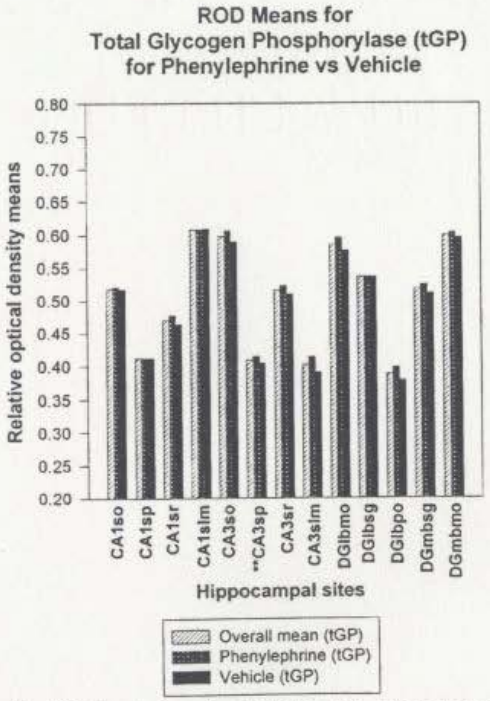

Graph 17. TGP levels for phenylephrine- and vehicle-treated sites in hippocampus. The double asterisks denote significance. See Table 16 for α levels. The mean of the phenylephrine and vehicle tGP levels is also included.

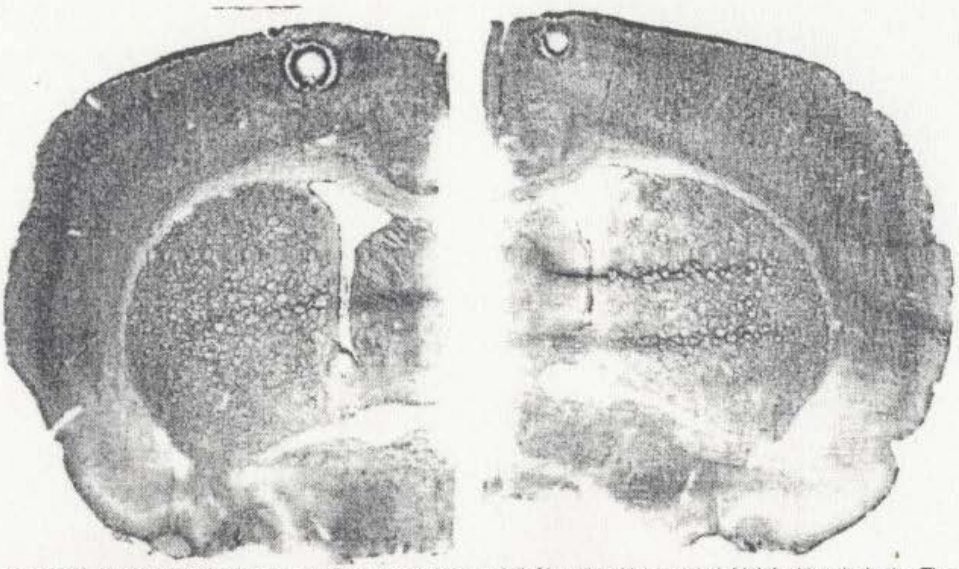

Image 24. A photograph showing a phenylephrine-treated (left) and vehicle-treated (right) chimeric brain. The difference in tGP staining intensity within the neocortex is not as salient as the difference in aGP staining for this same chimeric brain (See **Image 15**).

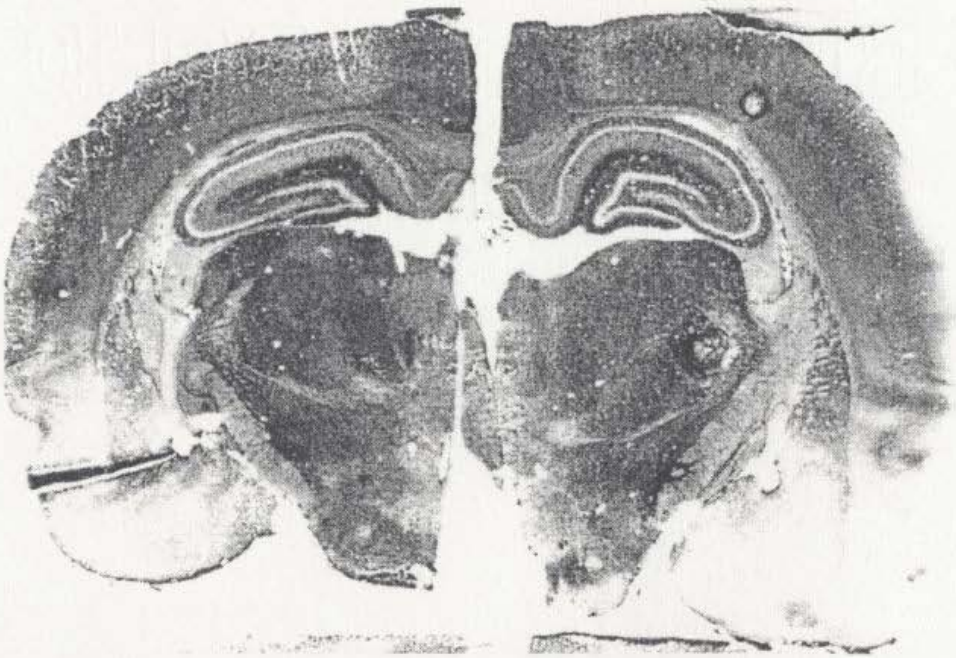

Image 25. A photograph showing an phenylephrine-treated (left) and vehicle-treated (right) chimeric brain. The difference in tGP staining intensity within the hippocampus is not as salient as the difference in aGP staining for this same chimeric brain (See **Image 16**).

Prazosin and propranolol treatment condition

Neocortical and hippocampal sites

T-test analysis ($\alpha \leq 0.05$, df = 6, two-tailed t(crit) ≤ 2.447) of mean differences for neocortical, hippocampal, thalamic and striatal sites showed significant decreases in levels of tGP in both the polymorphic layer of the lateral blade and the granular layer of the medial blade of the dentate gyrus in response to administration of prazosin and propranolol. No sites in the neocortex showed a similar decrease in tGP in response to the application of the α1- and β-adrenergic antagonists. See Table 18; Graphs 18-20; and Images 26 and 27. As with the pyramidal layer of CA3 in the phenylephrine group, the size of the box used to measure the granular layer may have been too large. See Image 13. Consequently some of the surrounding areas, the polymorphic and the molecular layers (both of which stain quite darkly for tGP), may have been included in the measurements for this region. The unexpected finding that the polymorphic layer of the dentate gyrus is significantly darker on the vehicle side, may be a statistical anomaly.

Table 18

A Comparison of Levels of Total Glycogen Phosphorylase Between Prazosin and Propranolol-Treated and Vehicle-Treated Sites Using T-Test Statistical Analysis

Site	Mean Diff	Std Dev	SE	T-Test	Alpha (Sig)
BF3	-0.011	0.079	0.032	-0.341	
BF4	-0.009	0.062	0.025	-0.356	
BF5a	-0.001	0.063	0.026	-0.039	
BF5b	0.011	0.068	0.028	0.396	
BF5	0.007	0.056	0.023	0.306	
SSS3	-0.037	0.074	0.030	-1.225	
SSS4	-0.017	0.064	0.026	-0.651	
SSS5a	-0.013	0.059	0.024	-0.540	
SSS5b	0.004	0.058	0.024	0.169	
SSS6	0.001	0.047	0.019	0.052	
SSPll3	-0.003	0.067	0.027	-0.110	
SSPll4	-0.018	0.049	0.020	-0.900	
SSPll5a	0	0.050	0.020	0.000	
SSPll5b	-0.015	0.050	0.020	-0.735	
SSPll6	-0.005	0.021	0.009	-0.583	
SSPul3	-0.014	0.039	0.016	-0.879	
SSPul4	-0.018	0.050	0.020	-0.882	
SSPul5a	-0.008	0.050	0.020	-0.392	
SSPul5b	-0.006	0.055	0.022	-0.267	
SSPul6	0.004	0.066	0.027	0.148	
CA1so	-0.008	0.029	0.012	-0.676	
CA1sp	0.023	0.046	0.019	1.225	
CA1sr	-0.007	0.023	0.009	-0.745	
CA1slm	-0.010	0.025	0.010	-0.980	
CA3so	-0.017	0.041	0.017	-1.015	
CA3sp	-0.041	0.044	0.018	-2.282	
CA3sr	-0.016	0.056	0.023	-0.700	
CA3slm	-0.037	0.045	0.018	-2.014	
Dglbmo	-0.019	0.046	0.019	-1.012	
Dglbsg	-0.048	0.043	0.018	-2.734	p<0.050
Dglbpo	-0.043	0.033	0.013	-3.191	p<0.050
Dgmbsg	-0.041	0.050	0.020	-2.008	
Dgmbmo	-0.025	0.040	0.016	-1.531	

Two-tailed t-test of the difference between the prazosin and propranolol group means and the vehicle group means for tGP reactivity. $\alpha = 0.050$, df = 5, t(crit) = 2.571, SE(avr) = 0.020

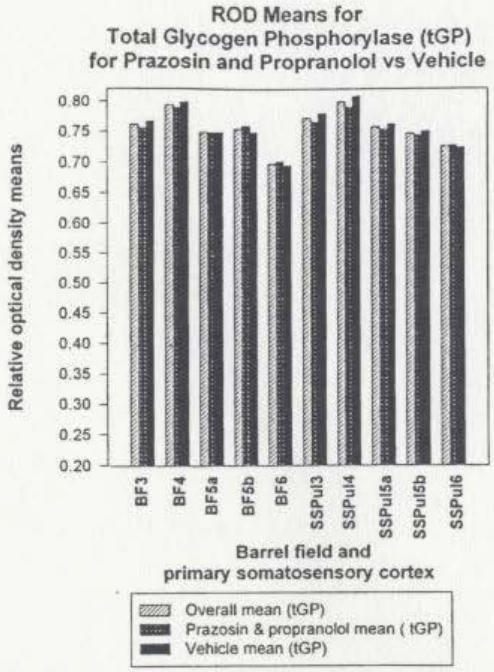

Graph 18. TGP levels for prazosin and propranolol- and vehicle-treated sites in the barrel field and upper limb portion of the primary somatosensory cortex. The mean of the phenylephrine and vehicle tGP levels is also included since there were no significant differences between the two groups.

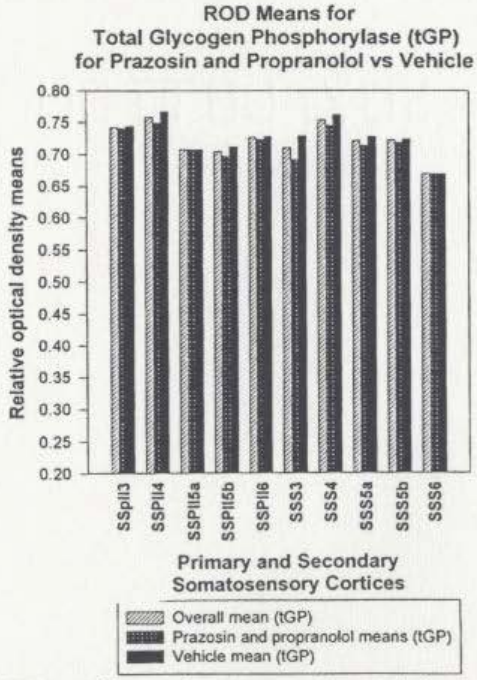

Graph 19. TGP levels for prazosin and propranolol- and vehicle-treated sites in the lower limb portion of the primary somatosensory cortex and the secondary somatosensory cortex. The mean of the phenylephrine and vehicle tGP levels is also included since there were no significant differences between the two groups.

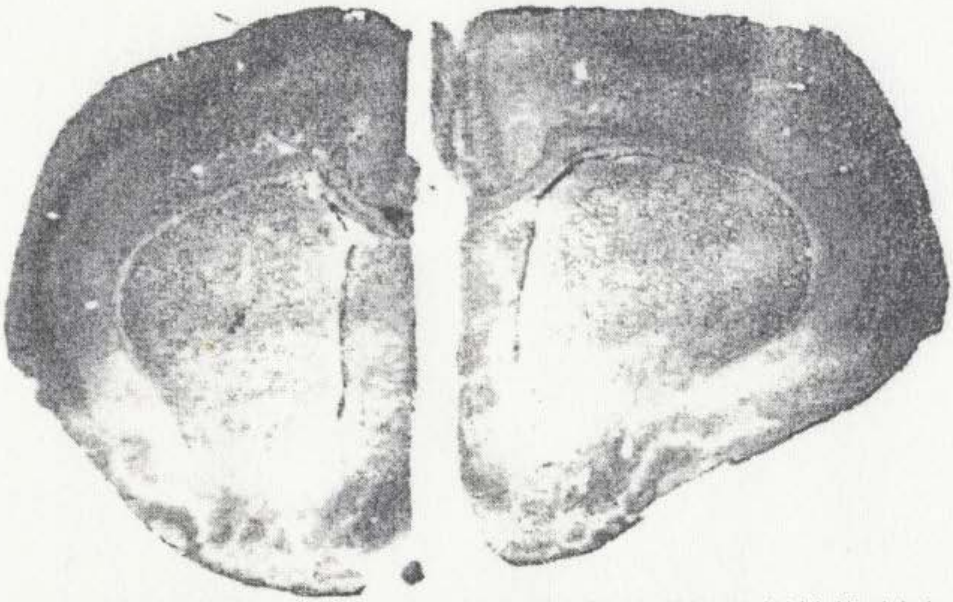

Image 26. A photograph showing a prazosin and propranolol-treated (left) and vehicle-treated (right) chimeric brain. The difference in tGP staining intensity within the neocortex is not as salient as the difference in aGP staining for this same chimeric brain (See **Image 17**).

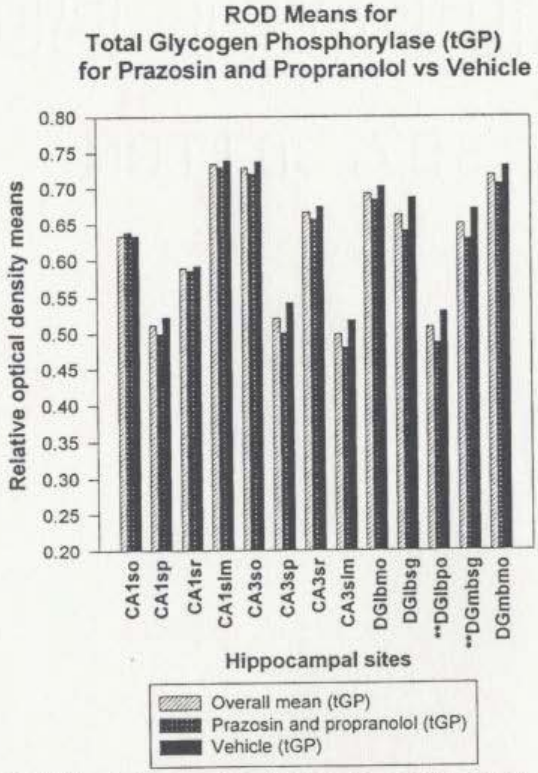

Graph 20. TGP levels for prazosin and propranolol- and vehicle-treated sites in the hippocampus. The mean of the phenylephrine and vehicle tGP levels is also included. The double asterisks denote significant differences between the two groups. See Table 17 for α levels.

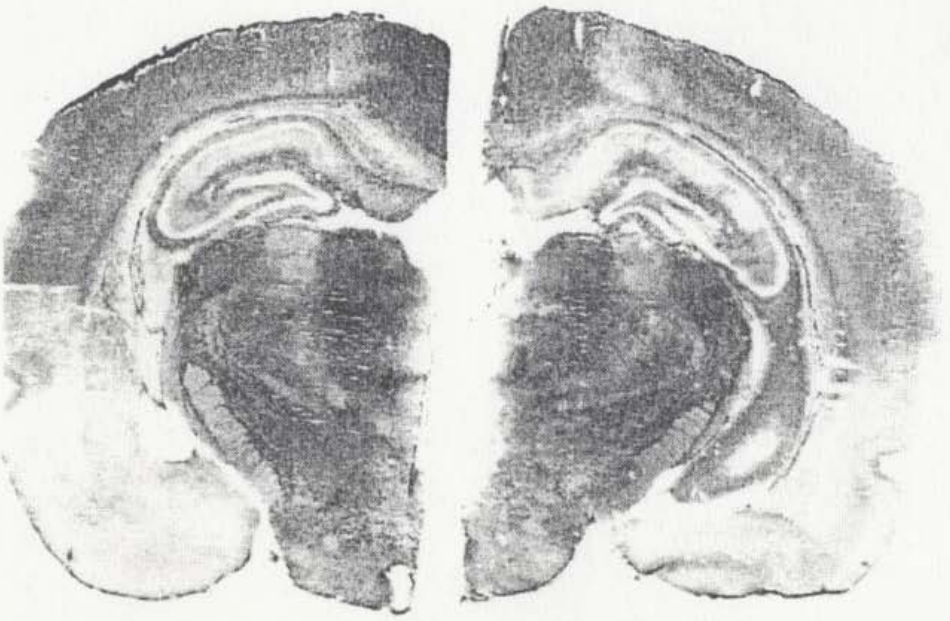

Image 27. A photograph showing a prazosin and propranolol-treated (right) and vehicle-treated (left) chimeric brain. The difference in tGP staining intensity within the hippocampus is not as salient as the difference in aGP staining for this same chimeric brain (**See Image 18**).

Patterns of basal aGP expressed as percent of total

These calculations were made to determine the amount of aGP present in nervous tissue under normal conditions (vehicle-treated) and the increase in levels of aGP in response to drug activation (drug-treated) calculated as percent of total. All brain sections were histochemically assessed for aGP and tGP and random slices from each chimeric brain were histochemically processed without immersion in incubation medium to determine the basal ROD value of tissue in the absence of aGP. As there were no significant differences in the ROD values obtained for the drug-treated versus vehicle-treated portions of the unincubated chimeric brains, an overall mean value was calculated (0.0951) which was subtracted from the mean tGP, drug aGP and vehicle aGP ROD values for each site to obtain corrected mean values. For each site the corrected vehicle-treated aGP value was divided by the corrected mean tGP value and multiplied by 100 to

determine the levels of aGP present normally as percent of total. As well, the corrected vehicle-treated aGP value was subtracted from the corrected drug-treated aGP value and the resulting number was divided by the corrected mean tGP value and multiplied by 100 to arrive at the percent of total increase/decrease in activation in response to drug application.

Levels of aGP activation calculated as percent of tGP

There is no ratio that can consistently describe the levels of basal aGP activity compared to tGP available. The ratio of basal aGP to tGP varies from region to region. Part of this inconsistency is likely due to the lability of the aGP measure, the fact that it is dependent on the activity of the rat prior to decapitation. Whatever behavioural or attentional stimulation the subject received prior to decapitation which selectively activated GP in brain, would be preserved by our histological procedures. The measure of basal aGP to tGP is expected to vary. One salient result remained consistent, however: basal GP activity is never activated beyond approximately 80% of total. See Tables 19-21. The highest level of basal GP activity estimated by our ROD analysis is 77% of total. Across the vehicle-treated sections of the three experimental conditions, the majority of the high basal level as percent of total values was found in the hippocampus. Within the idazoxan treatment condition, the medial habenula and the two fiber tracts demonstrated high levels of aGP in relation to all available GP. The following layers were consistently most activated as a percentage of total across the vehicle controls of the three treatment groups: layer 6 of all the neocortical regions measured and in the hippocampus, the molecular layer of the dentate gyrus and the stratum laconosum moleculare of the CA1 region.

Layer 6 of all neocortical regions studied appears to consistently exhibit the highest ratio of aGP activation as a percent of total. In the hippocampus there is a correspondence between the sites that showed the highest ratio of activation and those that exhibited the highest levels of basal aGP activity and tGP activity since the stratum laconosum moleculare of CA1 and the molecular layer of the dentate gyrus both show highest levels for basal aGP activity, tGP and basal aGP as percent of total.

In the idazoxan treatment condition, the levels of aGP present in the cortical regions studied ranged from 53% to 77% of total amount of aGP possible. See Table 19. The granular layer of the dentate gyrus lateral (hidden) blade contained the lowest level of aGP and the medial habenula contained the highest level of aGP as a percentage of total. The fornia fimbrix and the internal capsule show 77% and 75% activation of available GP. In one sense this is surprising because neither of these two sites contains very much GP to begin with. Whatever little GP is present in these sites must be in active form following exposure to noradrenergic activation. In comparison, other sites that demonstrated relatively low levels of tGP such as the pyramidal and granular layers of the hippocampus do not show a similar degree of aGP activation as percent of total. Indeed these tracts show the highest basal aGP as percent of total activity.

In the phenylephrine treatment condition, the lowest percent activation was 43% of total, demonstrated by layer 3/4 of upper limb of the primary somatosensory cortex and the secondary somatosensory cortex, and the stratum oriens of CA3. The highest percent activation of 64% was found in the granular layer of the lateral blade of the dentate gyrus. In general, the range of percent activation, for vehicle-treated sections in the phenylephrine treatment condition was about 10% lower than in the idazoxan treatment condition. This may reflect the quality of the slices following histochemical

processing rather than actual levels of GP. The staining intensity of the chimeric sections in the phenylephrine treatment condition was considerably lighter than those in the idazoxan treatment condition.

Table 19

Levels of Basal (Vehicle-Treated) and Idazoxan-Induced Increases in Active Glycogen Phosphorylase Calculated as Percent of Total Glycogen Phosphorylase

Site	A	B	C	D	E
BF3	0.559	0.408	0.374	66.8	6.2
BF4	0.606	0.451	0.405	66.7	7.7
BF5a	0.588	0.418	0.372	63.2	7.8
BF5b	0.609	0.427	0.376	61.7	8.4
BF6	0.583	0.427	0.399	68.4	4.9
SSS3	0.546	0.400	0.381	69.8	3.5
SSS4	0.600	0.455	0.429	71.6	4.3
SSS5a	0.574	0.417	0.387	67.5	5.1
SSS5b	0.592	0.428	0.389	65.7	6.6
SSS6	0.555	0.408	0.378	68.1	5.3
SSPll3	0.588	0.418	0.375	63.8	7.3
SSPll4	0.604	0.428	0.395	65.3	5.5
SSPll5a	0.561	0.388	0.356	63.4	5.7
SSPll5b	0.576	0.400	0.363	63.0	6.5
SSPll6	0.610	0.456	0.423	69.4	5.3
SSPul3	0.611	0.426	0.376	61.5	8.2
SSPul4	0.650	0.470	0.401	61.7	10.6
SSPul5a	0.615	0.429	0.366	59.5	10.1
SSPul5b	0.617	0.438	0.371	60.1	10.8
SSPul6	0.611	0.451	0.393	64.2	9.5
CA1so	0.491	0.376	0.314	64.0	12.6
CA1sp	0.363	0.237	0.198	54.5	10.8
CA1sr	0.444	0.320	0.277	62.3	9.8
CA1slm	0.602	0.499	0.428	71.1	11.7
CA3so	0.517	0.416	0.381	73.8	6.7
CA3sp	0.376	0.240	0.234	62.2	1.6
CA3sr	0.497	0.385	0.339	68.3	9.3
CA3slm	0.593	0.490	0.416	70.1	12.4
Dglbmo	0.582	0.416	0.375	64.5	7.0
Dglbsg	0.394	0.233	0.210	53.3	6.0
Dglbpo	0.530	0.384	0.342	64.6	7.8
Dgmbsg	0.371	0.192	0.214	57.6	-5.8
Dgmbmo	0.549	0.367	0.377	68.6	-1.7
CP	0.529	0.326	0.304	57.4	4.2
FF	0.369	0.291	0.285	77.3	1.6
GP	0.578	0.428	0.411	71.1	2.9
LD	0.527	0.329	0.297	56.4	5.9
PVT	0.530	0.312	0.289	54.5	4.5
IC	0.360	0.276	0.271	75.2	1.5
RT	0.598	0.444	0.406	68.0	6.3
MH	0.587	0.446	0.450	76.6	-0.6

Column A: corrected mean** tGP ROD values

Column B: corrected mean** aGP ROD values for idazoxan side

Column C: corrected mean** aGP ROD values for vehicle side

Column D: Basal aGP activity Calculated as Percent of tGP (Column C/Column A * 100)

Column E: Percent activation of aGP by idazoxan [(Column B - Column C)/Column A] * 100

**Please note that corrected means result from subtraction of the mean unincubated ROD value (staining in the absence of aGP or tGP reactivity).

Table 20

Levels of Basal (Vehicle-Treated) and Phenylephrine-Induced Increases in Active Glycogen Phosphorylase, Calculated as Percent of Total Glycogen Phosphorylase for Each Site

Site	A	B	C	D	E
BF3	0.541	0.303	0.249	46.0	10.0
BF4	0.583	0.327	0.284	48.6	7.5
BF5a	0.541	0.291	0.256	47.3	6.5
BF5b	0.532	0.284	0.244	45.8	7.5
BF6	0.492	0.279	0.245	49.8	7.0
SSS3	0.519	0.293	0.228	43.9	12.6
SSS4	0.575	0.322	0.271	47.1	9.0
SSS5a	0.530	0.292	0.246	46.3	8.7
SSS5b	0.522	0.243	0.243	46.5	0.0
SSS6	0.464	0.253	0.232	49.9	4.6
SSPll3	0.522	0.273	0.237	45.4	6.9
SSPll4	0.532	0.257	0.238	44.8	3.6
SSPll5a	0.487	0.239	0.233	47.7	1.3
SSPll5b	0.472	0.231	0.224	47.4	1.6
SSPll6	0.501	0.267	0.239	47.7	5.5
SSPul3	0.560	0.315	0.243	43.4	12.9
SSPul4	0.588	0.330	0.270	46.0	10.1
SSPul5a	0.548	0.302	0.258	47.1	8.0
SSPul5b	0.528	0.284	0.247	46.8	7.1
SSPul6	0.512	0.304	0.261	51.1	8.3
CA1so	0.423	0.271	0.256	60.4	3.5
CA1sp	0.316	0.193	0.187	59.2	1.6
CA1sr	0.375	0.222	0.193	51.5	7.5
CA1slm	0.513	0.301	0.250	48.6	10.0
CA3so	0.502	0.273	0.219	43.5	10.9
CA3sp	0.314	0.168	0.144	45.7	7.7
CA3sr	0.421	0.236	0.198	47.1	9.0
CA3slm	0.307	0.173	0.141	46.0	10.4
Dgibmo	0.491	0.290	0.249	50.7	8.4
Dglbsg	0.441	0.302	0.284	64.4	4.1
Dglbpo	0.293	0.185	0.170	58.2	5.1
Dgmbsg	0.422	0.258	0.231	54.8	6.3
Dgmbmo	0.504	0.304	0.258	51.2	9.1

Column A: corrected mean** tGP ROD values
Column B: corrected mean** aGP ROD values for phenylephrine side
Column C: corrected mean** aGP ROD values for vehicle side
Column D: Basal aGP activity Calculated as Percent of tGP (Column C/Column A * 100)
Column E: Percent activation of aGP by phenylephrine [(Column B - Column C)/Column A] * 100
**Please note that corrected means result from subtraction of the mean basal ROD value (staining in the absence of aGP or tGP reactivity).

Table 21

Levels of Basal (Vehicle-Treated) and Prazosin and Propranolol-Induced Decreases in Levels of Active Glycogen Phosphorylase Calculated as Percent of Total Glycogen Phosphorylase for Each Site

Site	A	B	C	D	E
BF3	0.666	0.307	0.342	51.4	-5.3
BF4	0.699	0.315	0.335	48.0	-3.0
BF5a	0.653	0.302	0.350	53.6	-7.3
BF5b	0.659	0.300	0.329	50.0	-4.4
BF6	0.602	0.323	0.352	58.5	-4.8
SSS3	0.615	0.282	0.321	52.1	-6.3
SSS4	0.659	0.315	0.341	51.7	-3.9
SSS5a	0.626	0.282	0.352	56.3	-11.2
SSS5b	0.627	0.288	0.342	54.6	-8.7
SSS6	0.575	0.291	0.337	58.6	-8.1
SSPll3	0.648	0.290	0.274	42.3	2.4
SSPll4	0.664	0.296	0.304	45.8	-1.2
SSPll5a	0.613	0.288	0.296	48.3	-1.2
SSPll5b	0.610	0.281	0.296	48.5	-2.5
SSPll6	0.631	0.346	0.321	50.9	4.0
SSPul3	0.677	0.301	0.315	46.5	-2.0
SSPul4	0.704	0.324	0.359	50.9	-5.0
SSPul5a	0.662	0.301	0.354	53.6	-8.1
SSPul5b	0.651	0.307	0.333	51.1	-4.0
SSPul6	0.629	0.355	0.354	56.2	0.2
CA1so	0.539	0.358	0.390	72.3	-5.9
CA1sp	0.416	0.277	0.283	68.0	-1.4
CA1sr	0.494	0.325	0.335	67.8	-2.0
CA1slm	0.639	0.436	0.441	69.1	-0.8
CA3so	0.634	0.397	0.427	67.4	-4.7
CA3sp	0.426	0.298	0.285	66.8	3.2
CA3sr	0.571	0.376	0.377	66.0	-0.2
CA3slm	0.403	0.270	0.268	66.5	0.4
Dglbmo	0.598	0.389	0.387	64.7	0.3
Dglbsg	0.569	0.421	0.429	75.4	-1.4
Dglbpo	0.413	0.287	0.289	70.0	-0.5
Dgmbsg	0.555	0.388	0.382	68.8	1.1
Dgmbmo	0.624	0.434	0.433	69.4	0.1

Column A: corrected mean** tGP ROD values
Column B: corrected mean** aGP ROD values for drug side
Column C: corrected mean** aGP ROD values for vehicle side
Column D: Basal aGP activity Calculated as Percent of tGP (Column C/Column A * 100)
Column E: Percent inhibition of aGP by prazosin and propranolol [(Column B - Column C)/Column A] * 100
**Please note that corrected means result from subtraction of the mean unincubated ROD value (staining in the absence of aGP or tGP reactivity)

The lowest percent activation demonstrated by vehicle-treated sites in the prazosin and propranolol treatment condition was found in layer 3/4 of the lower limb portion of the primary somatosensory cortex (42%). The highest percent activation was found in the granular layer of the lateral blade of the dentate gyrus (75%). The range of

percent activation values is much larger for this group than either of the other two. The possible reasons for this increased variability are discussed on p. 107.

Idazoxan versus vehicle (idazoxan-induced activation calculated as % of total)

The greatest activational increase from vehicle basal aGP activity was 12%. The range of activation, across various sites, by idazoxan was 1.6 - 12.6 %. Three sites in the hippocampus were activated most strongly by idazoxan: CA1 and CA3 stratum lacunosum moleculare, as well as CA1 stratum oriens. Levels of aGP in stratum lacunosum moleculare of CA1 increased 11%, CA1sp, SSPul4, SSPul5a and SSPul5b increased 10%, CA3 stratum radiatum, SSPul6 and CA1 stratum radiatum increased 9%, BF5b and SSPul3/4 increased 8% in response to idazoxan administration. See Table 19. These sites were found to demonstrate significantly higher levels of aGP ($\alpha \geq 0.05$, df = 6, t(crit) $\leq$ 1.943) on the idazoxan treated site compared to corresponding sites on the vehicle portion of the chimeric brain. Sites showing less than an 8% increase in aGP were not consistently significant. BF4, BF5a and SSPll3/4, for instance showed about 7% increase in aGP on the idazoxan treated sites, but of these sites only BF5a was found to be significantly more reactive on the idazoxan treated site ($\alpha \geq 0.05$, df = 6, t(crit) $\leq$ 1.943). See Tables 13 and 14. It may be possible the sites showing a 7% increase in aGP are significantly affected by the experimental condition, but that variability was high for these sites and so statistical significance was not found.

Several thalamic and striatal sites, which were activated less than 7%, did show significantly more aGP in the drug-treated condition than in the vehicle-treated condition (caudate putamen - 4.216, laterodorsal nucleus - 5.935, paraventricular nucleus - 4.457, and reticular nucleus - 6.323). Interestingly, idazoxan effects are not observed in the

medial habenula where highest basal aGP activity is found. This area may already be maximally active under normal conditions. See Table 19.

Phenylephrine versus vehicle (phenylephrine-induced activation)

The range of activation by phenylephrine was consistent with the range found for idazoxan, 0 - 12%. Maximal activation by phenylephrine occurred at site SSPul3 and SSS3 (12% increase). Phenylephrine also produced a greater than 10% increase in the following sites: BF3, SSPul4, CA1slm, CA3so and CA3slm. A greater than 8% increase in aGP levels was found in SSS4, SSS5a, SSPul6, CA3sr, Dglbmo and Dgmbmo. See Table 20. Of these listed sites, only SSS3, SSPul3and SSPul6 were found to demonstrate significantly higher levels of aGP in the phenylephrine treated site ($\alpha \geq 0.05$, df = 6, t(crit) $\leq$ 1.943). SSPul5b, which demonstrated only a 7% increase in aGP levels in response to drug treatment, was also found to contain significantly higher levels of aGP in the drug-treated side. Although idazoxan and phenylephrine both increased metabolism in neocortex and hippocampus, phenylephrine effects may not be reliable. The lack of agreement between these data and the idazoxan data may relate to the greater variability found in this group or to a selective effect of á1-AR activation. The methodological problems encountered with this experiment group, which likely contributed to the heightened variability will be discussed later.

Prazosin and propranolol versus vehicle (prazosin and propranolol-induced inhibition)

Administration of prazosin and propranolol combined decreased the reactivity of basal aGP by a range of 0 to 11%. The greatest decreases (> 7% decrease) occurred in SSS5a (11%), SSS5b, SSS6, SSPul5a (8%). See Table 21. The effects of the double

blockers seem to be predominantly within the region of the neocortex, specifically the secondary somatosensory cortex, and even more specifically, layer 5a. None of these sites were found to demonstrate significantly less aGP following application of prazosin and propranolol ($\alpha \geq 0.05$, df = 6, t(crit) $\leq$ 1.943). While noradrenergic â1 and â1/2-ARs may contribute little or nothing to the maintenance of basal aGP it should be noted that there was large variability in this group. Possible methodological sources of the variability will be considered in the following sections.

Methodological considerations

Differences in variability

In comparing the histochemically processed tissue obtained from each experiment there were evident differences in the quality and reliability of staining intensity. Statistical analysis found that the later experiments (phenylephrine and prazosin and propranolol treatment conditions) contained considerably more variability than the idazoxan treatment condition. The standard error of the mean values for the idazoxan group ranged between 0.007 to 0.032, mean = 0.018 for the aGP-stained and between 0.010 to 0.029 for the tGP-stained, mean = 0.015. The standard error of the mean values for the phenylephrine group ranged between 0.012 to 0.044, mean = 0.027 for the aGP-stained and between 0.003 to 0.039, mean = 0.021 for the tGP-stained. In the prazosin and propranolol group, the standard error ranged between 0.020 to 0.050, mean = 0.032 for the aGP-stained and between 0.009 to 0.032, mean = 0.020 for the tGP stained. Also see Table 3. The tGP staining seemed more consistent than the aGP staining. Though the tGP staining error variance was still greater in the later two experiments than in the first,

the difference is not as pronounced as in the aGP stained tissue. This is probably related to ceiling effects with tGP, but also suggests that aGP-staining is more labile and vulnerable to disruption. Table 3 presents the lightest and darkest staining intensities from sites where experimental manipulation was found to have a statistically significant effect. From these readings it is clear that the prazosin and propranolol group generated the highest range of ROD values for the sites measured. The ROD values for the lightest and darkest stained batches of the phenylephrine group had a slightly higher range than the idazoxan group but the difference is not considerable. That the standard error of the mean for this group is considerably higher than for the idazoxan group is more likely related to the inconsistency of the effect of phenylephrine (at the dose selected) compared to the effect of the idazoxan dose. In some chimeric brains the vehicle sites were found to have higher levels of aGP than the corresponding phenylephrine-treated sites. This can be readily discerned by examination of raw data for some chimeras. (See Table 3.)

There were also differences in other, possibly salient, variables between the first experiment (idazoxan group) and later experiments (phenylephrine group and prazosin and propranolol group). The first experiment was conducted in the winter. Winter room temperatures during tissue processing were more consistent than those later during the summer, when experiments 2 and 3 were carried out. The processing room did not have air-conditioning and had large windows, higher and fluctuating room temperatures occurred during this period. Secondly, the vehicle used in the idazoxan experiment was physiological saline whereas for the later experiments, alcohol was included in the vehicle formulation. It was necessary to use alcohol because prazosin did not dissolve easily in saline or even in mild hydrochloric acid. Although we used a dilute concentration of 95% ethanol (0.025% of the total volume of vehicle used), the effects of

alcohol cannot be ruled out as a potential contributor to the increase in variance. Alcohol is known to exert metabolic effects with direct consequences on aGP activity (Cusso *et al.*, 1989). In addition, serious cryostat frosting occurred during summer sectioning due to a malfunctioning fuse. This problem was not successfully identified or corrected until sectioning had been completed.

Although difficulties during the summer sectioning period resulted in variable overall staining from an overall yellow/brown or light brown to the rich dark brown typical of the winter experiment, all sections for a given chimeric brain were similar in staining quality. Thus vehicle versus treatment comparisons could be made although floor effects related to staining quality may have obscured differences. ROD values were examined to determine whether larger differences in ROD values between drug and control group could be predicted more for overall lightly versus darkly stained sections, but observations were inconclusive.

DISCUSSION

Patterns of aGP

Visual inspection of sections reacted for both aGP and tGP in the present study suggested the reactivity patterns were consistent with those previously described by Harley and Bielajew (1992). In sensory neocortex, an intense band of staining is seen in layer 4, while a broader, but less intense, band can be observed in the deeper layers. In the present study, the most superficial layers, which appeared less reactive were not sampled. The neocortical layers sampled did not differ significantly from each other

overall in the aGP measures. The barrel fields region layers 5b, 5a and 4 were most reactive. In tGP, the visual impression was confirmed quantitatively with the strongest reactions in layer 4 for both upper and lower limb primary somatosensory cortex. Interestingly, upper limb primary somatosensory cortex, rather than the barrel field region, showed the highest levels of overall reactivity in tGP. The aGP pattern in the neocortex is thus not a weaker version of the total levels of GP available but likely reflects functional demands in the premortem period. In the present study, animals were relatively quiet in their home cages and after anesthetic injection; it is possible that whisker activity may have been the predominant somatosensory input in the premortem period but this was not assessed directly. Swanson *et al.* (1992) have shown that whisker manipulation significantly enhances utilization of C14-labelled glycogen in the barrel field region of primary somatosensory cortex and in the thalamic and brainstem relay stations for this input. Future studies manipulating somatosensory input and evaluating aGP levels would be of interest. The total available GP would only be expected to change under conditions of chronic or prolonged manipulation, but the present data and Swanson's data support the hypothesis that astrocytic aGP levels and glycogenolysis can index transient alterations in metabolic demand. The high overall level of metabolic support available in layer 4 is consistent with results from studies of cytochrome oxidase and 2-DG uptake.

Within the hippocampus the CA1 and CA3 pyramidal cell layers and the dentate granule cell layer exhibit the least staining intensity, whereas the stratum lacunosum moleculare of CA1 and CA3 seems to have the darkest staining. The molecular layers of the dentate gyrus and the hilar area appear next most reactive. Stratum oriens and radiatum of CA3 also appear more reactive than the corresponding layers of CA1. In the

present quantitative tests of aGP distribution, the least reactive sites were the cell layers and the most reactive region was stratum lacunosum moleculare. Again the visual picture was best validated quantitatively in the data from tGP. CA1 and CA3 stratum lacunosum moleculare were most reactive; the molecular layer of the dentate gyrus was next most reactive, followed by the polymorph layer of the hilar region. CA3 stratum oriens and radiatum are more reactive than CA1 stratum oriens and radiatum. The cell body layers are least reactive. In aGP the pattern differs in that the medial, but not the lateral molecular layer, is significantly reactive supporting the hypothesis that aGP reflects differences in functional demand in the premortem state.

In the diencephalic, basal ganglia and fiber tract regions measured, the qualitative visual picture is again supported quantitatively by the measures of tGP. The medial habenula was most reactive, followed by the reticular nucleus of the thalamus and then globus pallidus. The fimbria fornix and the internal capsule were the least reactive and the caudate putamen, paraventricular nucleus and laterodorsal nucleus were intermediate. In aGP only the three most reactive structures were differentiated from the others. The order was the same as in tGP. This again suggests that active enzyme reflects transient demand rather than capacity.

Although the present measures use optical tissue density following staining of the glycogen generated rather than a direct colorimetric measure of enzymatic activity, e.g. liberated inorganic phosphate, as has been used in biochemical assays of brain GP activity, it is worth comparing the histochemical and biochemical estimates of aGP. From the earliest study of aGP in brain, the measure is given as a percentage of total activity. Different measures of enzyme activity yield different absolute values but both the forward and reverse reactions were initially reported to generate comparable percentage

values for aGP/tGP where tGP is defined as GP activity when AMP is added to the reaction medium. Breckenridge and Norman (1962) were the first to report very different measures of aGP levels as a function of time from decapitation. They used two methods of obtaining mouse brain: (1) decapitation followed by freezing of the head from 1 to 20 min postmortem and (2) direct freezing through the skull in restrained mice using surface applied Freon cooled with liquid nitrogen. The results from decapitated mice indicated a high level of aGP within 1 min, 70-75% of tGP; a lower level at 2 min of 50-55% and the lowest level (40-45%) by 5 min which remained unchanged up to 20 min. Cortex frozen *in situ*, however, had much lower levels of aGP, averaging 18%, as compared with 43% from cortex from mice decapitated into liquid nitrogen. This suggested GP in the cortex is primarily in the inactive form premortem, that it is activated within seconds on decapitation and inactivates again over a period of minutes. In a second set of experiments with drug administration, mice were decapitated into liquid nitrogen. Activity levels in control brain homogenate were 69% of tGP. Prior drug exposure to 18 hours of barbiturate anesthetic, 6 days of reserpine depletion, or 2 hr prior injection with chlorpromazine significantly reduced the aGP level from brains taken at the same time to 56-57% of tGP. Insulin-induced convulsions produce a significant activation of aGP to 83% of total. These values for decapitated animals based on histochemical measures are strikingly similar to the percentage activation levels calculated in the present study using a histochemical measure. The present values range from 43% to 77% depending on the area sampled and the experiment. A more recent study of aGP levels in rat brain caudate putamen homogenate from decapitated rats is higher (71% aGP) than the present value for caudate putamen (57%) but differences in the rate of removal may account for the higher level. The decapitation activation state is transient in that inactivation occurs over

minutes post mortem but may not completely return the brain to the lower *in situ* level of phosphorylase activity. The surprising finding, but one documented repeatedly beginning with Breckenridge and Norman's first experiments, is that premortem manipulations influence the level and pattern of postmortem phosphorylase activity (Breckenridge and Norman, 1962; Wallace, 1983; Woolf, 1985; and Coopersmith and Leon, 1995) despite decapitation related overall changes in the level of phosphorylase activity. Whether premortem manipulations would produce even larger percentage changes in aGP if *in situ* measures could be taken easily for these brain regions is not known.

The heterogeneous distribution of GP, active or available, is to be expected in the light of the discrete regional distribution of other metabolic enzymes such as cytochrome oxidase (Hevner *et al.*, 1995; and Wong-Riley, 1989), succinate dehydrogenase (Friede *et al.*, 1966), pyruvate dehydrogenase (Bagley *et al.*, 1989), malate dehydrogenase (Borowsky and Collins, 1989), and citrate synthetase (Shank and Campbell, 1984; and Wagman and Collins, 1988). Studies using [14C]2DG autoradiographic technique for measuring anatomically discrete changes in glucose metabolism have found that the brain does not utilize glucose uniformly (Sokoloff, 1979). Likewise, glycogen is not homogeneously utilized in the CNS. The distribution densities of GP may indicate which areas rely more heavily on glycogenolytic metabolism than others; highlight where astrocytes are more densely located, where more active synapses are located; and, perhaps, even which physiological functions are more dependent on energy derived through glycogenolytic means.

Links between glycogenolysis and functional regions of high neuronal activity

Numerous findings argue for links between neuronal activity and local glycogen utilization in mammalian brain suggesting that the brain may respond to sudden increases in energy demand partly through rapid metabolism of glycogen. As described previously, Swanson (1991) found that local increases in neuronal activity accelerated glycogenolysis in the rat brain. Areas that are highly reactive for tGP may denote areas where neurons are frequently stimulated. As reviewed in the Introduction, many astrocytic functions are closely tied to maintaining the integrity and efficiency of synaptic and neuronal functioning.

Enhanced glycogenolytic activity in discrete CNS regions therefore may indicate areas engaged in high levels of synaptic activity. Increased synaptic activity greatly increases the amount of work that astrocytes must perform in order to clear the synaptic space of glutamate, GABA and/or excess ions, to replenish depleted anaplerotic metabolites; and assist with CO_2 fixation. Because neuronal excitation results in increased astrocytic activity, there is also an increase in the amount of energy required by astrocytes, a need which may be fulfilled by glycogenolytic means.

Further evidence that high GP activity is linked to high neuronal activity comes from the parallel distribution of available GP and other metabolic enzymes such as cytochrome oxidase (CO). Harley and Bielajew (1992) reported similarities in reactivity for GP and CO across many brain regions. The quantitative results of the present study parallel the description of aGP distribution reported by the authors.

Further evidence that glycogenolytically active areas correspond to areas of enhanced neuronal activity is the probable connection between glycogenolysis and

glucose uptake activity. Cytochrome oxidase activity is also related to glucose uptake. In addition, the cytoarchitectural position of astrocytes between neuronal and vascular elements suggests that astrocytes form the first cellular barrier encountered by blood-borne substances entering the brain (Bunge *et al.*, 1962). This physiologically strategic position may indicate that astrocytes are key players in the channeling of nutrients, such as glucose, from vascular to neuronal elements (Pellerin and Magistretti, 1994).

Borowsky and Collins (1989) compared capillary density and metabolic enzyme activity throughout the rat brain and found that cytochrome oxidase activity parallelled capillary density whereas there was a negative correlation between lactate dehydrogenase activity and capillary density. They reported that the stratum lacunosum moleculare demonstrated the highest cytochrome oxidase activity, glucose utilization and capillary length, followed by the molecular layer of the dentate gyrus (inner blade). These results parallel our findings in that the stratum lacunosum moleculare of CA1 and CA3 were most reactive for aGP and tGP. The molecular layer was also reactive for these enzymes.

Shimada *et al.* (1992) compared circulatory microvessel and astroglial densities in each laminar region of the hippocampus and found that both densities were strongly correlated in all layers except in the pyramidal layers. The highest densities of microvessel and astroglia were found in the stratum radiatum and the lowest values were found in the granular layer. The stratum oriens and stratum lacunosum moleculare also show high GFAP-positive cell density and astroglial density. The stratum pyramidale, however, only exhibited high microvessel density without corresponding GFAP-positive cell density. The authors again speculate that this correspondence between vascular and astroglial density may be associated with glucose utilisation. The stratum lacunosum moleculare and the dentate molecular layer have also been found to demonstrate the

highest activities of succinate dehydrogenase (Friede *et al.*, 1966), malate dehydrogenase and citrate synthetase (Wagman and Collins, 1988).

It is important to note that while there is good correspondence in the distributions of GP, other metabolic enzymes and areas with enhanced microvessel and capillary density, the correspondence is not absolute. In some areas, heavy reliance on glycogenolytically derived energy, as inferred from higher levels of GP, may not be related to high neuronal activity but may, instead, indicate some primary function of astrocytes not directly related to neuronal excitation.

As mentioned previously, mapping of active glycogenolytic areas may not only indicate high levels of neuronal excitation but may also indicate the location of dense astrocytic processes or regions of dense connections between astrocytic processes and neuronal terminals. Isaacs *et al.* (1993) studied in astrocytic processes within the lamina of the dentate gyrus molecular layer. The highest density of astrocytic processes was found in the outer one-third of the molecular layer, where astrocytic processes and perikarya were numerous and neurons were sparse. The surface density of astrocytic processes was more widely dispersed in the inner region of the molecular layer of the dentate gyrus. A similar laminar result was observed for astrocytic process thickness in that the outer one-third of the molecular layer was found to contain the thickest processes. Harley and Rusak (1993) found the densest aGP patches in the middle molecular layer with lighter staining in the inner layer which may indicate that a simple relationship to astrocyte density does not occur. However examining tGP density in each subregion of the molecular layer would best test this hypothesis.

Noradrenergic activation of GP

Idazoxan group

Possible functions of NA's glycogenolytic effects

The noradrenergic system has been implicated in a wide variety of physiological processes including neuronal firing activity (Berridge *et al.*, 1993; and Bing *et al.*, 1992), attention (Devauges and Sara, 1990; Harley, 1991; Sara and Devauges, 1988; and; Sara *et al.*, 1994), curiosity (Dunn-Meynell and Levin, 1993), exploratory behaviour (Dunn-Meynell and Levin, 1993), learning (Coopersmith and Leon, 1995; and Sullivan *et al.*, 1994), mood and emotion (Kovachich *et al.*, 1993), and a host of psychiatric disorders (Iriye *et al.*, 1965). The pronounced differences in the ratio of AR subtypes among brain regions suggest that these subtypes may play different roles in neuronal function. These receptor subtypes and their varied association with discrete functional areas may provide a mechanism by which NA can activate a specific physiological process by stimulating neuronal activity and simultaneously initiating glycogenolysis to provide astroctyes with a rapid energy source to fuel the increased energy demands following neuronal excitation.

Idazoxan was found to significantly activate GP in layers 5a and 5b of the barrel fields, layer 5a of the lower limb and all layers of the upper limb sections of the primary somatosensory cortex. All the thalamic sites examined, the paraventricular, laterodorsal and reticular nuclei of the thalamus also demonstrated significant activation by idazoxan. These data suggest that NA may be involved in mediating glycogenolysis related to sensory processing. In the barrel fields, α1-ARs were found to be quite sensitive to decreases in afferent sensory input via vibrissectomy which caused a decrease in

[^{3}H]prazosin binding (Dunn-Meynell and Levin, 1993). The latter result suggests input levels and the potentiation for metabolic support may be functionally coupled.

Signal to noise ratio

NA has been described as a neuromodulator which enhances the signal-to-noise ratio in cortical sensory systems (Woodward *et al.*, 1979). While the major hypotheses describing NA's action in promoting signal and decreasing noise has related to neuronal neuromodulation effects, glia may also contribute to this action. One way in which NA may serve this function is by stimulating glycogen breakdown in order to fuel astrocytic processes, which include terminating rapidly and efficiently the effects of glutamate in the synaptic cleft, and buffering of ionic concentrations and other functions which are crucial to maintaining the integrity of synaptic conditions. The underlying mechanism by which NA is able to perform this function may be connected, in part, to its glycogenolytic effects - by providing astrocytes with the requisite rapidly accessible energy source to carry out synaptic clearance functions. NA also has direct effects on astrocytic activity following neuronal excitation.

As previously stated, astrocytes perform a variety of functions related to the restoration of homeostasis following neuronal activation. NA mediates many of these functions. Hansson and Ronnback (1992) reported that NA stimulates the re-uptake of several neurochemicals, including GABA, glutamate and taurine. Adrenergic agents mediate clearance of glutamate from the extracellular space (Hertz, 1992) through modulation of Na^+ dependent high affinity amino acid transporters (Kanai *et al.*, 1994) found on both neuronal and astrocytic loci (Kanai *et al.*, 1995).

While low concentrations of NA have been reported to result in a reduction of glutamate uptake, an effect that is linked to β-AR mediation (Hansson and Ronnback, 1981), higher concentrations of NA have been reported to increase glutamate uptake, an effect mediated by α1b-AR activation (Hansson and Ronnback, 1991; and Alexander *et al.*, (manuscript). An *in vivo* study reported that glutamate reuptake, as measured by levels of L-Glu, is increased in a dose-dependent manner by phenylephrine (α1-adrenergic agonist). This increase was attenuated by phentolamine (a1-adrenergic antagonist) (Isaacs *et al.*, 1993).

Learning, mnemonic and attentional processes

Studies have implicated the ascending dorsal noradrenergic bundle of the LC system in cognitive processes such as memory, learning and selective attention. However, it has also been suggested that NA is crucial in cognitive functions associated with the frontal lobes including prevention of distractibility by irrelevant stimuli. Idazoxan administration (1.0 mg/kg, i.p.) has been found to enhance attention/decrease distractability in rats (Bunsey and Strupp, 1995). The present finding of idazoxan effects on glycogen metabolism in the same regions implicated in the learning and memory studies suggests glial metabolic changes may be intimately linked to these effects. A critical role for glial glycogenolysis in such functions could be examined with inhibitors of glial glycogen metabolism.

NA's glycogenolytic effects may also be related to neuronal activation that occurs during learning and mnemonic processes. In our results, idazoxan administration enhanced glycogenolysis in layers 5a and 5b of both barrel fields and primary

somatosensory cortex upper limb section, as well as in layer 5b of lower limb section. One potential function of noradrenergic modulation in these layers may be to provide energy to fuel learning processes. Nowicky *et al.* (1992) reported that β-ARs modulate synaptic transmission and postsynaptic induction of associative LTP in layer 5 neurons of rat sensorimotor cortical slices.

Even in the olfactory bulb, a region not examined in our analysis, noradrenergic activation of glycogenolysis is associated with olfactory learning. Coopersmith and Leon (1995) found evidence to suggest that noradrenergic stimulation of glycogenolysis in the olfactory bulb accompanies olfactory stimulation in young rats. Neonatal rats were reported to exhibit aGP "hot spots" to peppermint in the olfactory bulb after being conditioned by pairing peppermint odour and body stroking. Enhanced aGP activity was absent in these areas in unconditioned rat pups. Sullivan *et al.* (1994) also reported similar findings. Following bilateral impairment of the LC using 6-OHDA, they found an attenuation of neonatal rats'olfactory associative learning. Thus, in the rat olfactory bulb, NA has been reported to enhance glycogenolytic activity and mediate associative olfactory learning.

In the hippocampus, in particular, where idazoxan-induced NA release was found to activate glycogenolysis in layers of CA1, CA3 and the dentate gyrus, there is a strong connection between NA and learning and mnemonic processes. Several studies of NA in the dentate gyrus support a role for the LC noradrenergic system in facilitating both short- and long-term enhancement of responses to complex sensory inputs (Sara *et al.*, 1994; and for review see Harley, 1991). NA release was found to enhance perforant path evoked potentials in the dentate gyrus of anaesthetized rats (Harley *et al.*, 1996). The mechanism through which projections from the LC may mediate memory processes is by

promoting or permitting changes in network configurations at critical times when environmental events may require changes in behavioural output. A study by Sara *et al.* (1994) reported that LC cells responded to novelty or change in incoming information but did not demonstrate a sustained response to stimuli, even when these stimuli were biologically significant. This suggests that the pattern of NA release from the LC to target sensory systems might serve to promote selective attention to relevant stimuli at the critical moment of change. Devauges and Sara (1990) reported that activation of the noradrenergic system facilitated an attentional shift in the rat. Rats were trained on a fixed path of six successive choices in a linear maze, the task was subsequently changed to a visual discrimination task in which the spatial configuration of the correct path was indicated by visual cues and changed on each daily trial. The drug treatment had no effect on the acquisition of either the successive place learning or the visual discrimination, but it was effective during the shift phase of the experiment, where the idazoxan-treated rats required fewer trials to reach criterion than control rats. According to the authors, hippocampal cells have been shown to respond selectively to specific places in the environment through a process of Hebbian association. They appear to become coupled to a set of distal environmental cues such that any subset of those cues is effective in activating the map. Sara and Devauges (1988) previously reported that low-level electrical stimulation of the LC immediately prior to testing rats in a 6-unit linear maze to which they had previously been trained resulted in significantly fewer performance errors than rats which did not receive priming LC stimulation, demonstrating that LC priming facilitates memory retrieval in the rat.

Electroencephalographic alterations

Inhibition of LC noradrenergic input to the neocortex and hippocampus has been reported to result in alterations of electro-encephalographic activity in these areas. The neocortical response to bilateral LC inhibition by clonidine (an α2-AR agonist) was characterized by a shift from low-amplitude, high-frequency to large-amplitude, slow-wave activity. In the hippocampus, theta-dominated activity was replaced with mixed frequency activity following noradrenergic inhibition (Berridge *et al.*, 1993). Bing *et al.*, (1992) also reported that NA exerts effects on the thalamic firing patterns of freely moving rats. They found that peripheral administration of the α1 antagonist, prazosin and the α2-agonists xylazine and clonidine increased the incidence and duration of thalamic and neocortical high voltage spike and wave spindles. These results demonstrate that the LC noradrenergic system exerts a potent and tonic activating influence on forebrain electroencephalographic state, which may modulate behavioral state and/or state-dependent processes and which may also be linked to the metabolic changes described here.

Receptor mediation

The effect of idazoxan-induced NA release in the neocortex is likely to be mediated at least in part by β-ARs since it is known that NA stimulates the formation of cAMP in this area (Rosenberg and Li, 1995). Using I-pindolol binding Rainbow *et al.* (1984) found high levels of predominantly β1-AR binding only in the superficial layers (layers 1 and 2) of the cerebral cortex. They reported that layers 4 and 5b of the neocortex contained comparable levels of both β1- and β2-AR subtypes and that layer 6 of

neocortex contained predominantly β2-ARs. In the primary somatosensory cortex, α1-ARs are most densely localized in layers 5 and 6, layers 3/4 and 4 have relatively less dense levels of α1 binding sites, with the lowest densities occurring in layers 1 and 2 (Zilles *et al.*, 1993). Our results consistently revealed that the levels of aGP in the deeper layers of neocortex (layers 3/4, 4, 5a, 5b and 6 of primary somatosensory cortex, upper limb section, in layer 5b of lower limb section and in layers 5a and 5b of barrel fields) were significantly enhanced by idazoxan-induced NA release. Based on these results, it is difficult to infer that one AR subtype is more greatly involved in mediating NA's glycogenolytic effects in the neocortex than another. Perhaps each receptor mediated region-specific glycogenolysis or perhaps ARs act in cooperation in this area.

Previous studies have reported that most hippocampal regions investigated in our study (the rostral and caudal portions of CA1, CA3 and dentate gyrus) demonstrate primarily β1- as opposed to β2-ARs (Bartholini, 1980; and Rainbow *et al.*, 1984). α1-ARs are almost exclusively distributed in the CA3 region of the rat hippocampus in the following strata: oriens, pyramidal, lucidum, radiatum and lacunosum moleculare and in dentate gyrus, particularly in the hilus (Zilles *et al.*, 1993). Our study found that sites examined in CA1, CA3 (with the exception of stratum pyramidale) and dentate gyrus (with the exception of granular and molecular layers) showed significant enhancement of aGP levels in response to idazoxan-induced NA release. These effects may be mediated by both α1- and β1-ARs, although the failure to observe significant differences in glycogenolysis in the hippocampus with phenylephrine suggests β1-ARs may play the dominant role. In CA1, where there is very little α-AR labelling, and predominantly β1 binding, the effects are likely to be mediated by β1-ARs.

The involvement of β-ARs in NA's glycogenolytic effects in the hippocampus are not surprising considering the fact that NA is known to stimulate formation of cAMP in the hippocampus (Stanton and Sarvey, 1985). The physiological relevance of this system, however, has yet to be established. Production of cAMP is involved in the expression of long-term potentiation and NA-induced long-lasting potentiation in the dentate gyrus (Stanton and Sarvey, 1985). Glial cAMP production via noradrenergic activation of β-ARs is hypothesized to mediate activation of neuronal immediate early gene (IEG) expression in the rat cerebral cortex (Bing *et al.*, 1992; Bing *et al.*, 1991; and Stone *et al.*, 1991). In support of this hypothesis, Stone *et al.* (1993) reported that administration of yohimbine, an α2-AR antagonist, or stress brought on by restraint, resulted in increases in *c-fos* immunoreactivity in the rat cerebral cortex. (Interestingly, stress has also been found to affect receptor activity. Weiss *et al.* (1994) reported that the type of stress introduced differentially affects α2- receptor binding in the LC.)

The laterodorsal nucleus of the thalamus has been reported to contain mainly β1-ARs whereas the paraventricular and reticular nuclei demonstrated higher levels of β2-ARs (Rainbow *et al.*, 1984). Anasuma (1992) reported dense noradrenergic innervation of the thalamus. He found the density of dopamine beta hydroxylase (the enyzyme that converts dopamine into NA) containing boutons within the reticular nucleus neuropil was found to be greater than that found in the relay nuclei of the dorsal thalamus (with the exception of the anterior group nuclei). The thalamus contains predominantly α1-ARs, with the greatest densities occurring in the lateral ventral and medial ventral regions (Zilles *et al.*, 1993). We found significant enhancement of glycogenolysis in the laterodorsal, paraventricular and reticular nuclei of the thalamus, sites which contain both

AR subtypes.

Our investigation found that idazoxan administration significantly enhanced glycogenolytic activity in the caudate putamen. This finding is potentially problematic since there is no evidence for a noradrenergic projection to this area from the LC. It is possible, however, that the β1-Ars, which are found in this region (Bartholini, 1980), are activated by NA release from other NA-containing cell groups (Room *et al.*, 1981). Release of 5HT is also inhibited by presynaptic α2-ARs (McCormick, 1991; and Feuerstein *et al.*, 1993). Idazoxan's effects in the striatum may be related to the serotonergic consequences of α2-AR antagonism by idazoxan. The glycogenolytic effects observed in the caudate may result from increased release of serotonin. These α2 presynaptic receptor effects, though, have only been demonstrated in neocortex and hippocampus to date (Feuerstein *et al.*, 1993; and Feuerstein, 1985).

In summary, both α- and β-ARs appear to mediate NA's glycogenolytic effects. In the neocortex, the areas in which α1-ARs are most abundant (namely layers 5a and 5b) were found, in the idazoxan study, to be particularly responsive to noradrenergic enhancement of glycogenolysis. However, results of the phenylephrine manipulation, activating á1-ARs primarily demonstrated greater sensitivity in layer 3/4. In the hippocampus, again, both α1 and β-ARs might contribute to noradrenergic enhancement of glycogenolysis, but phenylephrine effects were not significant. In CA1, particularly, where there is little α1-AR labelling, the present glycogenolytic effects are likely to be mediated by β1-ARs, which are more predominantly localized in the hippocampal areas examined than β2-ARs.

Idazoxan has been reported to cause reductions in cortical glucose use in certain

LC projection areas. In various cortical, hippocampal and thalamic regions, idazoxan administration was associated with a 13-20% reduction in glucose use (French *et al.*, 1995). It is unclear whether this represents a switch from glucose uptake to glycogen breakdown or if other factors related to the timing of metabolic measurements explain the differences from the present histochemical approach.

Possible confounds arising from use of idazoxan

As previously stated in the introduction, idazoxan activates many kinds of noradrenergic α2-ARs including autoreceptors, postsynaptic receptors, heteroreceptors, imidazoline receptors, with a particular affinity for the I2 subtype (Miralles *et al.*, 1993) but not I1-imidazoline binding sites (Ernsberger *et al.*, 1995), and 5HT2 receptors (Nilsson *et al.*, 1991). There are several subtypes of α2-ARs. Radioligand binding studies have demonstrated the existence of discrete regional distributions for each specific subtype. Different ligands, such as rawolscine, yohimbine and idazoxan show marked disparities in binding affinities which are affected by subtype selectivity of the ligand used to antagonize the receptor (Wamsley *et al.*, 1992). By examining the distribution of the mRNA coding for the three subtypes of α2-ARs (α2A, α2B and α2C), it has become possible to map those regions in the brain which possess cells that synthesize specific subtypes. MacDonald and Scheinin (1995) reported that regional differences in the localization of mRNA coding for α-AR subtypes, the subtype of which autoreceptors are primarily comprised, are found abundantly throughout the brain. Heal *et al.* (1995), using receptor binding and functional studies, found evidence suggesting that post-synaptic α2-ARs in the rat cortex are primarily of the α2D subtype. An electrophysiological study

investigating noradrenergic suppression of dorsal pyramidal neuronal firing rate in the CA1 and CA3 of the rat hippocampus, found that this effect was mediated primarily by α2-ARs (Curet and Montigny, 1988). MRNA for the α2B postsynaptic receceptors was found only in the thalamus whereas the α2C mRNA had a wider distribution with especially intense mRNA expression in basal ganglia (MacDonald and Scheinin, 1995).

α2-presynaptic receptors have been reported to elicit diverse physiological consequences. For instance, α2 antagonism has previously been reported to release brain serotonin (Dillen *et al.*, 1987), a neurotransmitter also known to exert glycogenolytic effects. As well, activation of α2-heteroreceptors has been found to facilitate NMDA-evoked tritium overflow in the rat brain cortex (Fink and Gothert, 1993). This effect was found to be mediated by α2-receptors since the preferential α1-AR antagonist prazosin was ineffective at evoking the response. In addition, idazoxan occupation of α2-heteroreceptors, located at least partly on serotonergic nerve terminals, facilitated, whereas NA reduced, the NMDA evoked 5-HT release (Fink *et al.*, 1995).

The effects of post-synaptic α2-AR activation on glycogenolysis are somewhat controversial. Most of the α2-ARs in the neocortex are found in layer 4. There is some labelling of the α2-AR subtype in the more superficial layers (1, 2, and 3/4) and almost none in layers 5 and 6 (Zilles *et al.*, 1993). In the barrel fields, α2-ARs are distributed almost homogeneously across the entire barrel field (Dunn-Meynell and Levin, 1993). α2-ARs are localized primarily to CA1 of the hippocampus (Zilles *et al.*, 1993) and in several thalamic nuclei (King *et al.*, 1995). We had thought that any direct antagonism of idazoxan administration on post-synaptic α2-ARs would further enhance glycogenolysis because these receptors inhibit cAMP production via inhibition of adenylyl cyclase.

Subbarao and Hertz (1990), however, reported that administration of the α2-AR agonist, clonidine, resulted in enhancement of glycogenolysis in astrocyte cultures and that NA's glycogenolytic effects could be inhibited by yohimbine, an α2-AR antagonist. Though there is little doubt that cAMP and Ca^{2+} play a role in the enhancement of glycogenolysis, the release of these intracellular messengers does not fully account for neurotransmitter activation of glycogenolysis. Some neurotransmitters, which can enhance release of Ca^{2+}, and/or increase cAMP production, such as glutamate, do not exert glycogenolytic effects.

Our results, when compared with the distribution of post-synaptic α2-adrenergic receptos, suggest that α2-ARs may decrease NA's glycogenolytic effects. Antagonism by idazoxan resulted in clear activation of glycogenolysis in layer 3/4 of neocortex and CA1 of hippocampus, regions where there is an abundance of α2-ARs. Since β-Ars are densely distributed in these areas, these results may indicate that, in these areas, β- and not α-ARs mediate NA's glycogenolytic effects here (Rainbow *et al.*, 1984). Nevertheless, the possibility remains that, in the idazoxan condition, NA's full glycogenolytic effects were not observed because possible stimulation via α2-ARs was masked by idazoxan antagonism.

Imidazoline effects

Idazoxan has been shown to recognize non-AR sites with high affinity (Mallard *et al.*, 1992). Autoradiography studies found I2 receptor subtypes in the following sites: subfornical organ, arcuate nucleus, interpeduncular nucleus, medial habenular nucleus, lateral mamillary nucleus, LC, dorsal raphe and dorsomedial hypothalamic nucleus (MacKinnon *et al.*, 1995). The direct effects of idazoxan on imidazole-receptor activation

do not appear to significantly alter glycogenolysis since glycogenolytic activity in regions known to contain I2 receptors, such as the medial habenula, were not found to be significantly modified by idazoxan. The sites we investigated are relatively free of confounding effects of imidazoline receptor activation. Several studies investigating the autoradiographic localization of imidazoline receptors do not report their presence in the thalamus, hippocampus and neocortex, the primary areas we studied King *et al.*, 1995; and MacKinnon *et al.*, 1995). Imidazoline binding sites have been reported on monoamine oxidase (both a and b) (Raddatz *et al.*, 1995), which suggest that it may affect the degradation of monoaminergic neurochemicals. However, idazoxan's effect on imidazole receptors may be minor since studies have reported that the major component of [3H]idazoxan binding was to sites that are alpha 2-adrenergic rather than non-adrenergic in nature (Raymond *et al.*, 1992). It would have been interesting to examine other areas where imidazoline receptor binding sites are abundantly found, which we did not do in this study.

Phenylephrine group

Phenylephrine, an α1-AR agonist, was administered to determine which regional glycogenolytic activational effects of idazoxan were mediated by α1-ARs. Phenylephrine was expected to enhance glycogenolysis in the neocortex because α1-ARs are found abundantly in the neocortical layers where significant effects were observed with idazoxan administration (Zilles *et al.*, 1995). Similarly, in the hippocampus, with the exception of CA1 areas, α1-ARs are localized densely in regions where we observed significant glycogenolytic effects, though β-ARs are also found in these regions. As well,

microdialysis studies have found that administration of phenylephrine in brain increases *in vivo* NA levels to 225% basal levels (Van Velhuizen *et al.*, 1993). Our study, however, found that systemic administration of phenylephrine only enhanced glycogenolytic activity in a few neocortical areas (SSS3/4, SSPul3/4, SSPul5b and SSPul6) and not in any hippocampal regions. The present data were only consistent with possible glycogenolytic involvement of á1-ARs in neocortex although they do not rule out a synergistic role for á1-ARs in concert with β-AR activation in other areas.

Prazosin and propranolol group

Under normal conditions, in the absence of experimental manipulation, the LC maintains a basal release of NA which increases with arousal level. A prazosin (á1 antagonist) and propranolol (β1/2 antagonist) cocktail, administered to determine whether basal noradrenergic release contributes to basal glycogenolytic activity, revealed that administration of prazosin and propranolol significantly inhibited basal glycogenolytic activity only in layer 3/4 of the barrel fields. The data suggest little support for NA involvement in basal glycogenolysis. This is consistent with the low level of basal NA neuronal activity in rats during quiet waking (Aston-Jones and Bloom, 1981). Although the data from the two sets of experiments suggest (a) little or no role for LC NA release in supporting basal aGP and (b) a relatively modest role for á1-ARs in enhancing aGP, certain caveats should be noted.

Time constraints prevented the systematic evaluation of the optimal dosages and time interval parameters for both the phenylephrine group and the prazosin and propranolol group.

Secondly, ethanol, which was used in the vehicle for these experiments has been linked to increased brain glycogen. Garriga *et al.* (1994) reported that 8 minutes after i.p. administration of ethanol (7 M, 0.75 ml ethanol/100 g animal weight) glycogen concentration increased in the hippocampus, striatum, cortex and thalamus which likely indicates inhibition of GP (Garriga *et al.*, 1994). Activational effects of NA may have been depressed by the use of ethanol (Cusso *et al.*, 1989).

Thirdly, as described earlier, these latter two experiments were conducted in the summer and brains were subjected to greater variations in temperature during the sectioning and histochemical processes. The increased overall staining variability necessarily reduced the sensitivity of the experiment despite the use of chimeric sections.

AGP in relation to tGP

In brain areas that demonstrated an overall increase in GP activation of 8% following idazoxan administration there was significantly more aGP reactivity as measured by ROD levels on the idazoxan-treated half of the chimeric brain. Some sites, which showed an activational enhancement of approximately 7%, were also found to have higher levels of aGP in the idazoxan side. In the thalamus, however, sites, which demonstrated between 4.2-6.3% activational increase in aGP were found to be significantly more reactive on the idazoxan side. Interestingly, the range of activational enhancement in response to idazoxan and phenylephrine administration is similar: 1.6-12.6% and 0-12% respectively. The range of attenuation by the double blocker cocktail is also similar, 0-11%.

Several questions are raised by the results of this study. For instance, why is there never 100% activation of all GP present in a particular region of the brain? In the present context, it might be suggested that one neurotransmitter is not sufficient to induce complete activation of all available GP in any area of the brain. There are many known activators of glycogenolysis. The neurochemicals adenosine (Magistretti *et al.*, 1986; Quach *et al.*, 1982; and Sorg and Magistretti, 1991), cAMP (Folbergrova, 1995; and Takarama and Graves, 1991), Ca^{2-} ions (Medrano *et al.*, 1992; and Ververken *et al.*, 1982) and K^{-} ions (Cambray Deakin *et al.*, 1988; and Subbarao *et al.*, 1995), ammonia, arachidonic acid (Sorg *et al.*, 1995), and ATP (Woolf, 1987) have been reported to activate breakdown of glycogen. Neurotransmitters and neuromodulators have also been found to exert glycogenolytic effects, including vasoactive intestinal peptide (Sorg and Magistretti, 1992; and Sorg *et al.*, 1995), histamine (Medrano *et al.*, 1992; and Quach *et al.*, 1978), serotonin (Chen *et al.*, 1995; and Quach *et al.*, 1982), NA (Cambray-Deakin *et al.*, 1988; Sorg and Magistretti, 1992; and Sorg *et al.*, 1995) and substance P (Subbarao *et al.*, 1995). The effects of dopamine (Cambray-Deakin *et al.*, 1988), glutamate (Woolf, 1987) and acetylcholine (Cambray-Deakin *et al.*, 1988) remain controversial with consensus leaning toward the conclusion that they are ineffective in directly modulating glycogen metabolism.

It may be that a combination of different stimuli must be present before most if not all GP is converted to its active form. Converging activation from a combination of neurotransmitters, neurochemicals and behavioural factors may be required before close to 100% activation of available GP is observed.

Current theories concerning the function of glycogen breakdown

The function of the glycogen store is only now beginning to be elucidated. It appears to play a dynamic role in the daily functioning of the CNS since it has a rapid turnover rate (Watanabe and Passonneau, 1973). In other tissues, in muscle for instance, glycogen serves as an energy store that is rapidly utilized through glycolytic metabolism during times of increased energy demand. In brain, empirical evidence implicates the breakdown of glycogen in supplying emergency energy during pathological conditions (Harik *et al.*, 1982; and Swanson and Choi, 1993). At other times, however, the brain was believed to rely primarily on oxidative metabolism to supply the vast majority of its energy requirements. The high resting oxygen demand and the close match between local cerebral blood flow and local cerebral glucose consumption supported this notion. Local cerebral blood flow is presumed to supply neurons with O_2 and to remove CO_2 secreted by active neurons (Ueki *et al.*, 1988). The fact that glycogen is stored almost entirely in glia rather than in neurons also makes it an unlikely source of energy for neurons. However, the discovery that substances secreted following neuronal excitation are able to modulate glycogenolysis implies a functional metabolic coupling between neurons and glia, specifically astrocytes.

Current studies report that the brain may respond to local increases in energy demand by engaging non-oxidative metabolic mechanisms, specifically via the breakdown of glycogen. Lipton (1993), using fluorescence techniques in brain slice preparations, suggested that non-oxidative breakdown of glycogen, perhaps through glycogenolysis, occurs specifically at the onset of neuronal activity even when glucose availability is adequate. In addition, greater increases in local cerebral glucose utilization than can be accounted for by increases in local cerebral blood flow have been reported

following sensory stimulation (Ueki *et al.*, 1988). Using functional MRI, Raichle (1994) reported that the normal human brain exhibits non-oxidative metabolism during spurts of neuronal activity. In fact, this form of metabolism occurs despite the presence of abundant oxygen in the normal brain (Swanson and Choi, 1993). Blood flow associated with neocortical activation is also rapid, but not instantaneous (Leniger-Foller and Hossmann, 1979). This time lapse may require that energy be derived, at least initially, from anaerobic means prior to the arrival of blood-bourne oxygen. Increased local metabolic demands may initially be resolved by increased anaerobic breakdown of glycogen.

Glycogen is an obvious candidate substrate however the functional role of this energy source is still debated. Swanson (1991) argues that astrocytes metabolize glycogen in response to neuronal activation in order to fuel the resulting increases in their own energy demands following increases in neuronal activity As previously stated, neuronal activation is always accompanied by increases in levels of K^+ and neurotransmitter in the extracellular space.

The process of assisting with the restoration of membrane potential and neurotransmitter reuptake and/or inactivation, Swanson points out, is dependent on transport via the transmembrane glial Na^+ gradient, which has previously been reported to be preferentially fueled by glycolytically produced ATP (Swanson, 1991). Swanson further argues that there is no energetic advantage in cycling glucose through a glial pool for neuronal consumption in the presence of extracellular glucose. Blood glucose normally exceeds the levels of extractable blood oxygen except during severe hypoglycaemia (Siesjo, 1978).

When glucose supply is insufficient, oxygen supply will also be inadequate and

only an anaerobic metabolic route will generate energy under these conditions. Since pyruvate, lactate, malate and other TCA intermediates can only generate ATP through oxidative processes, the transfer of these intermediates to neurons by glia would not facilitate neuronal ATP production under anaerobic conditions.

Consistent with Swanson's argument is the fact that glycogenolysis causes the formation of glucose-6-phosphate (G-6-P) which is not permeable through cell membranes without the catalytic intervention of G-6-P phosphatase to cleave the phosphate from the molecule and makes it freely diffusable. Sokoloff *et al.* (1977) reported that phosphatase activity in the brain is fairly low, making this an unlikely possibility. Forsyth *et al.* (1993) suggests that this low phosphatase activity may be misleading. Western blot analysis has shown that cells from primary rat astrocyte cultures express a protein that cross-reacts with polyclonal antibodies to the catalytic subunit of rat hepatic glucose 6-phosphatase. They also note that the cerebral glucose-6-phosphatase system lacks a glucose -6-phosphate translocase, based largely on the failure of brain microsomes to distinguish mannose 6-phosphate and glucose 6-phosphate, which may also not accurately reflect the true situation. In additon, a glucose transporter, GLUT1, has been reported to be localized in astrocytes from the blood brain barrier in humans (Morgello *et al.*, 1995), rabbits (Dwyer and Pardridge, 1993) and rats (Bagley *et al.*, 1989).

The glycogen story is further complicated by the fact that glia have been reported to release substances which can be metabolized by neurons to yield cellular energy (ATP) such as lactate and pyruvate (Brazitikos and Tsacopoulos, 1991; Fray *et al.*, 1996; Magistretti *et al.*, 1993; Sonnewald *et al.*, 1993; and Sorg and Magistretti, 1992). It is possible that glycogen may function in the brain in a manner similar to its function in

other tissues. Glycogen may serve as an energy reserve that can be immediately utilized to meet sudden increases in energy demand occurring under normal physiological conditions

Neuronal firing per se likely does not require much energy to maintain. Primary synaptic activation may have the highest energy requirement, increases in energy demand may occur in astrocytes which have the demanding task of cleaning up the synaptic cleft and replenishing depleted neuronal supplies. The shifting of the energetic burden to astrocytes is supported by empirical reports that the anaerobic metabolism, which happens immediately in response to neuronal activation, occurs even in the presence of abundant oxygen (Fellows *et al.*, 1993; and Raichle, 1994). Glycogen breakdown, especially the first stage, glycogenolysis, does not require the presence of oxygen. The next step, glycolysis, can also occur in the absence of oxygen. See Figure 2.

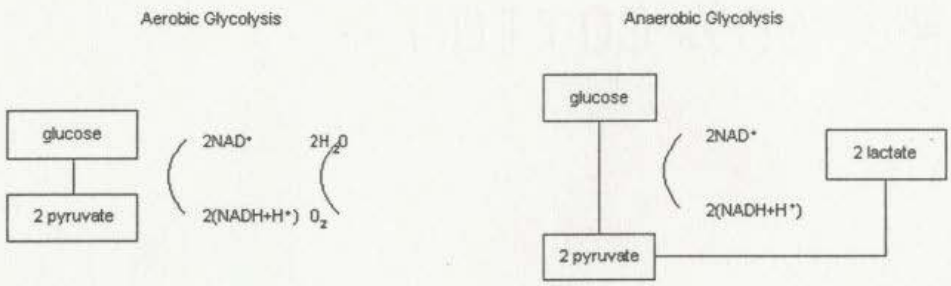

Figure 2

Increases in blood supply are likely necessary for predominantly neuronal but not astrocytic purposes. Increased blood supply would result in higher oxygen levels which could be utilized by neurons to metabolize the substances secreted by astrocytes such as lactate, pyruve and malate as these substances can only yield energy after undergoing the

TCA cycle which is a strictly aerobic process. See Figure 3.

Recent studies have shed some light into the possible nature of this energy interaction between neurons and astrocytes, using *in vitro* techniques. During times of high anaerobic metabolic activity, at the onset of neuronal activation, there is an increase in lactate production from astrocytes which can be transported to neurons possibly to fuel neuronal processes. However, the evidence to date does not support the notion that glycogen is metabolized to provide neurons with energy. Firstly, studies have demonstrated that the primary biproduct of glycogenolysis is glucose and not lactate (Boutelle *et al.*, 1993). During times of high anaerobic metabolic activity at the onset of neuronal activation described in fMRI studies, there is an increase in lactate but no significant increase in glucose levels. The transfer of glucose from astrocytes to neurons is not impossible, particularly in light of recent evidence of glucose-6-phosphatase activity in brain. However, from a biochemical standpoint, it makes better sense for neurons to be supplied with lactate rather than glucose. Lactate can immediately enter the TCA cycle, whereas glucose must first undergo glycolytic metabolism. See Figure 3.

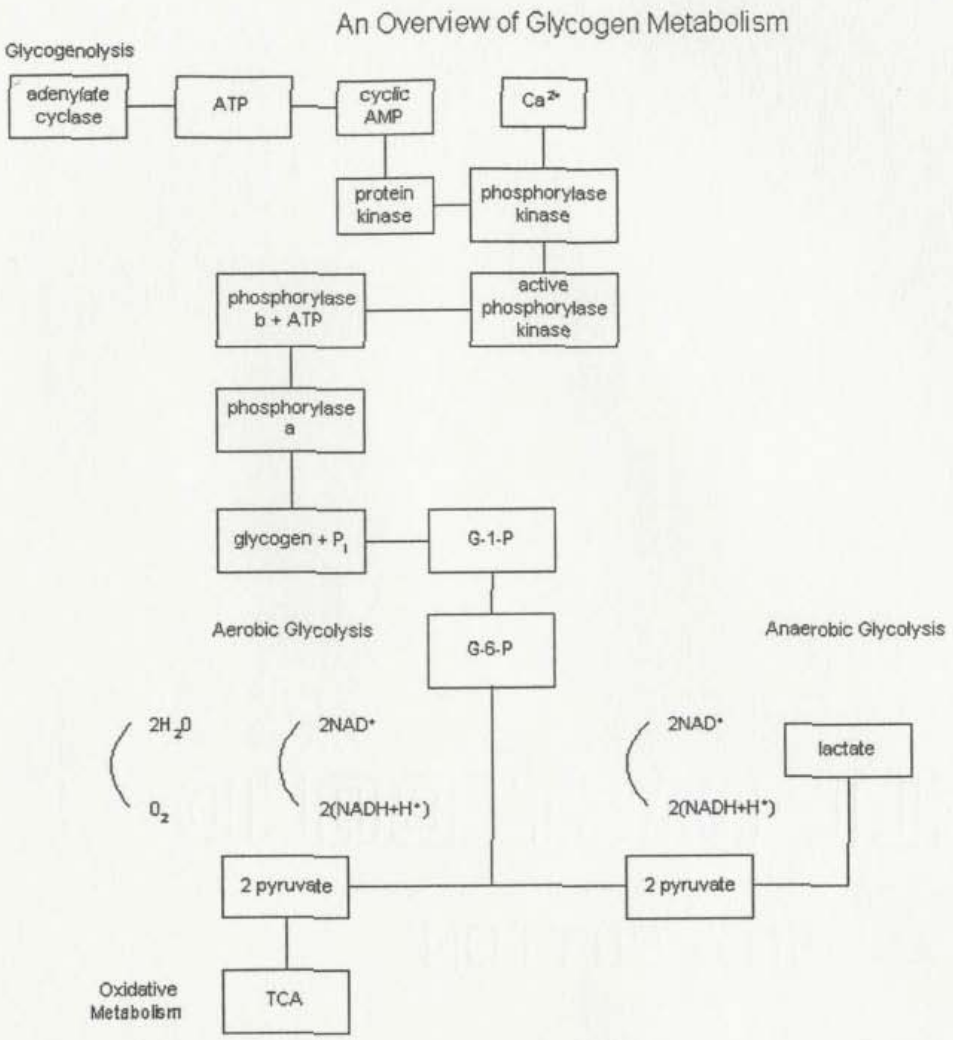

Figure 3

Pellerin and Magistretti (1994) suggest that lactate is the key player in the non-oxidative metabolic activity that occurs immediately after neuronal excitation. A transport system has recently been described in neurons (Pellerin and Magistretti, 1994). In addition they cite various *in vitro* studies which reported that synaptic activity can be demonstrated in cerebral cortical slices maintained in lactate or pyruvate in the absence of glucose; glucose deprivation – induced neurodegeneration in hippocampal slices can be prevented by the addition of lactate in the perfusing medium; lactate utilization by

nervous tissue occurs even in the presence of glucose. Though lactate cannot fully substitute for glucose as a metabolic substrate for brain because of its limited permeability across the blood brain barrier, Pellerin and Magistretti suggest that it could, at least in part, fulfill the brief, immediate, energetic needs of neurons at the onset of activation.

REFERENCES

1. Agullo, L and Garcia, A (1991) Norepinephrine increases cGMP in astrocytes by a mechanism dependent on nitric oxide synthesis. Eur J Pharmacol 206:343-346.

2. Alexander, GM, Grothsen, JR, Gordon, SW and Schwartzman, RJ. Intracerebral microdialysis study of glutamate reuptake in awake, behaving rats (manuscript).

3. Anasuma, C (1992) Noradrenergic innervation of the thalamic reticular nucleus: a light and electron microscopic immunohistochemical study in rats. J Comp Neurol 319:299-311.

4. Aoki, C, Joh, TH and Pickel, VM (1987) Ultrastructural localization of β-adrenergic receptor-like immunoreactivity in the cortex and neostriatum of rat brain. Brain Res 437:264-282.

5. Aston-Jones, G and Bloom, FE (1981) Activity of norepinephrine-containing locus coeruleus neurons in behaving rats anticipates fluctuations in the sleep-waking cycle. J Neurosci 1:876-886.

6. Attia, AM, Mostafa, MH, Richardson, BA and Reiter, RJ (1995) Night-time rise in rat pineal N-acetyltransferase due to carbaryl administration is reduced by propranolol treatment. Biomed Environ Sci 8:45-53.

7. Bagley, PR, Tucker, SP, Nolan,C. Lindsay, JG, Davies, A, Baldwin, SA, Cremer, JE and Cunningham, VJ (1989) Anatomical mapping of glucose transporter protein and pyruvate dehydrogenase in rat brain: An immunogold study. Brain Res 499:214-224.

8. Barford, D, and Johnson, LN (1989) Allosteric transition of glycogen phosphorylase. Nature 340:609-616.

9. Bartholini, G (1980) Interactions of dopaminergic, cholinergic and GABA-ergic neurons; relation to extrapyramidal function. Trends in Pharmacol Sci 1:138-140.

10. Berridge, CW, Page, ME, Valentino, RJ and Foote, SL (1993) Effects of locus coeruleus inactivation on electroencephalographic activity in the neocortex and hippocampus. Neurosci 55:381-393.

11. Bing, G, Chen, S, Zhang, Y, Hilman, D and Stone, EA (1992) Noradrenergic-induced expression of c-fos in rat cortex: neuronal localization. Neurosci Lett 140:260-264.

12. Bing, G, Filer, D, Miller, JC and Stone, EA (1991) Noradrenergic activation of immediate early genes in the rat cerebral cortex. Mol Brain Res 11:43-46.

13. Breckenridge, BM and Norman, JH (1962) Glycogen phosphorylase in brain. J Neurochem 9: 383-392.

14. Borowsky, IW and Collins, RC (1989) Metabolic anatomy of brain: a comparison of regional capillary density, glucose metabolism, and enzyme activities. J Comp Neurol 288:401–413.

15. Bowman CL, and Kimelberg HK (1987) Pharmacological properties of the norepinephrine-induced depolarization of astrocytes in primary culture: evidence for the involvement of an α1-adrenergic receptor. Brain Res 423:403-407.

16. Brazitikos, PD and Tsacopoulos, M (1991) Metabolic signaling between photoreceptors and glial cells in the retina of the drone (Apis mellifera). Brain Res 567: 33-41.

17. Brown, CM, MacKinnon, AC, Redfern, WS, Williams, A, Linton, C, Stewart, M, Clague, RU, Clark, R and Spedding, M (1995) RS–45041-190: a selective, high-affinity ligand for I2 imidazoline receptors. Br J Pharmacol 116:1737-1744.

18. Bunge, MD, Bunge, RP and Pappas, GD (1962) Electron microscopic demonstrations of connections between glia and myelin sheaths in the developing mammalian central nervous system. Cell Biol 12:448–453.

19. Bunsey, MD and Strupp, BJ (1995) Specific effects of idazoxan in a distraction task: evidence that endogenous norepinephrine plays a role in selective attention in rats. Behav Neurosci 109:903-911.

20. Burgess, SK, Trimmer, PA and McCarthy, KD (1985) Autoradiographic quantification of β-adrenergic receptors on neural cells in primary cultures. II. Comparison of receptors on various types of immunocytochemically identified cells. Brain Res 335:11-19.

21. Butterworth, RF (1993) Portal-Systemic Encephalopathy: A Disorder of Neuron-Astrocytic Metabolic Trafficking. Dev Neurosci 15:313-319.

22. Cambray-Deakin, M, Pearce, B, Morrow, C and Murphy, S (1988) Effects of extracellular potassium on glycogen stores of astrocytes in vitro. J Neurochem 51:1852-1857.

23. Cambray-Deakin, M, Pearce, B, Morrow, C and Murphy, S (1988) Effects of Neurotransmitters on astrocyte glycogen stores in vitro. J Neurochem 51:1852-1857.

24. Chen, Y, Peng, L, Zhang, X, Stolzenburg, J-U and Hertz, L (1995) Further evidence that fluoxetine interacts with a 5-HT2c receptor in glial cells. Brain Res Bul 38:153-159.

25. Clark, RB and Perkins, JP (1971) Regulation of adenosine 3':5'-cyclic monophosphate concentration in cultured human astrocytoma cells by catecholamines and histamine. Proc Natl Acad Sci USA 68:2757-2760.

26. Coopersmith, R and Leon, M (1995) Olfactory bulb glycogen metabolism: noradrenergic modulation in the young rat. Brain Res 674:230-237.

27. Curet, O and Montigny, D (1988) Electrophysiological characterization of adrenoceptors in the rat dorsal hippocampus. I. Receptors mediating the effect of microiontophoretically applied norepinephrine. Brain Res 475:35-46.

28. Cusso, R, Vernet, M, Cadefau, J and Urbano-Marquez, A (1989) Effects of ethanol and acetaldehyde on the enzymes of glycogen metabolism. Alcohol and Alcoholism 24:291-297.

29. Deecher, CD, Wilcox, BD, Dave, V, Rossman, PA and Kimelberg, HK (1993) Detection of 5-hydroxytriptamine2 receptors by radioligand binding, northern blot analysis and Ca^{2+} responses in rat primary astrocyte cultures. J Neurosci Res 35:246 -256.

30. Devauges, V and Sara, SJ (1990) Activation of the noradrenergic system facilitates an attentional shift in the rat. Behav Brain Res 39:19-28.

31. Devlin, TM (ed). (1992) Textbook of Biochemistry, With Clinical Correlations John Wiley and Sons, Inc., New York, New York.

32. Dillen, L, Claeys, M and DePotter, WP (1987) Effects of alpha-2 antagonist idazoxan on monoaminergic parameters measured in the cerebrospinal fluid of rabbits. Eur J Pharmacol 137:33-40.

33. Dunn-Meynell, AA and Levin, BE (1993) Alpha 1-adrenoceptors in the adult rat barrel field: effects of deafferentation and norepinephrine removal. Brain Res 623:25-32.

34. Dwyer, K and Pardridge, W (1993) Developmental modulatin of blood-brain-barrier and choroid plexus GLUT1 glucose transporter messenger ribonucleic acid and immunoreactive protein in rabbits. Endocrinology 132:558-565.

35. Ebersolt, C, Perez and M Bokaert, J (1981) Neuronal, glial and meningeal localizations of neurotransmitter-sensitive adenylate cyclases in cerebral cortex of mice. Brain Res 213:139-150.

36. Ernsberger, P, Fraves, ME, Graff, LM, Zakieh, N, Nguyen, P, Collins, LA, Westbrooks, KL, Johnson FF (1995) I1-imidazoline receptors. Definition, characterization, distribution and transmembrane signaling. Ann YY Acad Sci

763:22-42.

37. Fahrig, T (1993) Receptor subtype involved and mechanism of norepinephrine-induced stimulation of glutamate uptake into primary cultures of rat brain astrocytes. Glia 7:212-218

38. Fallon, JH and Moore, RY (1978) Catecholamine innervation of the basal forebrain III. Olfactory bulb, anterior olfactory neucli, olfactory tubercle and piriform cortex. J Comp Neurol 180:533-544.

39. Federoff S, Juurlink, BHJ and Doucette, R (eds.) (1993) Biology and pathology of astrocyte-neuron interactions. Plenum Press, New York, New York.

40. Fellows, LK, Boutelle, MG and Fillenz, M (1993) Physiological stimulation increases nonoxidative glucose metabolism in the brain of the freely moving rat. J Neurochem 60:1258-1263.

41. Feuerstein, TJ, Hertting, G and Jackisch, R (1985) Endogenous noradrenaline as modulator of hippocampal serotonin (5-HT) release. Dual effects of yohimbine, rauwolscine and coryn-anthine as α2-adrenoceptor antagonists and 5-HT-receptor agonists. Naunyn Schmiederbergs Arch Pharmacol 329:216-221.

42. Feurstein, TJ, Mutschler, A, Lupp, A, Van Velthoven, V, Schlicker, E and Gothert, M (1993) Endogenous noradrenaline activates α2-adrenoceptors on serotonergic nerve endings in human and rat neocortex. J Neurochem 61:474-480.

43. Fillenz, M (1990) Noradrenergic Neurons, Cambridge University Press, New York, New York.

44. Finch, EA, Turner, TJ and Goldin, SM (1991) Calcium as a coagonist of inositol 1,4,5-triphosphate-induced calcium release. Science 252:443-446.

45. Fink, K and Gothert, M (1993) Modulation of N-methyl-D-aspartate (NMDA)-stimulated noradrenaline release in rat brain cortex by presynaptic alpha 2-adrenoceptors. Naunyn Schmiedebergs Arch Pharmacol 348:372-378.

46. Fink, K, Schmitz, V, Boing, C and Gothert, M (1995) Stimulation of serotonin release in the rat brain cortex by activation of ionotropic glutamate receptors and its modulation via alpha 2-heteroreceptors. Naunyn Schmiedebergs Arch Pharmacol 352:394-401.

47. Finkbeiner, SM (1993) Glial calcium. Glia 9:83-104.

48. Folbergrova, J (1995) Glycogen phosphorylase activity in the cerebral cortex of rats during development: effect of homocysteine-induced seizures. Brain Res 694:128-132.

49. Fonnum, F (1984) Glutamate: A neurotransmitter in mammalian brain. J Neurochem 42:1-11.

50. Forsyth, RJ, Bartlett, K, Burchell, A, Scott, HM and Eyre, JA (1993) Astrocytic glucose-6 phosphatase and the permeability of brain microsomes to glucose 6-phosphate. Biochem J 294:145-151.

51. Fray, AE, Forsyth, RJ, Boutelle, MG and Fillenz, M (1996) The mechanisms controlling physiologically stimulated changes in rat brain glucose and lactate: a microdialysis study. J Physiol 496.1:49-57.

52. Freedman, JE and Aghajanian, GK (1984) Idazoxan (RX 781094) selectively antagonizes alpha 2-adrenoceptors on rat central neurons. Eur J Pharmacol 105:265-272.

53. French, N, Lalies, MD, Nutt, DJ and Pratt, JA (1995) Idazoxan-induced reductions in cortical glucose use are accompanied by an increase in noradrenaline release: complementary [14C]2-deoxyglucose and microdialysis studies. Neuropharmacol 34:605-613.

54. Friede, RL, Fleming, LM and Knoller, M (1966) A comparative mapping of enzymes involved in hexose monophosphate shunt and citric acid cycle in the brain. J Neurochem 10:263-277.

55. Garriga, J, Sust, M and Cusso, R (1994) Regional distribution of glycogen, glucose and phosphorylated sugars in rat brain after intoxicating doses of ethanol. Neurochem Intl 25:175-181.

56. Gilman, AG (1987) G proteins: transducers of receptor-generated signals. Ann Rev Biochem 56:615-650.

57. Gilman, AG (1989) G proteins and regulation of adenylyl cyclase. JAMA 262:1819-1825.

58. Gilman, AG and Nirenberg, M (1971) Effect of catecholamines on the adenosine 3':5'-cyclic monophosphate concentrations of clonal satellite cells of neurons. Proc Natl Acad Sci USA 68:2165-2168.

59. Hansson, E and Ronnback, L (1981) Regulation of glutamate and GABA transported by adrenoceptors in primary astroglial cell cultures. Life Sci 44:27-34.

60. Hansson, E and Ronnback, L (1991) Receptor regulation of glutamate, GABA and taurine high-affinity uptake into astrocytes in primary culture. Brain Res 548:215-221.

61. Hansson, E and Ronnback, L (1992) Adrenergic receptor regulation of amino acid neurotransmitter uptake in astrocyte. Brain Res Bul 29:297-301.

62. Hansson, E, Simonsson, P and Alling, C (1990) Interactions between cyclic AMP and inositol phosphate transduction systems in astrocytes in primary culture. Neuropharmacol 29:591-598.

63. Harik, SI, Busto, R and Martinez, E (1982). Norepinephrine regulation of cerebral glycogen utilization during seizures and ischemia. J Neurosci 2:409-414.

64. Harley, C (1991) Noradrenergic and locus coeruleus modulation of the perforant path-evoked potential in rat dentate gyrus supports a role for the locus coeruleus in attentional and memorial processes. Prog Brain Res 88:307-321.

65. Harley, CW and Bielajew, CH (1992) A comparison of glycogen phosphorylase and cytochrome oxidase histochemical staining in rat brain, J Comp Neurol 322:377-389.

66. Harley, CW, Lalies, MD and Nutt, DJ (1996) Estimating the synaptic concentration of norepinephrine in dentate gyrus which produces β-receptor mediated long-lasting potentiation in vivo using microdialysis and intracerebroventricular norepinephrine. Brain Res 710:293-298.

67. Harley, CW, Milway, JS and Fara-On, M (1995) Medial forebrain bundle stimulation in rats activates glycogen phosphorylase in layers 4, 5b and 6 of ipsilateral granular neocortex. Brain Res 685:217-223.

68. Harley, CW and Rusak, B (1993) Daily variation in active glycogen phosphorylase patches in the molecular layer of rat dentate gyrus. Brain Res 626:310-317.

69. Hassel, B, Paulsen, RE, Johnsen A and Fonnum, F (1992) Selective inhibition of glial cell metabolism in vivo by fluorocitrate. Brain Res 576:120-124.

70. Heal, DJ, Cheetham, SC, Butler, SA, Gosden, J, Prow, MR and Buckett, WR (1995) Receptor binding and functional evidence suggest that postsynaptic alpha 2-adrenoceptors in rat brain are of the alpha 2D subtype. Eur J Pharmacol 277:215-221.

71. Heal, DJ and Mardsen, CA (eds.), (1990) The pharmacology of noradrenaline in the central nervous system. Oxford University Press, New York, New York.

72. Hertz, L (1979) Functional interactions between neurons and astrocytes. I. Turnover and metabolism of putative amino acid transmitters. Prog Neurobiol 13:277-323.

73. Hertz, L (1992) Autonomic control of neuronal-astrocytic interactions, regulating metabolic activities, and ion fluxes in the CNS. Brain Res Bul 29:303-313.

74. Hevner, RF, Liu, S and Wong-Riley, MTT (1995) A metabolic map of cytochrome oxidase in the rat brain: histochemical, densitometric and biochemical studies. Neurosci 65:313-342.

75. Hirata, H, Slater, NT and Kimelberg, HK (1983) α-adrenergic receptor mediated depolarization of rat neocortical astrocytes in primary culture. Brain Res 270:358-362.

76. Hodges-Savola, C, Rogers, SD, Ghilardi, JR, Timm, DR and Mantyh, PW (1996) β-adrenergic receptors regulate astrogliosis and cell proliferation in the central nervous system in vivo. Glia 17:52-62.

77. Hosli, L, Hośli, E, Zehntner, C, Lehmann, R and Lutz, TW (1982) Evidence for the existence of α and β-adrenoceptors on cultured glial cells- an electrophysiological study. Neurosci 7:2867-2872.

78. Iriye, TT, Kuna, A and Simmonds, FA (1965) Glycogen phosphorylase levels in the brain of rats treated with psychotomimetic drugs and with tranquilizers. Biochem Pharmacol 14:1169-1171.

79. Iriye, TT and Simmonds, FA (1971) Possible involvement of glycogen phosphorylase of brain in the affective states. Intl Pharmacopsychiatry 6:98-110.

80. Isaacs, KR, Sirevaag, AM, Marks, AE, Chang, F-L and Greenough, WT (1993) A method for quantification of astrocytic processes reveals laminar differences in the dentate gyrus but not in CA1 of the hippocampal formation. J Neurosci Methods 48:141-148.

81. Jones, BE (1991) Noradrenergic locus coeruleus neurons: their distant connections and their relationship to neighboring (including cholinergic and GABAergic) neurons of the central gray and reticular formation. Prog Brain Res 88:15-30.

82. Kanai, Y, Smith, CP and Hediger, MA (1994) A new family of neurotransmitter transporters: the high-affinity glutamate transporters. FASEB J 8:1450-1459.

83. Kanai, Y, Bhide, PG, Difiglia, M and Hediger, MA (1995) Neuronal high-affinity glutamate transport in the rat central nervous system. Neuroreport 6:2357-2362.

84. Kandel, ER, Schwartz, JH and Jessop, TM (1991) Principles of Neural Science. Elsevier Science Publishing Co., Inc . New York, New York.

85. Kaufman, EE and Driscoll, BF (1993) Evidence for cooperativity between neurons and astroglia in the regulation of CO2 fixation in vitro. Dev Neurosci 15:299-305.

86. Killilea, SD, Brandt, H and Lee EYC (1976) Modulation of protein function by phosphorylation: the role of protein phosphatase. TIBS (February) pp30-33.

87. Kimelberg HK (ed.), (1988) Glial Cell Receptors. Raven Press, Albany, New York, p.1.

88. King, PR, Gundlach, AL and Louis, WJ (1995) Quantitative autoradiographic localization in rat brain of alpha 2-adrenergic and non-adrenergic I-receptor binding sites labelled by [3H] rilmedine. Brain Res 675:264-278.

89. Korf, J and Sebens, JB (1979) Cyclic AMP in the rat cerebral cortex after activation of noradrenaline neurons of the locus coeruleus. J Neurochem 32:463-468.

90. Kovachich, GB, Frazer, A and Aronson, CE (1993) Effect of chronic administration of antidepressants on alpha2 adrenoceptors in the locus coeruleus and its projection fields in rat brain determined by quantitative autoradiography. Neuropsychopharmacology 8:57-65.

91. Krebs, EG (1989) Role of the cyclic AMP-dependent protein kinase in signal transduction. JAMA 262:1815-1818.

92. Lajtha, AL, Maker, H and Clarke, DD (1981) Metabolism and transport of carbohydrates and amino acid GJ Siegerl, RW Albers, B Agranoff and R Katzman (eds.) Basic Neurochemistry. Litte, Brown and Co., Boston, Massachussetts pp329-353.

93. Lehninger, AL (1970) Biochemistry. Worth Publishers, Inc., New York, New York pp 499-500.

94. Leniger-Foller, E and Hossmann, K-A (1979) Simultaneous measurements of microflow and evoked potentials in the somatomotor cortex of the cat brain during specific sensory activation. Pflregers Arch 380:85-89.

95. Levitt, P and Moore, RY (1978). Noradrenaline neuron innervation of the neocortex in the rat. Brain Res 139:219-231.

96. Lindsay, RM (1979) Adult rat brain astrocytes support survival of both NGF-dependent and NGF-insensitive neurons. Nature 282:80-82.

97. Lindvall, O and Bjorklund, A (1974) The glyoxylic acid fluorescence histochemical method: a detailed account of the methodology for the visualization of central catecholamine neurons. Histochemistry 39:97-127.

98. Lipton, P (1973) Effects of membrane depolarization on nicotinamide nuclotide fluorescence in brain slices. Biochem J 136:999-1009.

99. Lopez-Sanudo, S and Arilla, E (1994) Changes in alpha 1-adrenergic neurotransmission alter the number of somatostatin receptors in the rat hippocampus. Neurosci Lett (Ireland) 177:107-110.

100. MacDonald E and Scheinin, M (1995) Distribution and pharmacology of alpha 2-adrenoceptors in the central nervous system. J Physiol Pharmacol 46:241-258.

101. MacKinnon, AC, Redfern, WS and Brown, CM (1995) [3H]-RS-45041-190: a selective high-affinity radioligand for I2 imidazoline receptors. Br J of Pharmacol 116:1729-1736.

102. Magistretti, PJ, Hof, PR and Martin, J-L (1986). Adenosine stimulates glycogenolysis in mouse cerebral cortex: a possible coupling mechanism between neuronal activity and energy metabolism. J Neurosci 6:2558-2562.

103. Magistretti, PJ, Sorg, O, Yu, N, Martin, J-L and Pellerin, L (1993) Neurotransmitters regulate energy metabolism in astrocytes: Implications for the metabolic trafficking between neural cells. Dev Neurosci 15:306-312.

104. Mallard, NJ, Hudson, AL, and Nutt, DJ (1992) Characterization and autoradiographical localization of non-adrenoceptor idazoxan binding sites in the rat brain. Br J Pharmacol 106:1019-1027.

105. Mancinelli, A, D'Arano, V, Stasi, MA, Lecci, A, Borsini, F and Meli, A (1991) Effect of enantiomers of propranolol on desipramine-induced anti-immobility in the forced swimming test in the rat. Phamacol Res 23:47-50.

106. McCarthy, KD and Vellis, D (1978) Alpha-adrenergic receptor modulation of beta-adrenergic, adenosine and prostaglandin E1 increased adenosine 3'5'-cyclic monophosphate levels in primary cultures of glia. J Cyc Nucleot Res 4:15-26.

107. McCarthy KD and Vellis, J (1979) The regulation of adenosine 3':5"-cyclic monophosphate accumulation in glia by alpha-adrenergic agonists. Life Sci 24:639-650.

108. McCormick, DA (1991) Electrophysiological consequences of activation of adrenoceptors in the CNS. Szabadi, E and Bradshaw, CM (eds.) In Adrenoceptors: Structure, Mechanisms, Function. Basel, Birkhauser Verlag, pp 159-169.

109. Medrano, S, Gruenstein, E and Dimlich, RVW (1992) Histamine stimulates glycogenolysis in human astrocytoma cells by increasing intracellular free calcium. Brain Res 592: 202-207.

110. Miralles A, Olmos, G, Sastre, M, Barturen, F, Martin, I and Garcia-Sevilla, JA (1993) Discrimmination and pharmacological characterization of I2-imidazoline sites with [3H]idazoxan and alpha-2 adrenoceptors with [3H]RX821002 (2-

methoxy idazoxan) in the human and rat brains. J Pharmacol Exp Therapeutics 264:1187-1197.

111. Morgello, S, Uson, RR, Schwartz, SJ and Haber RS (1995) The human blood-brain barrier glucose transporter (GLUT1) is a glucose transporter of gray matter astrocytes. Glia 14:43-54.

112. Murphy, S (ed.) (1993) Astrocytes: Pharmacology and Function. Academic Press Inc., San Diego, California

113. Nilsson, M, Hansson, E and Ronnback, L (1991) Adrenergic and 5HT2 receptors on the same astroglial cell. A microspectrofluorimetric study on cytosolic CA^{2+} response in single cells in primary culture. Dev Brain Res 63(1991)33-41.

114. Norenberg, MD and Martinez-Hernandez, A (1979) Fine structural localization of glutamine synthetase in astrocytes of rat brain. Brain Res 161:303-310.

115. Nowicky, AV, Christofi, G and Bindman, LJ (1992) Investigation of β-adrenergic modulation of synaptic transmission and postsynaptic induction of associative LTP in layer V neurones in slices of rat sensorimotor cortex. Neurosci Lett 137:270-273.

116. Otani, K, Kaneko, S and Bertilsson, L (1991) Studies on active transport of (E) - 100 hydroxynortriptyline in the kidney and brain of rats: effects of propranolol and quinidine. Pharmacol Toxicol 68:380-383.

117. Paudel, HK, Zwiers, H and Wang, JH (1993) Phosphorylase kinase phosphorylates the calmodulin-binding regulatory regions of neuronal tissue-specific proteins B-50 (GAP-43) and neurogranin. J Biol Chem 268:6207-6213.

118. Paulsen, RE, Contestabile, A, Villani, L and Fonnum, F (1987) An in vivo model for studying the function of brain tissue temporarily devoid of glial cell metabolism: the use of fluorocitrate. J Neurochem 48:1377-1385.

119. Pellerin, L and Magistretti, PJ (1994) Glutamate uptake into astrocytes stimulates aerobic glycolysis: A mechanism coupling neuronal activity to glucose utilization. Proc Natl Acad Sci USA 91:10625-10629.

120. Pentreath, VW, Seal, LH and Kai-Kai, MA (1982) Incorporation of [3H]2-deoxyglucose into glycogen in nervous tissue. Neurosci 7:759-767.

121. Peter, B, Van Waarde, MA, Vissink, A, 's-Gravenmade, EJ and Konings, AW (1995) Degranulation of rat salivary glands following treatment with receptor-selective agonists. Clin Exp Pharmacol Physiol 22:330-336.

122. Peters, A, Palay, SL and de F Webster, H (1991) The Fine Structure of the Nervous System: Neurons and Their Supporting Cells. 2nd ed. W.B. Saunders,

Philadelphia.

123. Pfeiffer, B, Meyermann, R and Hamprecht, B (1992) Immunohistochemical co-localization of glycogen phosphorylase with the astroglial markers glial fibrillary acidic protein and s-100 protein in rat brain sections. Histochemistry 97:405-412.

124. Quach, TT, Rose, C, Duchemin, AM and Schwartz, JC (1982) Glycogenolysis induced by serotonin in brain: identificaion of a new class of receptor. Nature 298:373-375.

125. Quach, TT, Rose, C and Schwartz, JC (1978) [3H]Glycogen hydrolysis in brain slices: Responses to neurotransmitters and modulation of noradrenaline receptors. J Neurochem 30:1335-1341.

126. Raichle, ME (1994) Visualizing the mind. Scientific American 270:58-64

127. Raddatz, R, Parini, A and Lanier, SM (1995) Imidazoline/guanidinium binding domains on monoamine osidases. Relationship to subtypes of imidazoline-binding proteins and tissue-specific interaction of imidazoline ligands with monoamine oxidase B. J Biol Chem 270:27961-27968.

128. Rainbow, TC, Parsons, B and Wolfe, BB (1984) Quantitative autoradiography of β1- and β2-adrenergic receptors in rat brain. Proc Natl Acad Sci USA 81:1585-1589.

129. Rakic, P (1971) Neuronal-glial relationships during granule cell migration in the developing cerebellar cortex. Golgi and electron microscopic study in the macacus rhesus. J Comp Neurol 141:282-312.

130. Rakic, P (1972) Mode of cell migration to the superficial layers of fetal monkey neocortex. J Comp Neurol 145:61-84.

131. Raymond, HK, Smith, TD and Leslie FM (1992) Further pharmacological characterization of [3H]idazoxan binding sites in rat brain; evidence for predominant labeling of alpha 2-adrenergic receptors. Brain Res 582:261-267.

132. Robison, GA, Butcher, RW, Oye, E, Morgan, HE and Sutherland EW (1965) The effect of epinephrine on adenosine 3'5'-phosphate levels in the isolated perfuse rat heart. Mol Pharmacol 1:168-177.

133. Room, P, Postema, F and Korf, J (1981) Divergent axon collaterals of rat locus coeruleus neurons: Demonstration by a fluorescent double labeling technique. Brain Res 221:219-230.

134. Rosenberg, PA and Li, Y (1995) Adenylyl cyclase activation underlies intracellular cyclic AMP accumulation, cyclic AMP transport, and extracellular adenosine accumulation evoked by β-adrenergic receptor stimulation in mixed

cultures of neurons and astrocytes derived from rat cerebral cortex. Brain Res 692:227-232.

135. Salm, AK and McCarthy, KD (1992) The evidence for astrocytes as a target for central noradrenergic activity: expression of adrenergic receptors. Brain Res Bul 29:265-275.

136. Sara, SJ and Devauges, V (1988) Priming stimulation of locus coeruleus facilitates memory retrieval in the rat. Brain Res 438:299-303.

137. Sara, SJ, Vankov, A and Herve, A (1994) Locus coeruleus-evoked responses in behaving rats: a clue to the role of noradrenaline in memory. Brain Res Bul 35:457-465.

138. Schousboe A and Westergaard N (1993) Pathologic consequences in hippocampus of aberrations in the metabolic trafficking between neurons and glial cells necessary for normal glutamate homeostasis. Hippocampus (special issue, eds. Nitsch, R and Ohm, TG) 3:165-170.

139. Schwartz, J-C, Gabarg, M and Pollard, H (1986) Histaminergic transmission in the brain. V.B. Mountcastle, F.E. Bloom and S.R. Geiger (eds.), Handbook of Physiology, The Nervous System Section I, Vol. IV, Chap. 5, Am Physiol Soc, Bethesda, MD, pp 257-316.

140. Shank, RP and Aprison, MH (1981) Present status and significance of the glutamine cycle in neural tissues. Life Sci 28:837-842.

141. Shank RP, Bennett, GS, Freytag, SO and Campbell, G Le M (1985) Pyruvate carboxylase, an astrocyte-specific enzyme implicated in the replenishment of amino acid neurotransmitter pools. Brain Res 329:364-367.

142. Shank, RP and Campbell, GL (1984). α-ketoglutarate and malate uptake and metabolism by synaptosomes: Further evidence for an astrocyte-to-neuron metabolic shuttle. J Neurochem 42:1153-1160.

143. Shimada, M, Akagi, N, Goto, H, Watanabe, H, Watanabe, H, Nakanishi, M, Hirose,Y and Watanabe, M (1992) Microvessel and astroglial cell densities in the mouse hippocampus. J Anatomy 180-89-95.

144. Siesjo, BK (1978) Brain energy metabolism. John Wiley and Sons, New York, New York.

145. Sokoloff, L (1979) Mapping of local cerebral functional activity by measurement of local cerebral glucose utilization with [14]2-deoxyglucose. Brain 102:653-668.

146. Sokoloff L, Reivich M, Kennedy C, Des Rosiers MH, Patlak CS, Pettigrew KD, Sakurada O, Shinohara M (1977) The [14C]deoxyglucose method for the

measurement of local cerebral glucose utilization: theory, procedure, and normal values in the conscious and anesthetized albino rat. J Neurochem May 28(5):897-916.

147. Sonnewald, W, Westergarrd, N, Petersen, S, Unsgard, G and Schousboe, A (1993) Metabolism of [U-C-13] glutamate in astrocytes studied by C-13 NMR spectroscopy - incorporation of more label into lactate than into glutamine demonstrates the importance of the tricarboxylic acid cycle. J Neurochem 61:1179-1182.

148. Sorg, O and Magistretti, PJ (1991) Characterization of the glycogenolysis elicited by vasoactive intestinal peptide, noradrenaline and adenosine in primary cultures of mouse cerebral cortical astrocytes. Brain Res 563:227-233.

149. Sorg, O and Magistretti, PJ (1992) Vasoactive intestinal peptide and noradrenaline exert long-term control on glycogen levels in astrocytes: blockade by protein synthesis inhibition. J of Neurosci 12:4923-4931.

150. Sorg, O, Pellerin, L, Stolz, M, Beggah, S and Magistretti, PJ (1995) Adenosine triphosphate and arachidonic acid stimulate glycogenolysis in primary cultures of mouse cerebral cortical astrocytes. Neurosci Lett 188:109-112.

151. Stanton, PK and Sarvey, JM (1985) The effect of high-frequency electrical stimulation and norepinephrine on cyclic AMP levels in normal versus norepinephrine-depleted rat hippocampal slices. Brain Res 358:343-348.

152. Stone, EA and Ariano, MA (1989) Are glial cells targets of the central noradrenergic system? A review of the evidence. Brain Res Rev 14:297-309.

153. Stone, EA and John, SM (1991) Further evidence for a glial localization of rat cortical β-adrenoceptors: studies of in vivo cyclic AMP responses to catecholamines. Brain Res 549:78-82.

154. Stone, EA, John, SM., Bing, G and Zhang, Y (1991) Studies on the cellular localization of biochemical responses to catecholamines in the brain. Brain Res Bul 29:285-288.

155. Stone, EA, Zhang, Y, John, S, Filer, D and Bing, G (1993) Effect of locus coeruleus lesion on c-fos expression in the cerebral cortex caused by yohimbine injections or stress. Brain Res 603:181-185.

156. Subbarao, KV and Hertz, L (1990) Effect of adrenergic agonists on glycogenolysis in primary cultures of astrocytes. Brain Res 536220-226.

157. Subbarao, KV and Hertz, L (1990) Noradrenaline induced stimulation of oxidative metabolism in astrocytes but not in neurons in primary cultures. Brain Res 527:346-349.

158. Subbarao, KV and Hertz, L (1991) Stimulation of energy metabolism by alpha-adrenergic agonists in primary cultures of astrocytes. J Neurosci Res 28:399-405.

159. Subbarao, KV, Stolzenburg, J-U and Hertz L (1995) Pharmacological characteristics of potassium-induced glycogenolysis in astrocytes. Neurosci Lett 196: 45-48.

160. Sullivan, RM, Wilson, DA, Lemon, C and Gerhardt, GA (1994) Bilateral 6-OHDA lesions of the locus coeruleus impair associative olfactory learning in newborn rats. Brain Res 643:306-309.

161. Swanson, LW (1992) Brain Maps: Structure of the Rat Brain. Elsevier, Amsterdam, pp. 239

162. Swanson, LW and Hartman, BK (1975) The central adrenergic system. An immunofluorescence study of the location of cell bodies and their efferent connections in the rat utilizing dopamine-β-hydroxylase as a marker. J Comp Neurol 163:467-506.

163. Swanson, RA (1991) Physiologic coupling of glycogen metabolism to neuronal activity in brain. Can J Physiol Pharmacol 70:S138-S144.

164. Swanson, RA and Choi, DW (1993) Glial glycogen stores affect neuronal survival during glucose deprivation in vitro. J Cereb Blood Flow and Metab 13:162-169.

165. Swanson, RA and Graham, SH (1994) Fluorocitrate and fluoroacetate effects on astrocyte metabolism in vitro. Brain Res 664:94-100.

166. Swanson, RA, Morton, MM, Sagar, SM and Sharp FR (1992) Sensory stimulation induces local cerebral glycogenolysis: Demonstration by autoradiography. Neurosci 51:451-461.

167. Takarama JF and Graves DJ (1991) Solution conformations of the N-terminal CNBr fragment of glycogen phosphorylase and its interaction with calmodulin. Biochimica et biophysica Acta 1077:371-378.

168. Taylor, SS, Buechler, JA and Yonemoto, W (1990) cAMP-dependent protein kinase: framework for a diverse family of regulatory enzymes. Ann Rev Biochem 59, 971-1005.

169. Trulson, ME and Jacobs, BL (1979) Raphe unit activity in freely moving cats: correlation with level of behavioral arousal. Brain Res 163:135-150.

170. Tsacopoulos, M.and Magistretti, PJ (1996) Metabolic Coupling between Glia and Neurons. J Neurosci 16:877-885.

171. Ueki, M, Linn, F and Hossmann, K-A (1988) Functional activation of cerebral blood flow and metabolism before and after global ischemia of rat brain. J Cereb Blood Flow Metab 8:486-494.

172. Van Calker, DV, Muller, M and Hamprecht, B (1978) Adrenergic α and β-receptors expressed by the same cell type in primary culture of perinatal mouse brain. J Neurochem 30:713-718.

173. Van Veldhuizen, MJ, Feenstra, MG and Boer, GJ (1994) Regional differences in the in vivo regulation of the extracellular levels of noradrenaline and its metabolites. Brain Res 635: 238-248.

174. Van Velhuizen, MJ, Feenstra, MG, Heinsbroek, RP and Boer, GJ (1993) In vivo microdialysis of noradrenaline overflow: effects of alpha-adrenoceptor agonists and antagonists measured by cumulative concentration-response curves. British J Pharmacol 109:655-660.

175. Ververken, D, Van Veldhoven, P, Proost, C, Carton, H and De Wulf, H (1982) On the role of calcium ions in the regulation of glycogenolysis in mounse brain cortical slices. J Neurochem 38:1286-1295.

176. Wagman, IL and Collins, RC (1988) Red and white metabolism in hippocampus. Neurol 38(Supp. 1):181.

177. Wallace, MN (1982) Modular organization of phosphorylase a activity in the rodent hippocampal region. J Physiol 329, 32P.

178. Wallace, MN (1983) Organization of the mouse cerebral cortex: A histochemical study using glycogen phosphorylase. Brain Res 267: 201-216.

179. Wamsley, JK, Alburges, ME, Hunt, MA and Bylund DB (1992) Differential localization of alpha 2-adrenergic receptor subtypes in brain. Pharmacol Biochem Behav 41:267-273.

180. Watanabe, H and Passonneau, JV (1973) Factors affecting the turnover of cerebral glycogen and limit dextrin in vivo. J Neurochem 20:1543-1554.

181. Weiss, GK, Ratner, A, Voltura, A, Savage, D, Lucero, K and Castillo, N (1994) The effect of two different types of stress on locus coeruleus alpha-2 receptor binding. Brain Res Bul 33:219-221.

182. Wong-Riley, MTT (1989) Cytochrome oxidase: an endogenous metabolic marker for neuronal activity. TINS 12:94-101.

183. Woodward, DJ, Moises, HC, Waterhouse, BD, Hoffer, BJ and Freedman, R, (1979) Modulatory actions of norepinephrine in the central nervous sytem. Fed Proc 38:2109-2116.

184. Woolf, CJ (1987) Excitatory amino acids increase glycogen phosphorylase activity in the rat spinal cord. Neurosci Lett 73:209-214.

185. Woolf, CJ, Chong, MS and Rashdi, TA (1985) Mapping increased glycogen phosphorylase activity in the dorsal root ganglia and in the spinal cord following peripheral stimuli. J Comp Neurol 234:60-76

186. Yamaguchi, T, Kuraishi, Y, Minami, M, Yabuuchi, K and Satoh, M (1991) Involvement of central beta-adrenoceptors in the induction of hypothalamic interleukin-1 beta mRNA by methamphetamine. Neurosci Res (Ireland)12:432-439.

187. Yamamoto, T, Iwasaki, Y, Sato, Y, Yamamoto, H and Konno, H (1989) Astrocytic pathology of metionine sulfoximine-induced encephalopathy. Acta Neuropathol 77:357-368.

188. Yudkoff, M, Nissim, I, Daikhin, Y, Lin, Z-P, Nelson, D, Pleasure, D and Erecinska, M (1993) Brain glutamate metabolism: neuronal-astroglial relationships. Dev Neurosci 15:343-350.

189. Zilles, K, Qu, M and Schleicher, A (1993) Regional distribution and heterogeneity of α-adrenoceptors in the rat and human central nervous system. Journal fur Hirnforschung 34:123-132.